Jeffrey, Keller et al 1978

Edinburgh Wave Power Project

Fourth Year Report

Volume 1 of 3

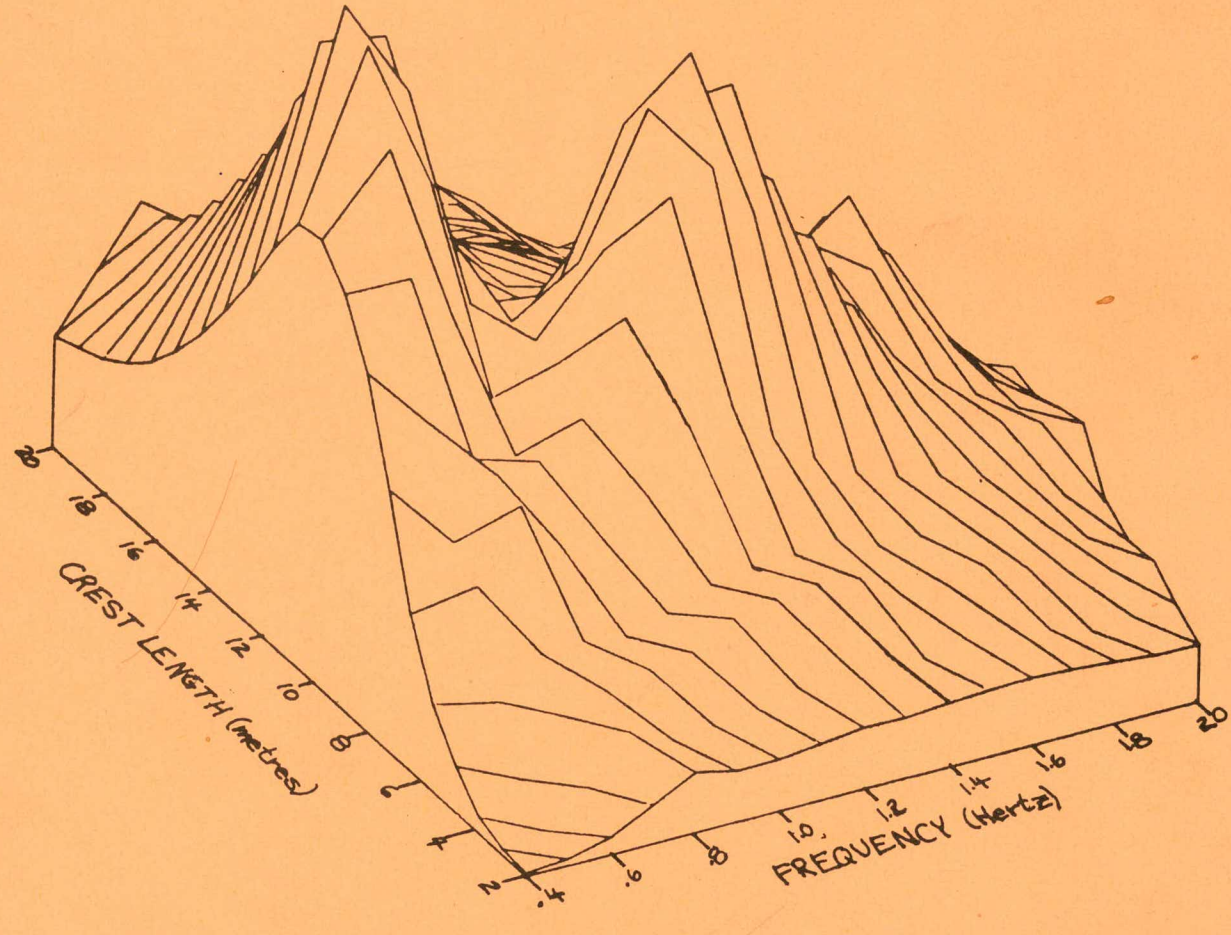

July 1978

FOURTH YEAR REPORT

on

EDINBURGH WAVE POWER PROJECT

"STUDY OF MECHANISMS FOR EXTRACTING POWER FROM SEA WAVES"

D. C. Jeffrey, G. J. Keller, Denis Mollison,

D.J.E. Richmond, S. H. Salter, J.R.M. Taylor, I.A. Young

Department of Mechanical Engineering,

University of Edinburgh,

Mayfield Road,

Edinburgh 9

CONTENTS

SEPARATE REPORTS:

VOLUME 2 SLAMMING TESTS

VOLUME 3 EDINBURGH WIDE TANK

The cover picture shows the relationship of bending moments to crest length and frequency for long backbones.

INTRODUCTION

The results of measurements carried out at the National Maritime Institute, Feltham in February 1977 confirmed that scaling laws operate well over the range from 1/150 to 1/15 and so we believe that it is safe to continue work in small tanks.

We have tested ducks on a variety of mountings in the narrow tank over the entire range of sea conditions found at OWS India. The results provide sufficient input data for the full-scale power take-off design.

We have developed techniques for generating very steep waves and have tested ducks in conditions likely to induce slamming. We are satisfied with duck behaviour in these conditions and do not regard slamming as our most serious problem. Photographs of the tests are contained in Volume 2 of this report.

We have explored duck behaviour on mountings of variable compliance, and have discovered some striking effects. We find that there are two regions of efficient operation, one of which requires no restraint in heave. Ducks on mountings with the right compliance can work better than those on fixed mountings and the right compliance can easily be achieved at full scale.

Most of our effort has gone into making a wide tank with control of directional characteristics of random seas. Its design may prove of interest to other groups. It was ready for use in January 1978 and the cost estimates proved accurate. Descriptions of the design and performance will be found in Volume 3 of this report.

Results from our first month of experiments on free-floating backbones without ducks show that bending moments fall in the central sections of very long backbones and that static beam theory is difficult to apply.

The full-time engineering strength of the team has risen to four with the arrival of Glenn Keller but I am sorry to report that we shall be losing two welcome visitors. Rick Jefferies, who has been working on non-linear problems for his Cambridge doctorate, will be going to CEGB, Marchwood. Ian Young is leaving us to read computer science here at Edinburgh.

I would like to draw the attention of WESC to reports by my colleague David McComb on polymer additions for hydraulic power transmission, by Graham Dixon on the anomalous heave force behaviour of horizontal cylinders and by Rick Jefferies on theoretical frequency and time domain models for ducks.

S. H. Salter

July 1978

SCATTER DIAGRAM TESTS IN THE NARROW TANK

In our 1976 report we described the behaviour of ducks in small to medium regular waves. We now report

(1) measurements in more realistic conditions, including pseudo-random seas;

(2) comparisons between fixed and moving mountings.

The same duck with the same ballasting (see page 3.2) was used for all tests. The tests were chosen to cover the range of sea conditions experienced at OWS India by a 15 metre duck.

On both kinds of mounting, tests covered RMS wave height from 0.2 to 4.3 metres, and energy period (T_e) from 7.4 to 13.3 seconds. In the fixed-axis tests, the torque limits ranged from .5 MNm/m to 4 MNm/m. However, since the fixed-axis work yielded evidence that the economic torque limit would be close to 1 MNm/m, this limit was imposed for all tests on the moving rig.

There were several repeat tests and random checks including some to investigate anomalous heave force behaviour.

The test points are superimposed on the scatter diagram opposite.

We present our main conclusions first. Complete test results start on page 2.17.

STATION INDIA SCATTER DIAGRAM SHOWING TESTS PERFORMED

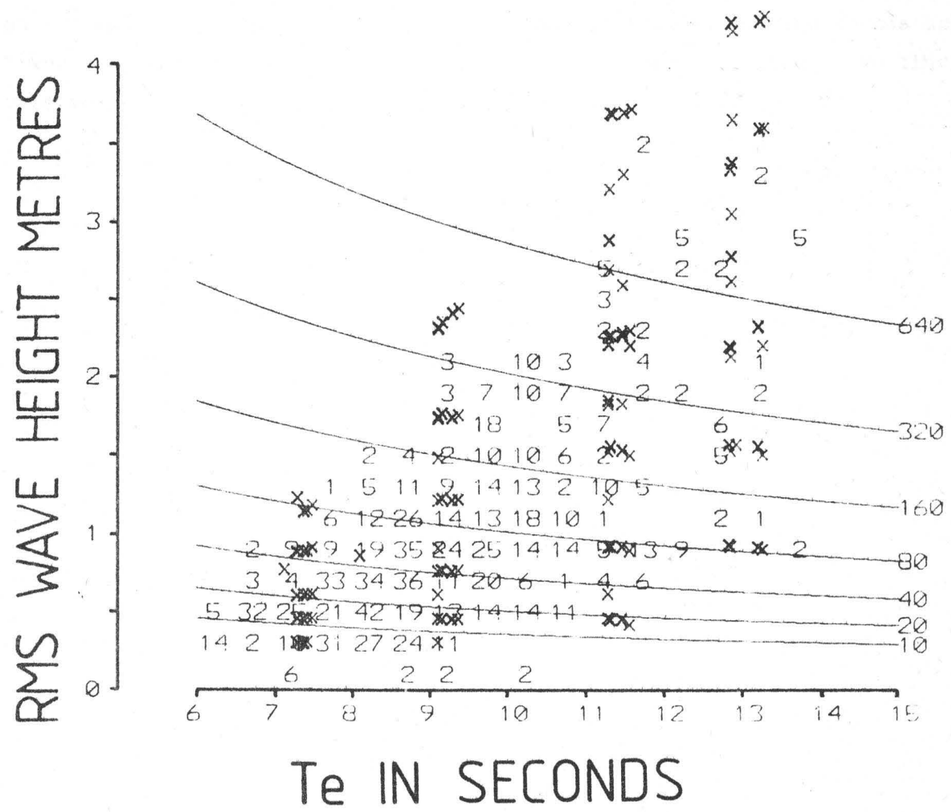

MAIN CONCLUSIONS

The major points noted in the tests were:

(1) Our simple force equation (see 2nd Year Report, page 2,2) survives random sea trials. The highest force coefficient recorded in this series is .79. The typical value for surge is .4 and for heave is .3.

(2) Duck power output is nearly independent of energy period in a random sea over the range tested. For a given RMS wave height, as the energy rises the power increase nearly balances the efficiency drop. On the fixed axis, a torque limit looks like a power limit. For example, a limit of 1 MNm/m of duck gives a mean power limit of 100 kW/m. A duck on a moving axis can get on average 20% more power with the same power limit because of better recovery from capsize.

(3) The biggest mooring force observed was 54 kN/m for a 15 metre full-scale duck on a fixed axis. But for models on the compliant axis, mooring forces are lower - typically 25 kN/m and they fall at large wave amplitude. We find this very encouraging.

SCATTER DIAGRAM TESTS IN THE NARROW TANK

MAJOR POINT 1: THE SIMPLE FORCE EQUATION SURVIVES

The opposite page shows all the force coefficients measured in the entire series of tests against RMS wave height.

Points include fixed and moving axis, RMS-derived and peak-derived values and all the energy periods. The coefficients greater than .5 in waves larger than 2 metres H_{rms} are for peak heave forces and occur only on a fixed axis (see page 2.52 for further explanation).

The two following pages show force coefficients for fixed and moving rig with the recommended torque limit (1 MNm/m).

ALL THE FORCE COEFFICIENTS

D0D19, wave scale for 15metre duck at INDIA (1/150)

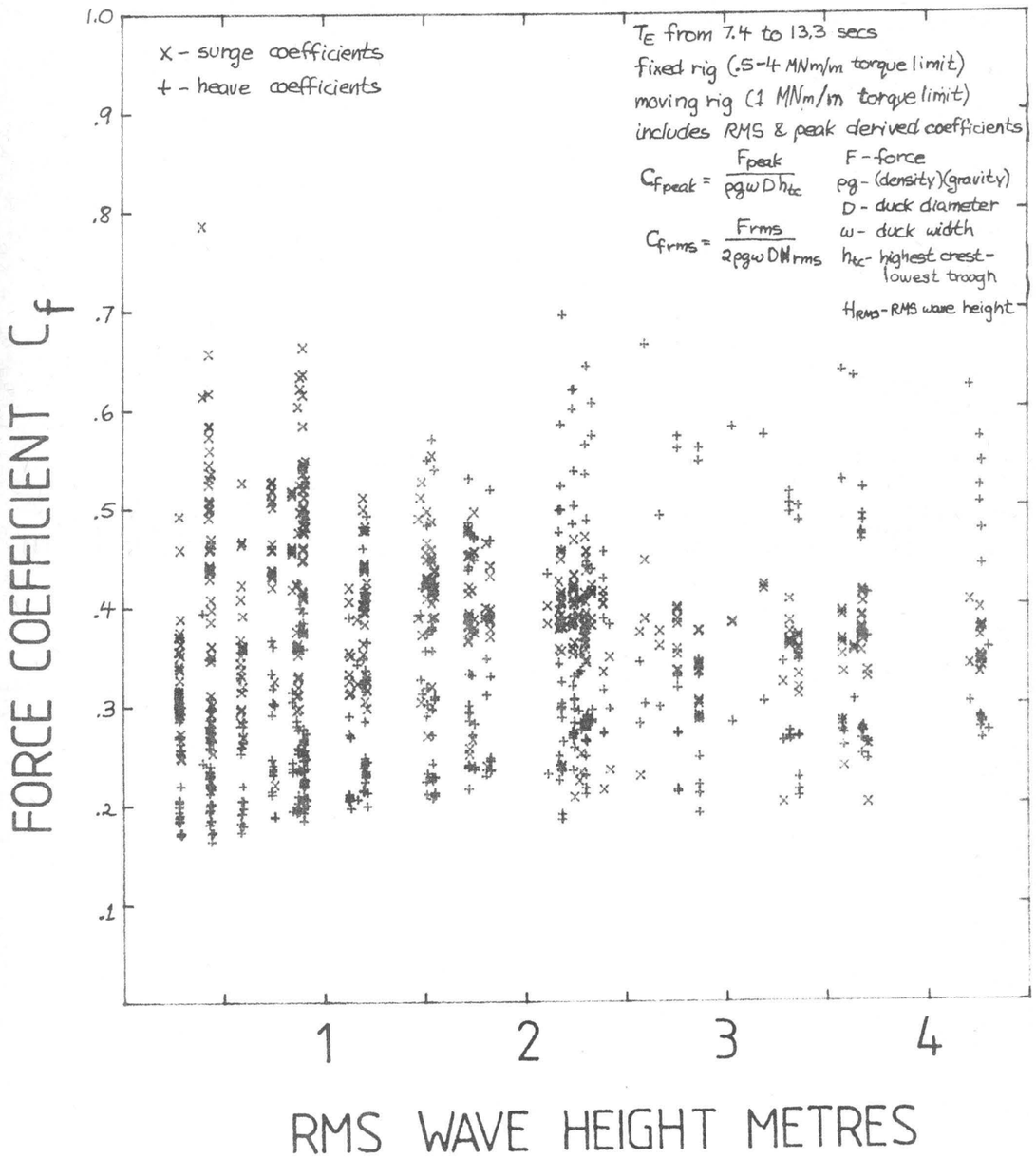

FORCE COEFFICIENTS ON FIXED AXES

DØØ19, assumed scale 1/150, 1 meganewton-metre/metre torque limit

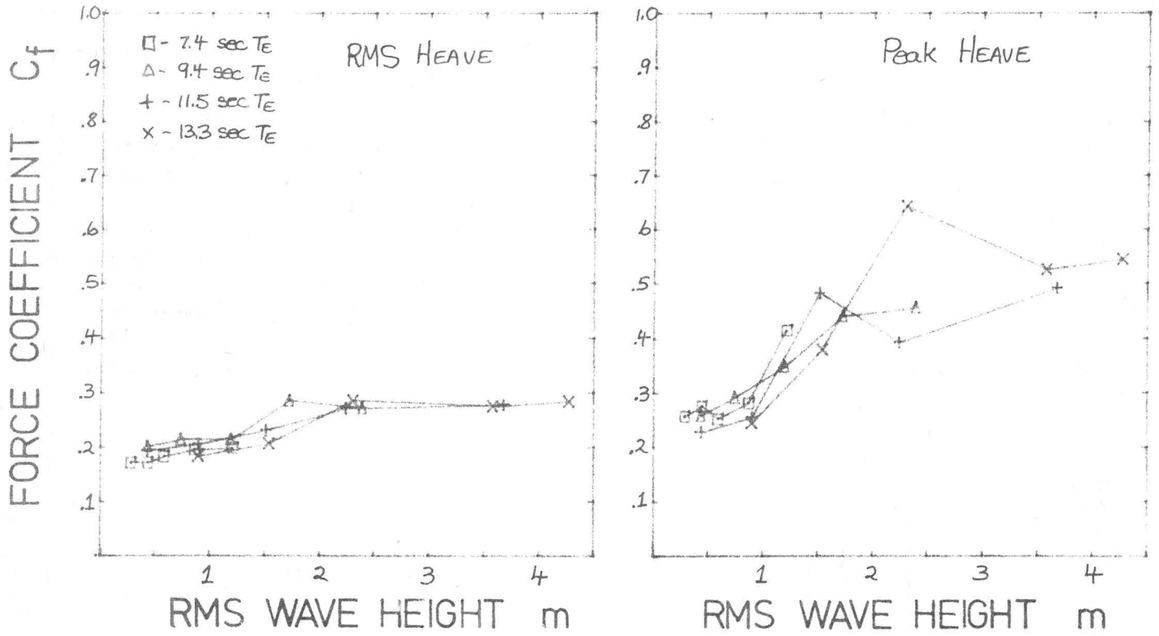

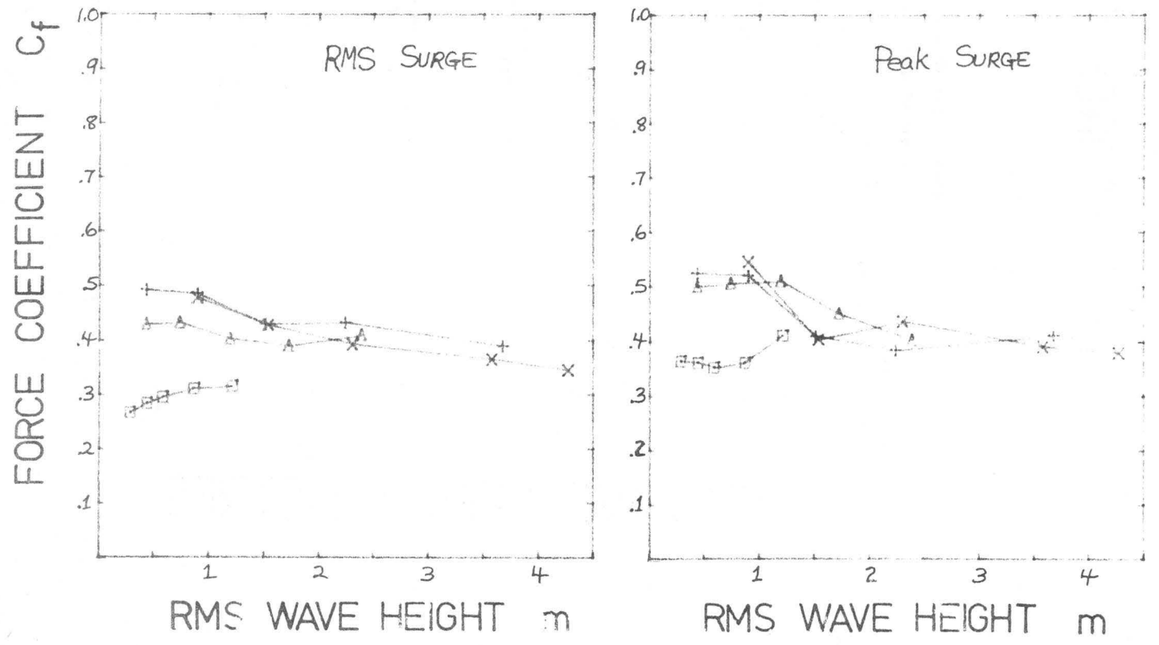

FORCE COEFFICIENTS ON MOVING AXES

DØØ19, assumed scale 1/150, 1 meganewton-metre/metre torque limit

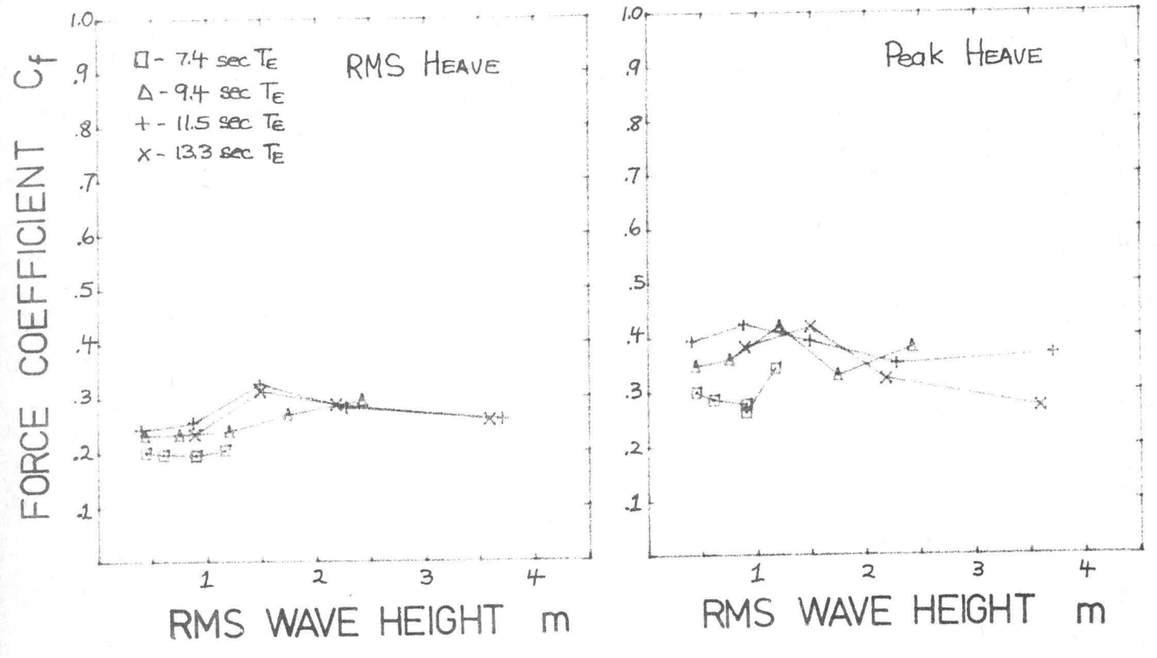

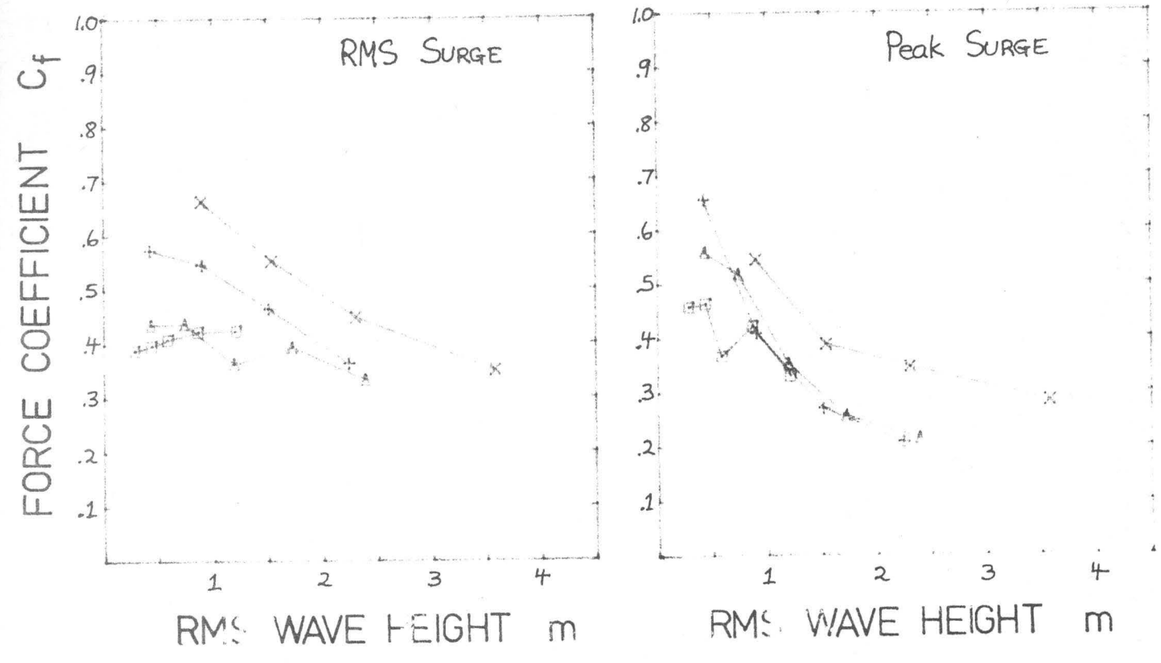

SCATTER DIAGRAM TESTS IN THE NARROW TANK

MAJOR POINT 2: DUCK POWER OUTPUT IS NEARLY INDEPENDENT OF T_e.

Scatter Diagram Tests

DUCK POWER

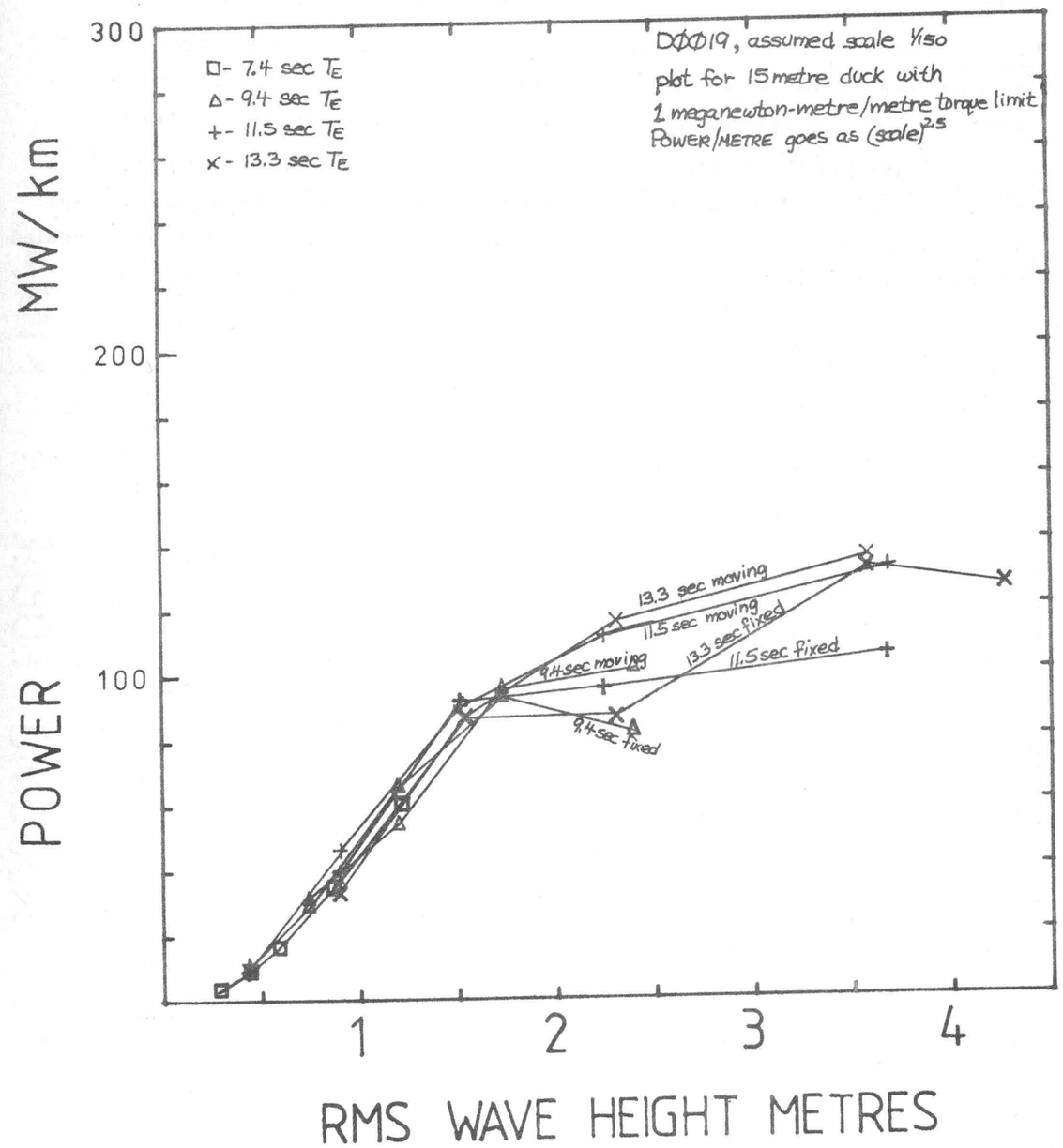

SCATTER DIAGRAM TESTS IN THE NARROW TANK

MAJOR POINT 3: MOORING FORCES ARE SMALL

The graph shows mooring force against H_{rms} for various energy periods on fixed and moving axes. Our mooring forces are measured as the long-term mean surge force on the assumption that there is a very low-rate mooring system.

The predicted values are so low that an intermediate mooring stiffness could be used to reduce surge excursions which might overstress the power cables. The lower values for the moving axis are caused by the transmission of waves behind the model, which occurs as soon as sufficient power has been taken.

MOORING FORCES ON FIXED AND MOVING AXES

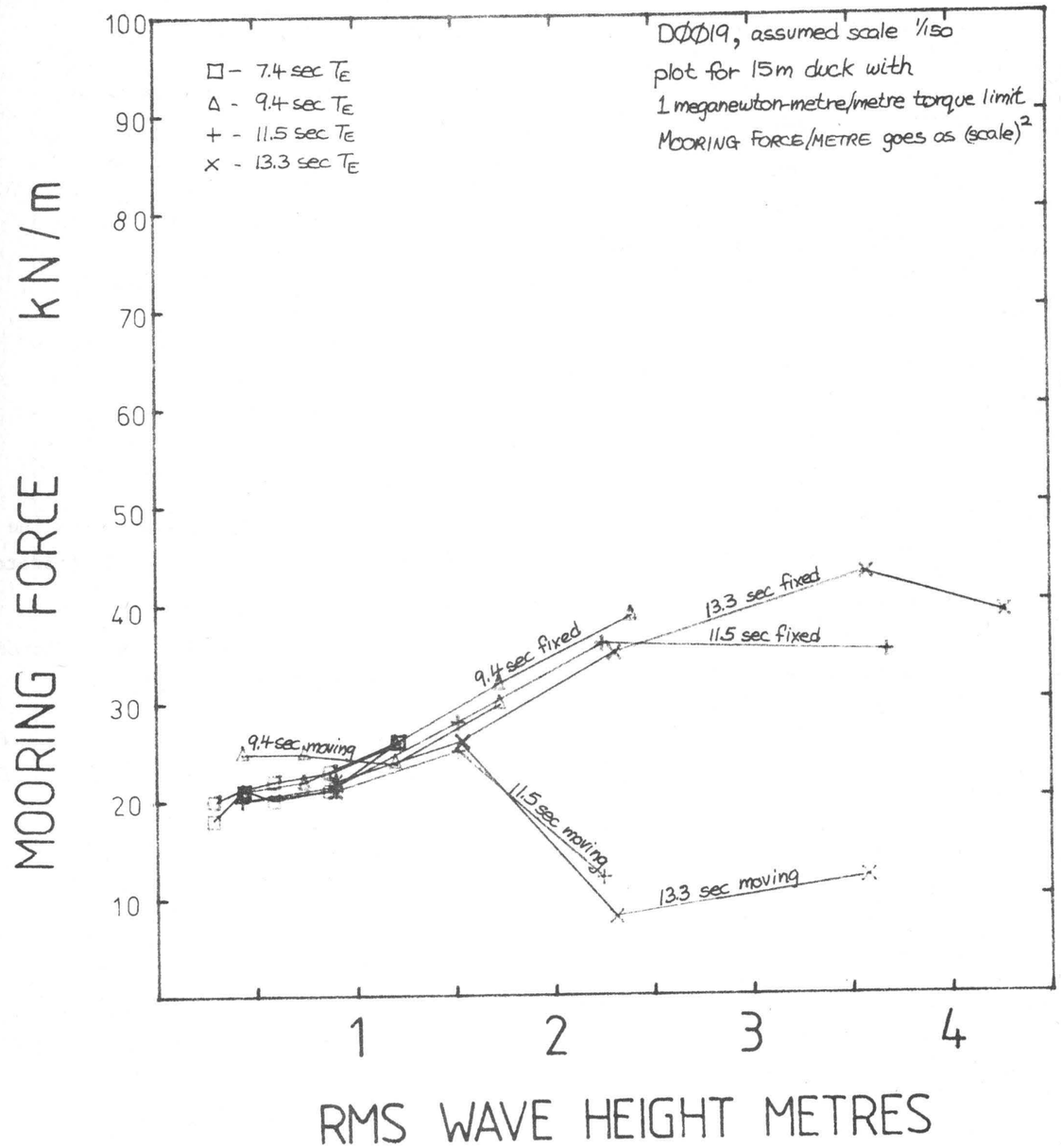

FULL-SCALE DESIGN VALUES

The values on the opposite page should give designers worst case data for calculations. The three following pages give typical working values for small medium and large seas. Each of the maxima is independent. Thus, for example, the maximum heave force coefficient does not necessarily come from the same test as the maximum heave force.

The table specifies, for each extreme value, the test conditions in which it was obtained.

H_{rms} = RMS wave height (metres)
T_e = energy period (seconds)
TLim = torque limit (MNm/m)
M/F = moving or fixed mounting
Test = test number

(The test number is included for our own reference.)

It should be noted that:

(1) the angle transducer is limited to a range of +1.4 to -.6 radians, and the angular range given is obtained from photographs and direct visual estimates;

(2) the peak/RMS ratio of waves in our tank is somewhat lower than is to be expected in the real sea and thus peak forces are probably better predicted using the RMS values and the Longuet-Higgins formula (see page 6.11).

PARAMETER	MAX. IN ALL TESTS						UNDER RECOMMENDED CONDITIONS MOVING RIG. 1MN/m TORQUE LIMIT			
	VALUE	TEST CONDITIONS					VALUE	TEST CONDITIONS		
		H_{rms}	T_e	TLim	M/F	Test		H_{rms}	T_e	Test
RMS WAVE AMPLITUDE (metres)	4.3	4.3	13.3	1	M	237	4.3	4.3	13.3	237
HIGHEST CREST-LOWEST TROUGH (metres)	24	4.3	13.3	1	M	90	24	4.3	13.3	90
SEA POWER (kilowatts/metre)	1950	4.3	13.3	1	M	237	1950	4.3	13.3	237
MEAN DUCK POWER (kilowatts/metre)	260	3.7	11.4	4	F	142	155	3.7	11.6	231
RMS DUCK ANGLE (radians)	.72	4.3	13.3	1	M	237	.72	4.3	13.3	327
DUCK ANGULAR RANGE (radians)	2.5 to -1.2	see opp. page					2.5 to -1.2	see opp. page		
RMS ANGULAR VELOCITY (radians/second)	.22	3.6	13.3	.5	F	129	.21	4.3	13.3	90
PEAK ANGULAR VELOCITY (radians/second)	.78	4.3	13.3	.5	F	131	.67	3.6	13.3	89
RMS DUCK TORQUE (Meganewton-metre/metre)	1.5	3.7	11.4	4	F	142	.94	3.6	13.3	71
PEAK TORQUE (Meganewton-metre/metre)	4.3	3.4	12.9	4	F	204	1.10	2.3	13.3	69
RMS HEAVE FORCE (kilonewtons/metre)	390	4.2	12.9	4	F	145	290	3.7	11.6	230
PEAK HEAVE FORCE (kilonewtons/metre)	2100	4.2	12.9	4	F	145	1340	3.7	11.6	231
RMS SURGE FORCE (kilonewtons/metre)	450	4.3	12.9	2	F	42	370	3.7	11.6	230
PEAK SURGE FORCE (kilonewtons/metre)	1400	4.3	12.9	1	F	21	840	3.7	11.6	230
SINKING FORCE (kilonewtons/metre)	360	4.3	12.9	2	F	42	155	3.7	11.6	230
MOORING FORCE (kilonewtons/metre)	54	4.3	12.9	3	F	58	31	1.75	9.4	223
RMS HEAVE FORCE COEFFICIENT	.33	1.5	11.6	1	M	227	.33	1.5	11.6	227
PEAK HEAVE FORCE COEFFICIENT	.69	2.2	11.4	4	F	166	.44	2.3	13.3	70
RMS SURGE FORCE COEFFICIENT	.66	.9	13.3	1	M	67	.66	.9	13.3	67
PEAK SURGE FORCE COEFFICIENT	.79	.4	11.6	1	M	225	.79	.4	11.6	225

FULL SCALE PARAMETERS

TYPICAL SMALL SEA (7.4 sec T_e)

	.5 MNm/m FIXED RIG TEST 113	1 MNm/m FIXED RIG TEST 93	RECOMMENDED CONDITIONS 1 MNm/m MOVING RIG TEST 74	2 MNm/m FIXED RIG TEST 24
RMS WAVE AMPLITUDE (metres)	.59	.59	.59	.59
HIGHEST CREST-LOWEST TROUGH (metres)	3.3	3.3	3.3	3.6
SEA POWER (kilowatts/metre)	20	20	20	20.5
MEAN DUCK POWER (kilowatts/metre)	15.5	17	17	18.5
EFFICIENCY (percent)	77	83	84	92
RMS DUCK ANGLE (radians)	.072	.062	.064	.064
DUCK ANGULAR RANGE (radians)	.46	.36	.34	.36
RMS ANGULAR VELOCITY (radians/second)	.055	.049	.049	.050
PEAK ANGULAR VELOCITY (radians/second)	.175	.15	.13	.145
RMS DUCK TORQUE (Meganewtons-metres/metre)	.28	.34	.34	.38
PEAK TORQUE (Meganewton-metres/metre)	.54	.95	.86	1.10
RMS HEAVE FORCE (kilonewtons/metre)	31	33	41	37
PEAK HEAVE FORCE (kilonewtons/metre)	170	127	160	140
RMS SURGE FORCE (kilonewtons/metre)	51	53	73	56
PEAK SURGE FORCE (kilonewtons/metre)	175	177	185	185
SINKING FORCE (kilonewtons/metre)	30	26	22	24
MOORING FORCE (kilonewtons/metre)	24	22	20	22
RMS HEAVE FORCE COEFFICIENT	.175	.185	.23	.205
PEAK HEAVE FORCE COEFFICIENT	.33	.25	.31	.26
RMS SURGE FORCE COEFFICIENT	.285	.30	.41	.31
PEAK SURGE FORCE COEFFICIENT	.34	.35	.37	.34

TYPICAL MEDIUM SEA

	Te=9.4 sec .5 MNm/m FIXED RIG TEST 118	Te=9.4 sec 1 MNm/m FIXED RIG TEST 98	Te=9.4 sec RECOMMENDED CONDITIONS 1 MNm/m MOVING RIG TEST 79	Te=9.2 sec 2 MNm/m FIXED RIG TEST 30	Te=9.2 sec 3 MNm/m FIXED RIG TEST 46
RMS WAVE AMPLITUDE (metres)	1.2	1.2	1.2	1.2	1.2
HIGHEST CREST-LOWEST TROUGH (metres)	5.9	5.9	6.0	6.3	6.3
SEA POWER (kilowatts/metre)	105	105	105	105	105
MEAN DUCK POWER (kilowatts/metre)	50	66	55	77	79
EFFICIENCY (percent)	48	63	52	74	75
RMS DUCK ANGLE (radians)	.225	.175	.155	.16	.155
DUCK ANGULAR RANGE (radians)	1.35	1.0	.89	.87	.83
RMS ANGULAR VELOCITY (radians/second)	.135	.11	.096	.10	.10
PEAK ANGULAR VELOCITY (radians/second)	.48	.38	.33	.31	.29
RMS DUCK TORQUE (Meganewton-metres/metre)	.41	.62	.58	.76	.79
PEAK TORQUE (Meganewton-metres/metre)	.55	1.05	1.05	2.0	2.3
RMS HEAVE FORCE (kilonewtons/metre)	86	77	78	84	85
PEAK HEAVE FORCE (kilonewtons/metre)	410	310	290	300	310
RMS SURGE FORCE (kilonewtons/metre)	145	145	130	150	150
PEAK SURGE FORCE (kilonewtons/metre)	450	460	320	450	460
SINKING FORCE (kilonewtons/metre)	57	47	38	47	44
MOORING FORCE (kilonewtons/metre)	27	26	24	28	28
RMS HEAVE FORCE COEFFICIENT	.24	.21	.215	.23	.235
PEAK HEAVE FORCE COEFFICIENT	.46	.35	.32	.32	.32
RMS SURGE FORCE COEFFICIENT	.40	.40	.36	.41	.41
PEAK SURGE FORCE COEFFICIENT	.50	.51	.35	.48	.48

TYPICAL LARGE SEA

	Te=13.3 sec	Te=13.3 sec	Te-13.3 sec	Te=12.9 sec	Te=12.9sec
			RECOMMENDED CONDITIONS		
	.5 MNm/m FIXED RIG TEST 129	1 MNm/m FIXED RIG TEST 109	1 MNm/m MOVING RIG TEST 71	2 MNm/m FIXED RIG TEST 41	3 MNm/m FIXED RIG TEST 57
RMS WAVE AMPLITUDE (metres)	3.6	3.6	3.6	3.3	3.3
HIGHEST CREST-LOWEST TROUGH (metres	18.5	18.5	20	18.5	18.5
SEA POWER (kilowatts/metre)	1350	1350	1350	1100	1100
MEAN DUCK POWER (kilowatts/metre)	80	130	135	210	225
EFFICIENCY (percent)	6	10	10	19	20
RMS DUCK ANGLE (radians)	.59	.59	.64	.55	.54
DUCK ANGULAR RANGE (radians)	2.5*	2.4*	2.2*	2.4*	2.3*
RMS ANGULAR VELOCITY (radians /second)	.22	.20	.19	.18	.17
PEAK ANGULAR VELOCITY (radians/second)	.74	.68	.62	.65	.57
RMS DUCK TORQUE (Meganewton-metres/metre)	.43	.73	.76	1.15	1.3
PEAK TORQUE (Meganewton-metres/metre)	.55	1.05	1.05	2.05	3.1
RMS HEAVE FORCE (kilonewtons/metre)	310	300	280	270	275
PEAK HEAVE FORCE (kilonewtons/metre)	1800	1450	820	1400	1450
RMS SURGE FORCE (kilonewtons/metre)	390	400	360	360	360
PEAK SURGE FORCE (kilonewtons/metre)	1100	1100	720	1050	1050
SINKING FORCE (kilonewtons/metre)	275	280	150	225	230
MOORING FORCE (kilonewtons/metre)	45	43	25	45	43
RMS HEAVE FORCE COEFFICIENT	.285	.275	.26	.27	.275
PEAK HEAVE FORCE COEFFICIENT	.64	.53	.27	.50	.52
RMS SURGE FORCE COEFFICIENT	.36	.37	.33	.36	.36
PEAK SURGE FORCE COEFFICIENT	.40	.39	.245	.37	.39

* possible over-range

DETAILED RESULTS OF SCATTER DIAGRAM TESTS

POWER OUTPUT

Duck power output is nearly independent of energy period T_e. A torque limit on the fixed rig causes the duck power output in kW/m to level off at about 100 times the torque limit in MNm/m (for a 15 metre duck). The moving rig results show an additional 30% of output for the same torque limit due to faster recovery from capsize. The power output on the fixed rig was nearly the same as on the moving rig, up to the torque limit.

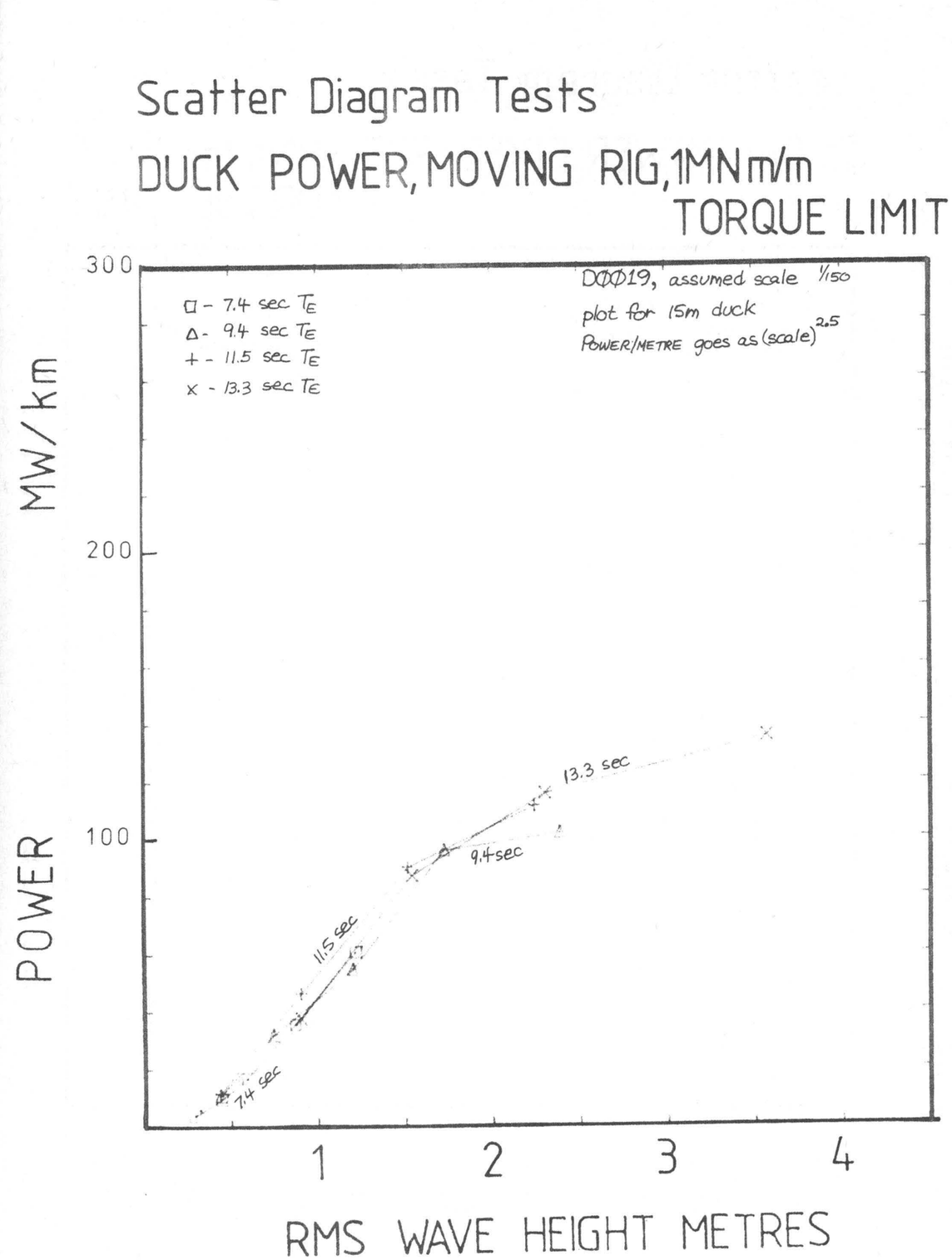

Scatter Diagram Tests

DUCK POWER, FIXED RIG, ·5MNm/m TORQUE LIMIT

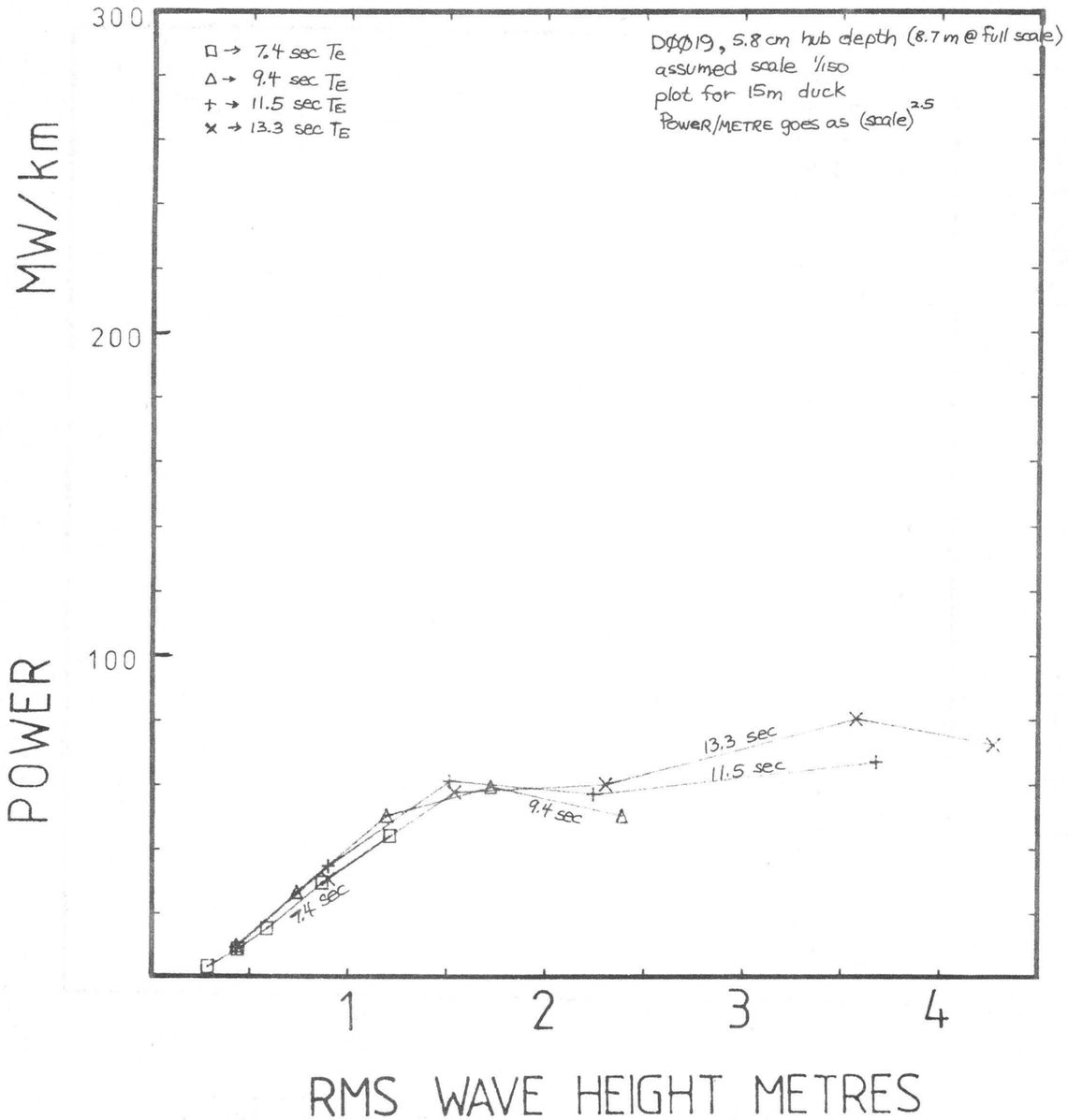

Scatter Diagram Tests

DUCK POWER, FIXED RIG, 1MNm/m TORQUE LIMIT

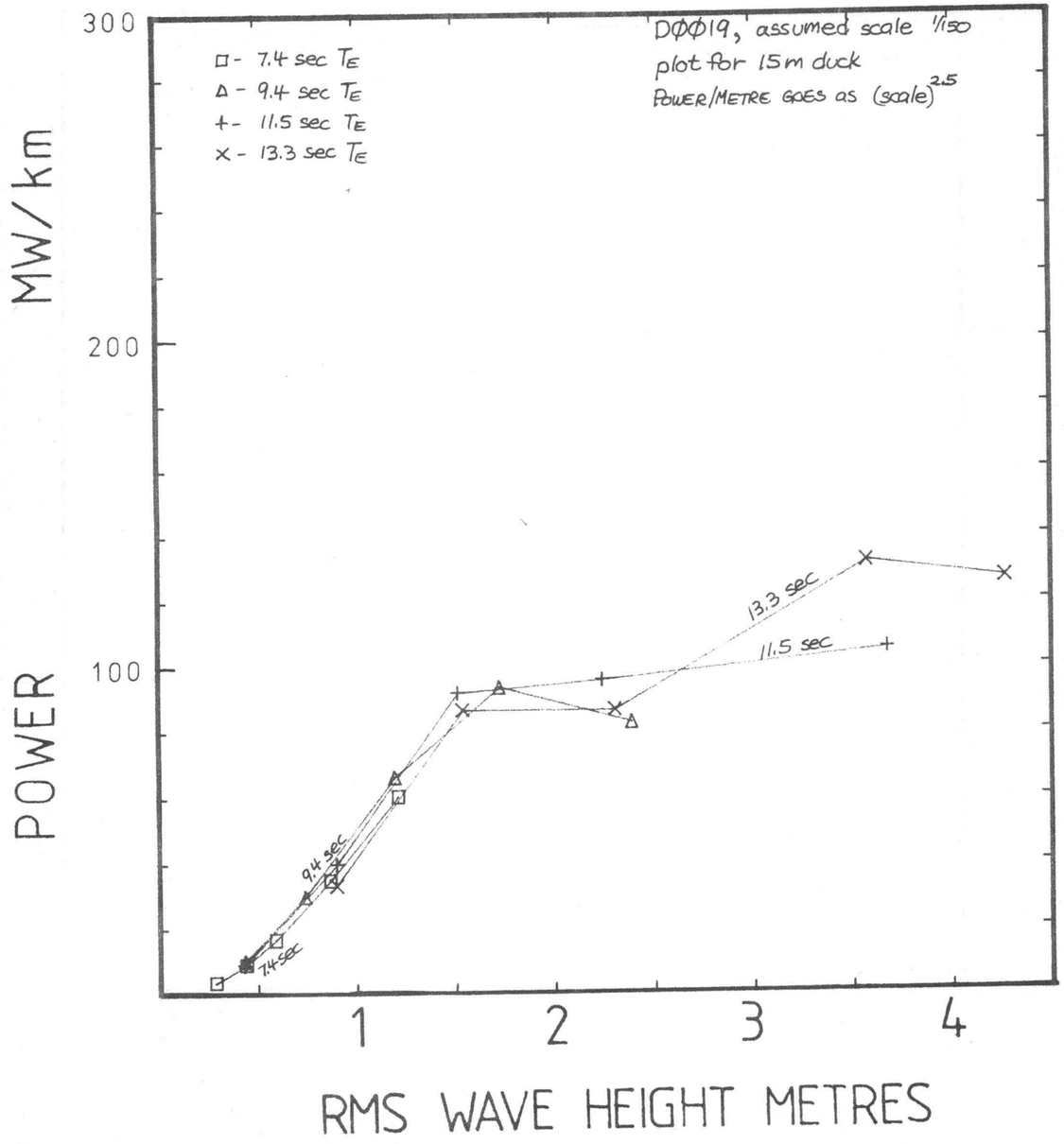

Scatter Diagram Tests

DUCK POWER, FIXED RIG, 2MNm/m TORQUE LIMIT

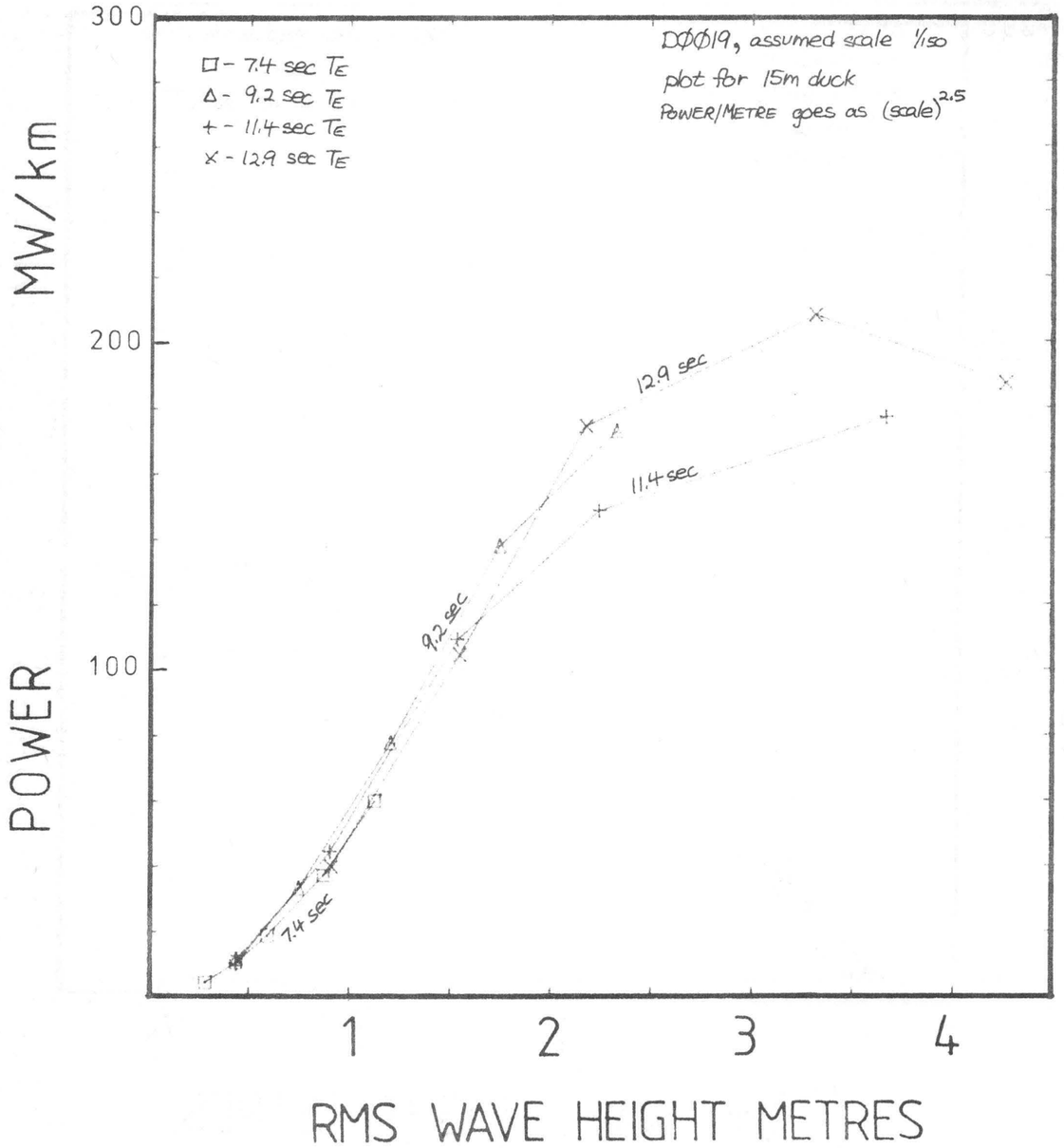

Scatter Diagram Tests

DUCK POWER, FIXED RIG, 3MNm/m TORQUE LIMIT

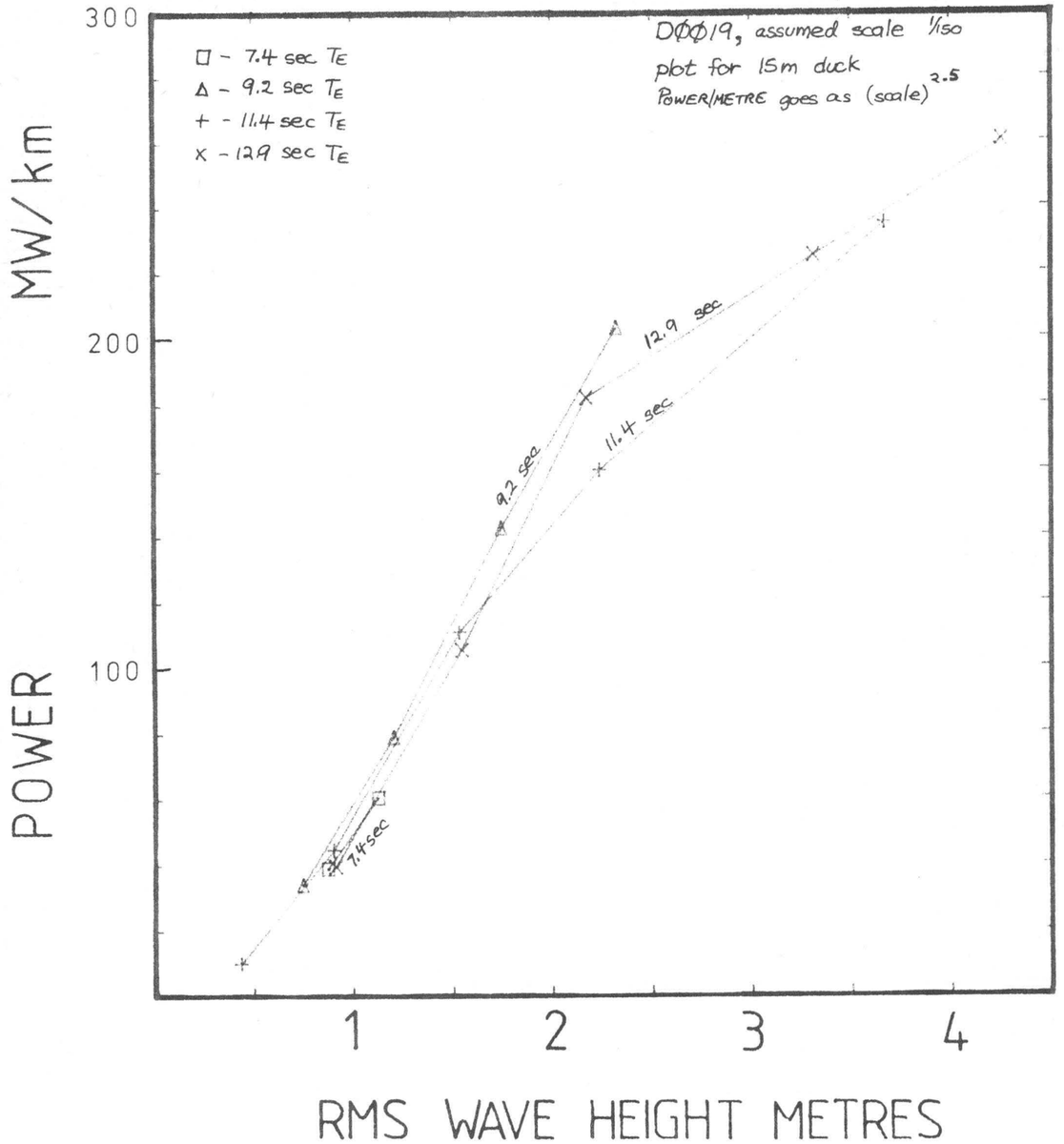

Scatter Diagram Tests
DUCK POWER, FIXED RIG

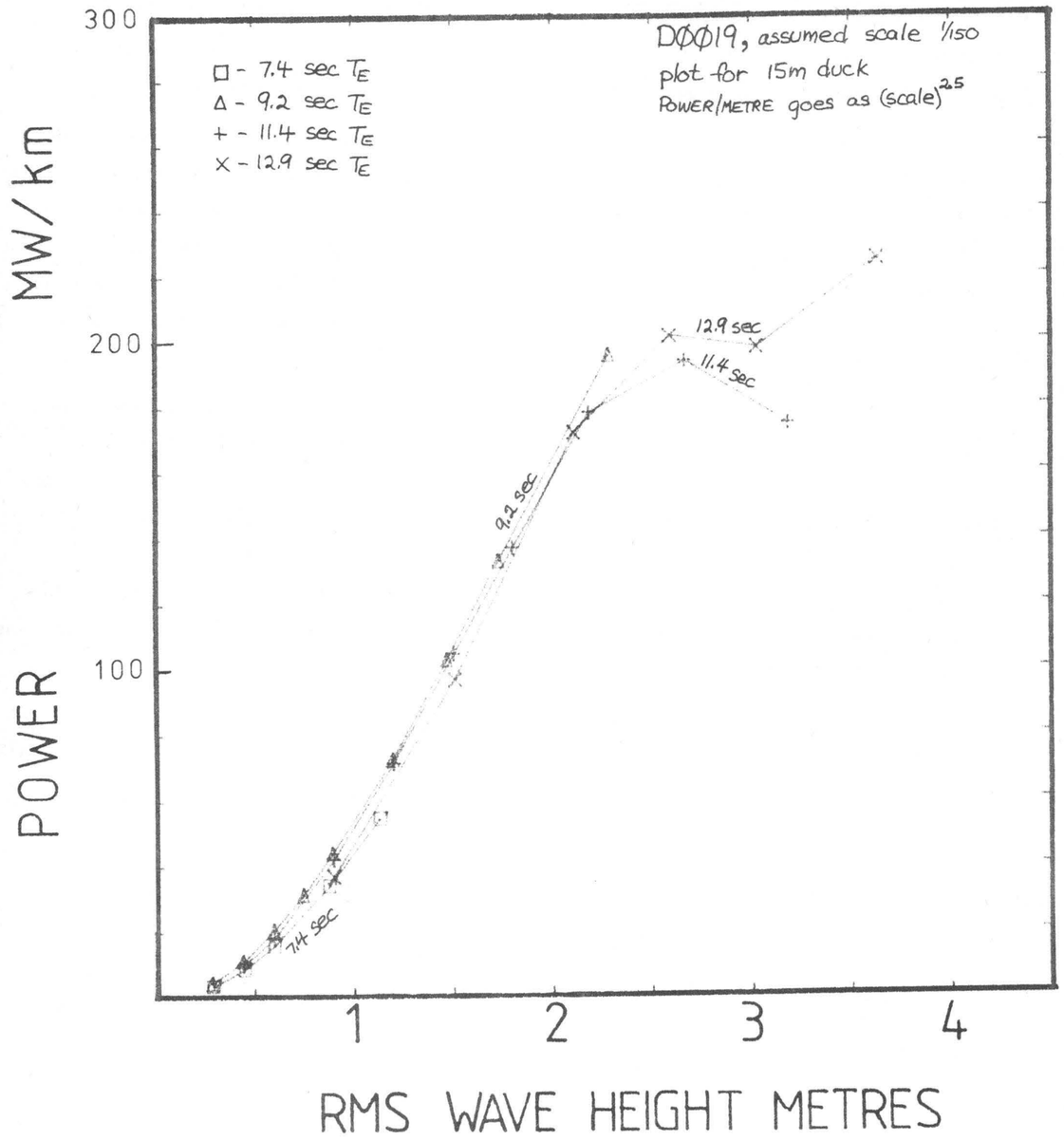

EFFICIENCY

This is the one parameter that varied significantly with energy period. In general, the 7.4 second seas gave the highest efficiencies (around 85%).

The very high readings shown on page 2.28 call for some comment. We analyse results as the tests are carried out and these trials were repeated eight times. The sea was also re-measured and no large errors were discovered. We remain dubious about the results but offer the following explanation.

Most efficiency curves show a drop in performance below .5 metre RMS amplitude for which there is no hydrodynamic explanation. It is almost certainly caused by bearing friction in the model mounting. This could easily amount to several milliwatts at model scale, and is not accounted for in efficiency calculations. The very high efficiency curves do not show this fall off and so it may be that for this test the model was assembled with its bearings very well aligned, giving less friction than usual.

As the energy period increased, the efficiency dropped. It is notable that the efficiency drop was nearly matched by the rise in power in the sea (at the same amplitude), thus making the duck power output dependent only on the RMS wave amplitude. As the wave height increased, the efficiency dropped, with each drop starting around H_{rms} = .5 metre for the torque limits of 0.5 MNm/m and H_{rms} = 1 metre for torque limits of 1 MNm/m and above. Efficiencies on the moving rig were somewhat higher than on the fixed rig for the 9 and 11 second seas, at low amplitudes but the drop-off started sooner.

Scatter Diagram Tests

DUCK EFFICIENCY, MOVING RIG, 1MNm/m TORQUE LIMIT

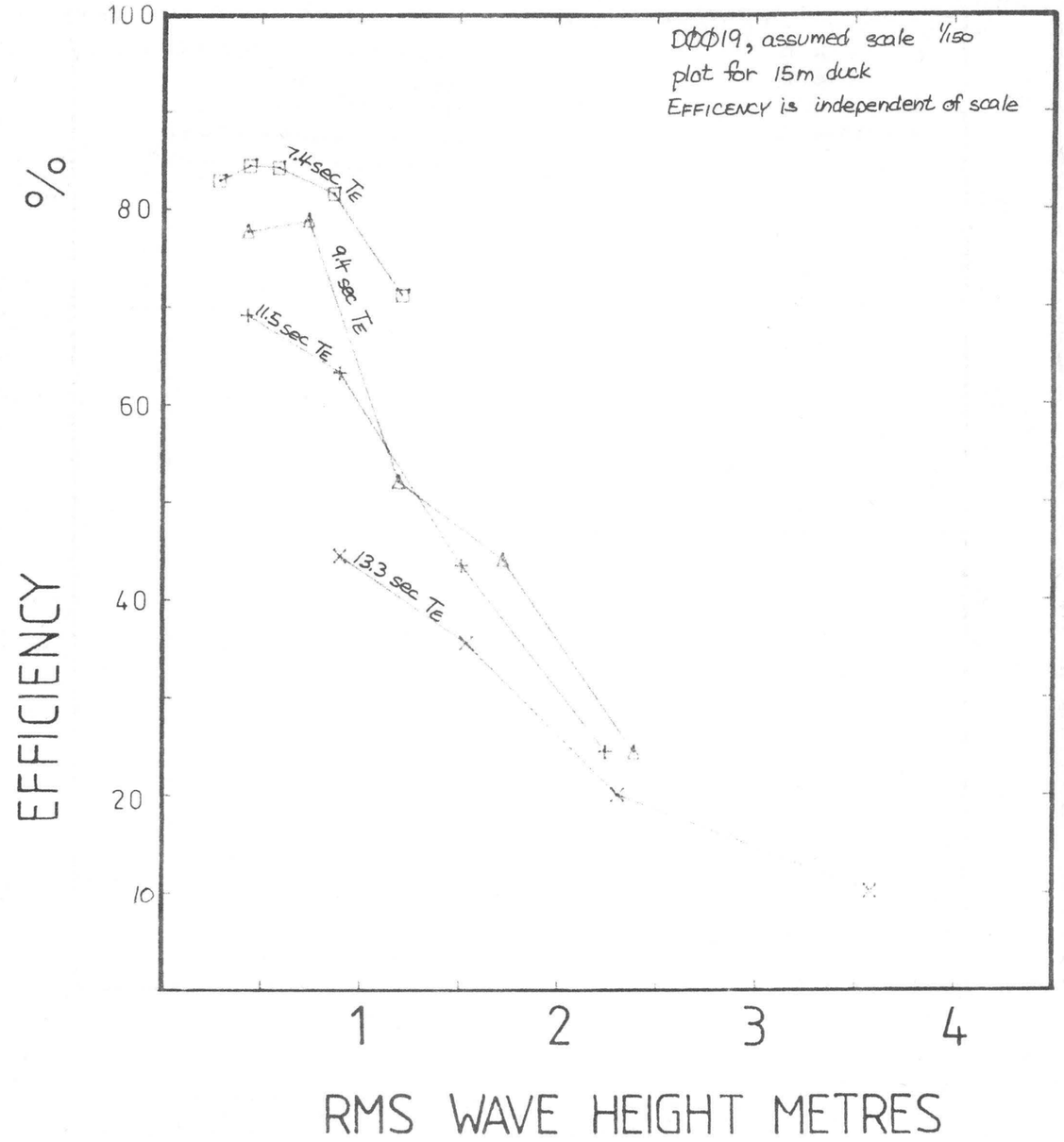

Scatter Diagram Tests

EFFICIENCY, FIXED RIG, ·5MNm/m TORQUE LIMIT

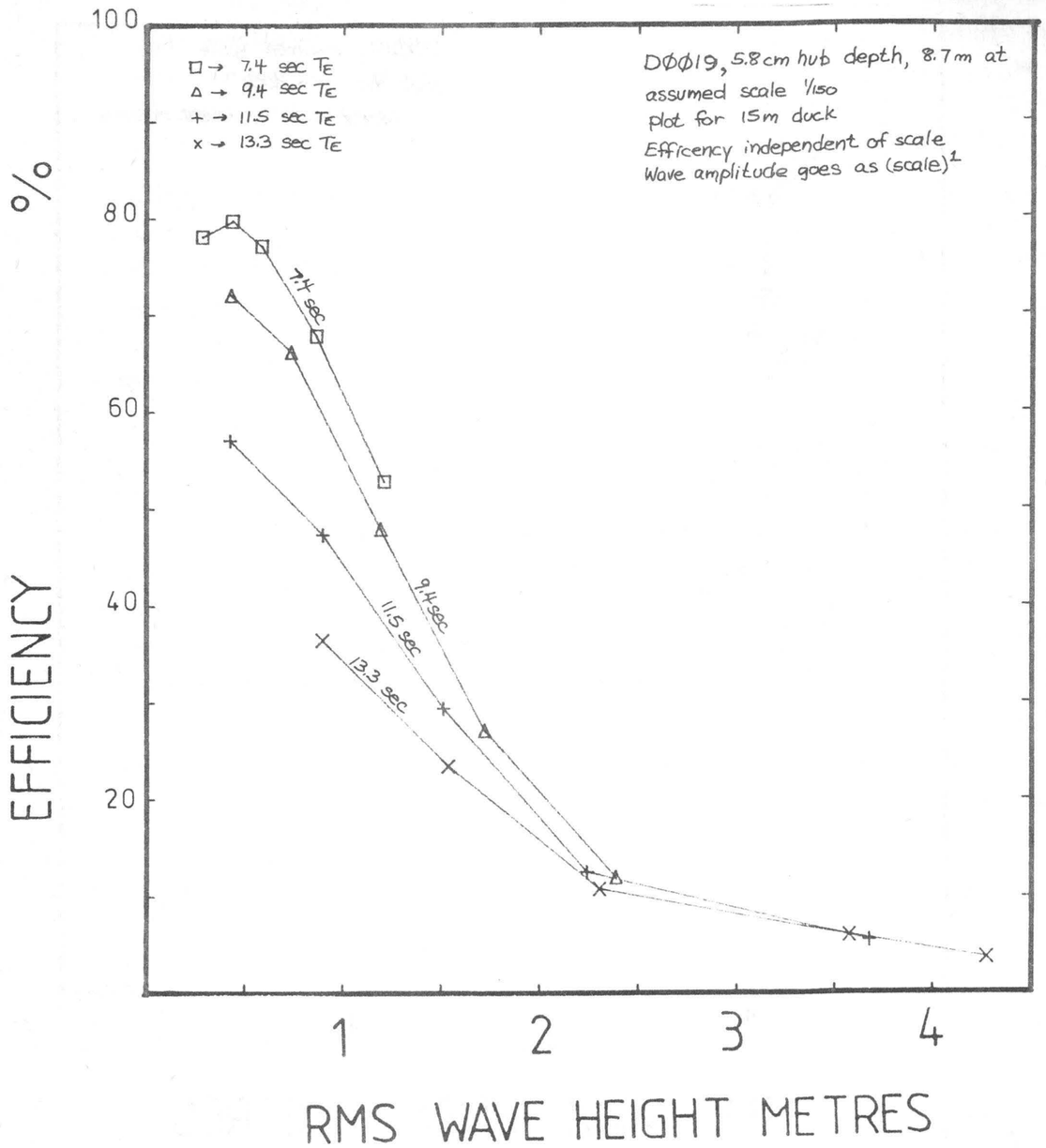

Scatter Diagram Tests

DUCK EFFICIENCY, FIXED RIG, 1MNm/m TORQUE LIMIT

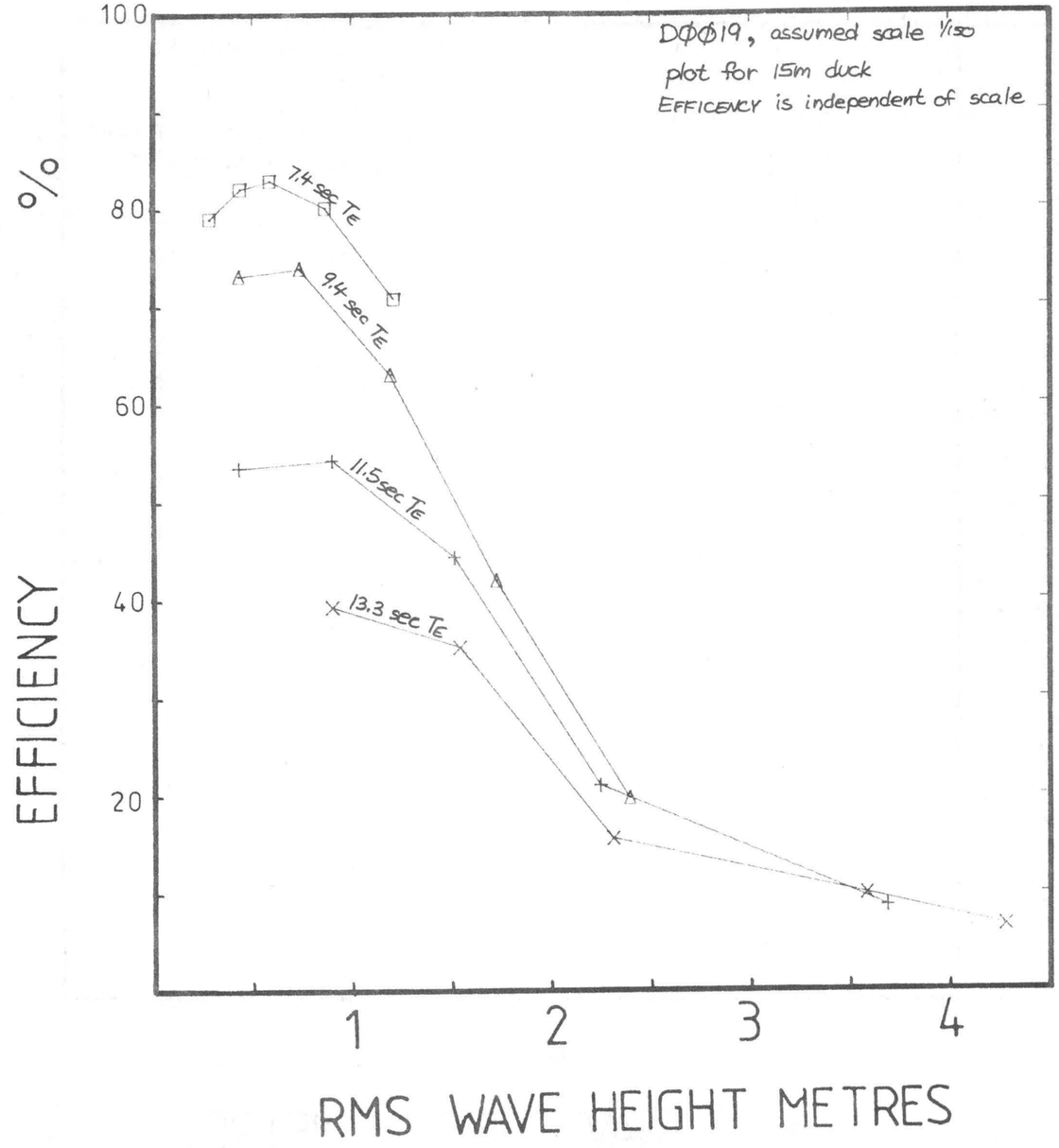

Scatter Diagram Tests

EFFICIENCY, FIXED RIG, 2MNm/m TORQUE LIMIT

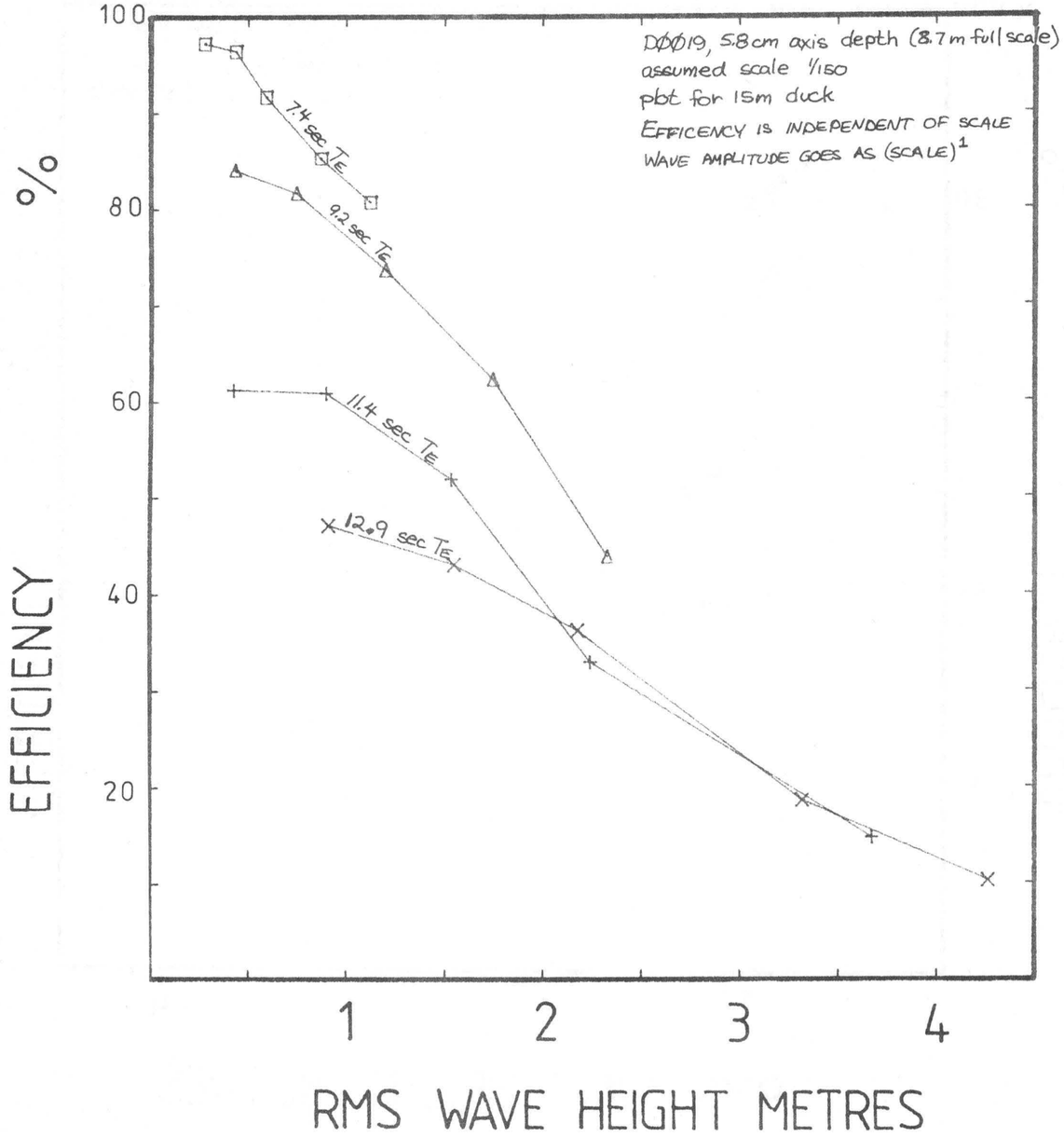

Scatter Diagram Tests

DUCK EFFICIENCY, FIXED RIG, 3MNm/m TORQUE LIMIT

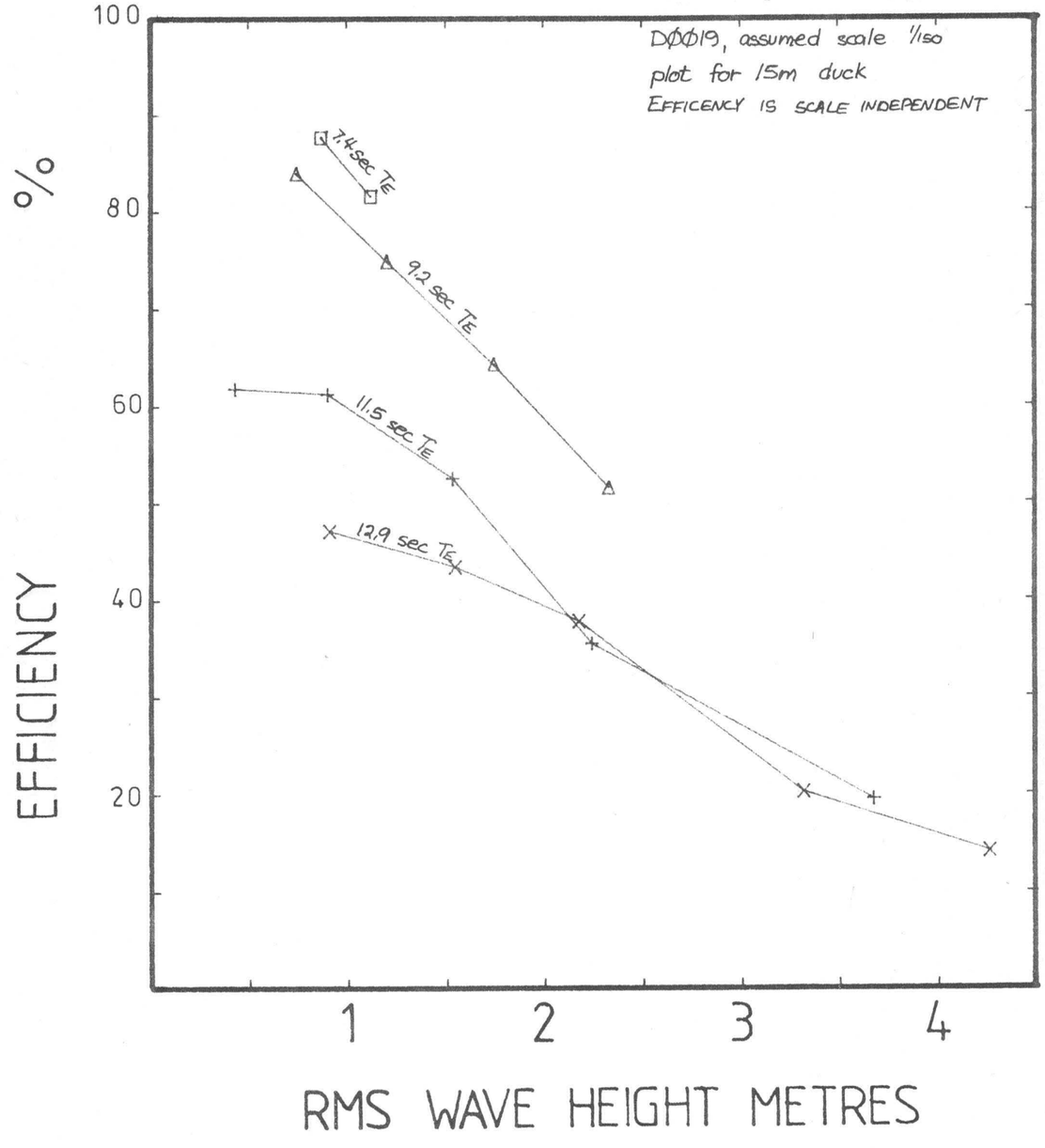

Scatter Diagram Tests
DUCK EFFICIENCY, FIXED RIG

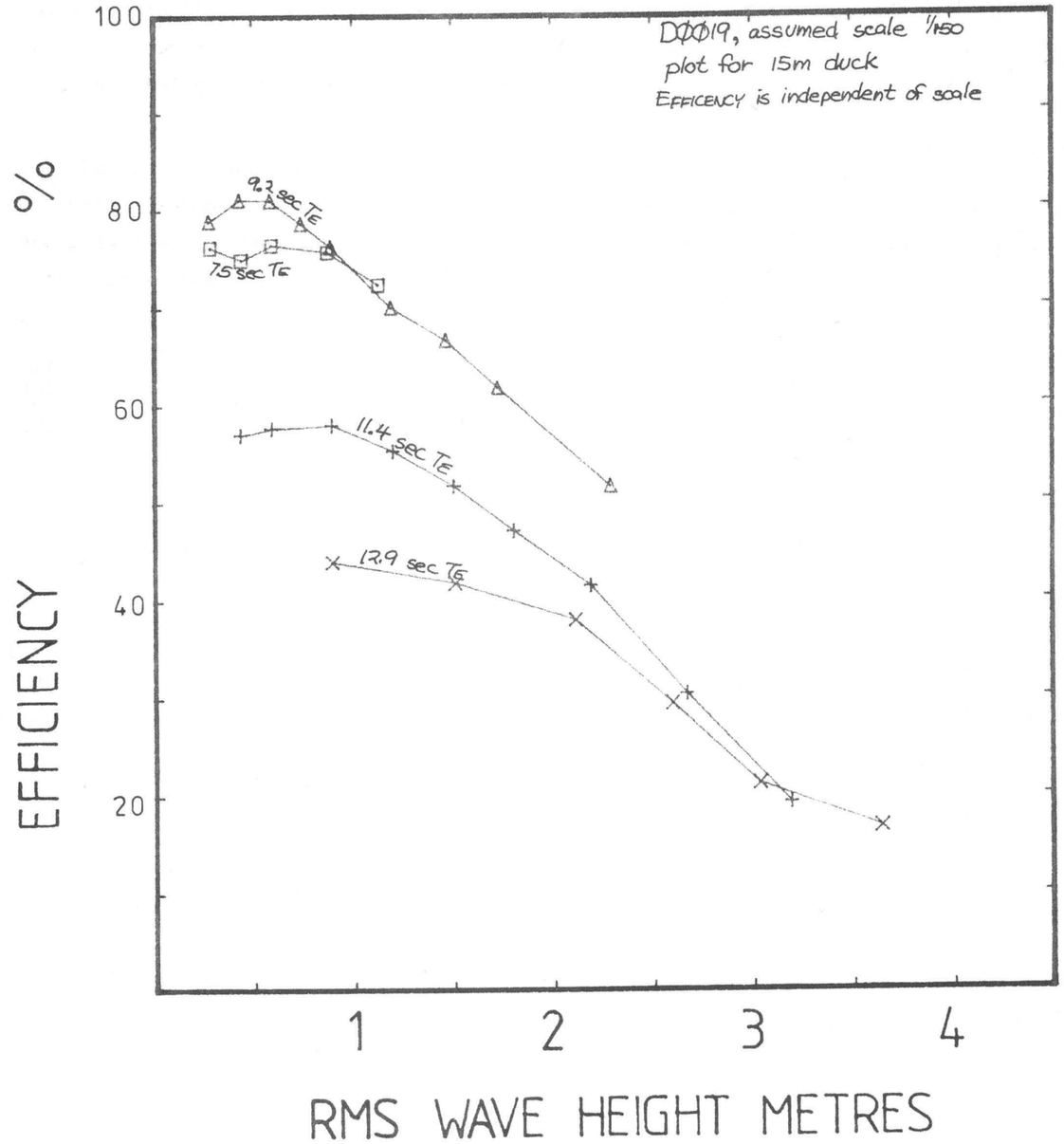

DUCK ANGLE

Duck angle varies considerably with energy period, the shortest seas giving about 50% less RMS angle than the longest ones. The RMS angle levels off at about 0.6 radians for all torque limits. The levelling-off happens at about H_{rms} = 2 metres for all tests, with the higher torque limits levelling off more slowly. The moving rig gives RMS angles similar to those on the fixed rig. The biggest difference is in the largest seas, where the moving rig angles are about 20% less.

Peak duck angles should not be considered reliable beyond 1.2 radian, which is the maximum angle for reasonable signals from the transducer. From photographic and "eyeball" inspection, we believe the angle of the duck will not go beyond the range +2.5 to -1.2 radians in any sea. (Positive angles put the duck over on its back.)

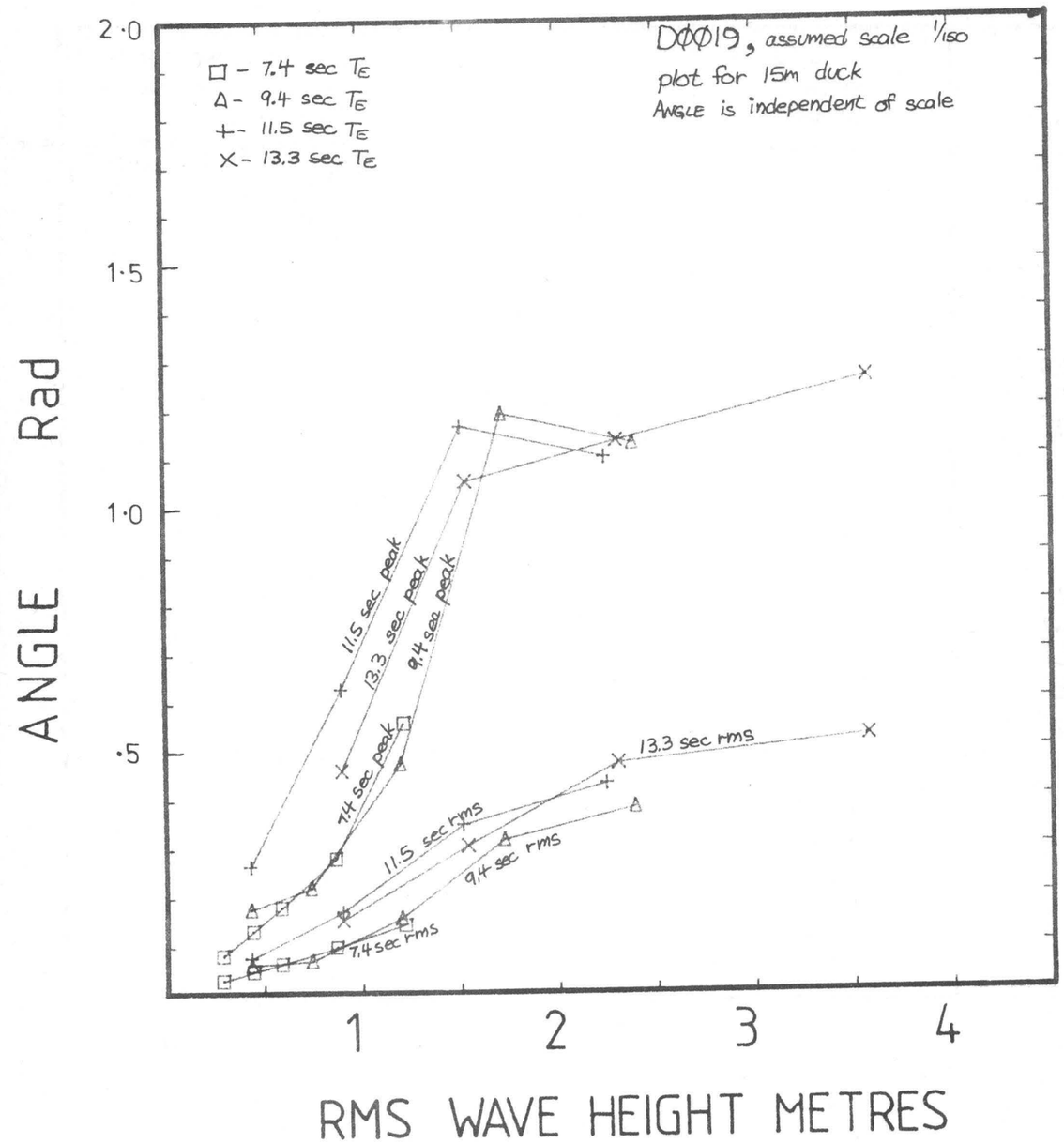

Scatter Diagram Tests

DUCK ANGLE, FIXED RIG, ·5MNm/m TORQUE LIMIT

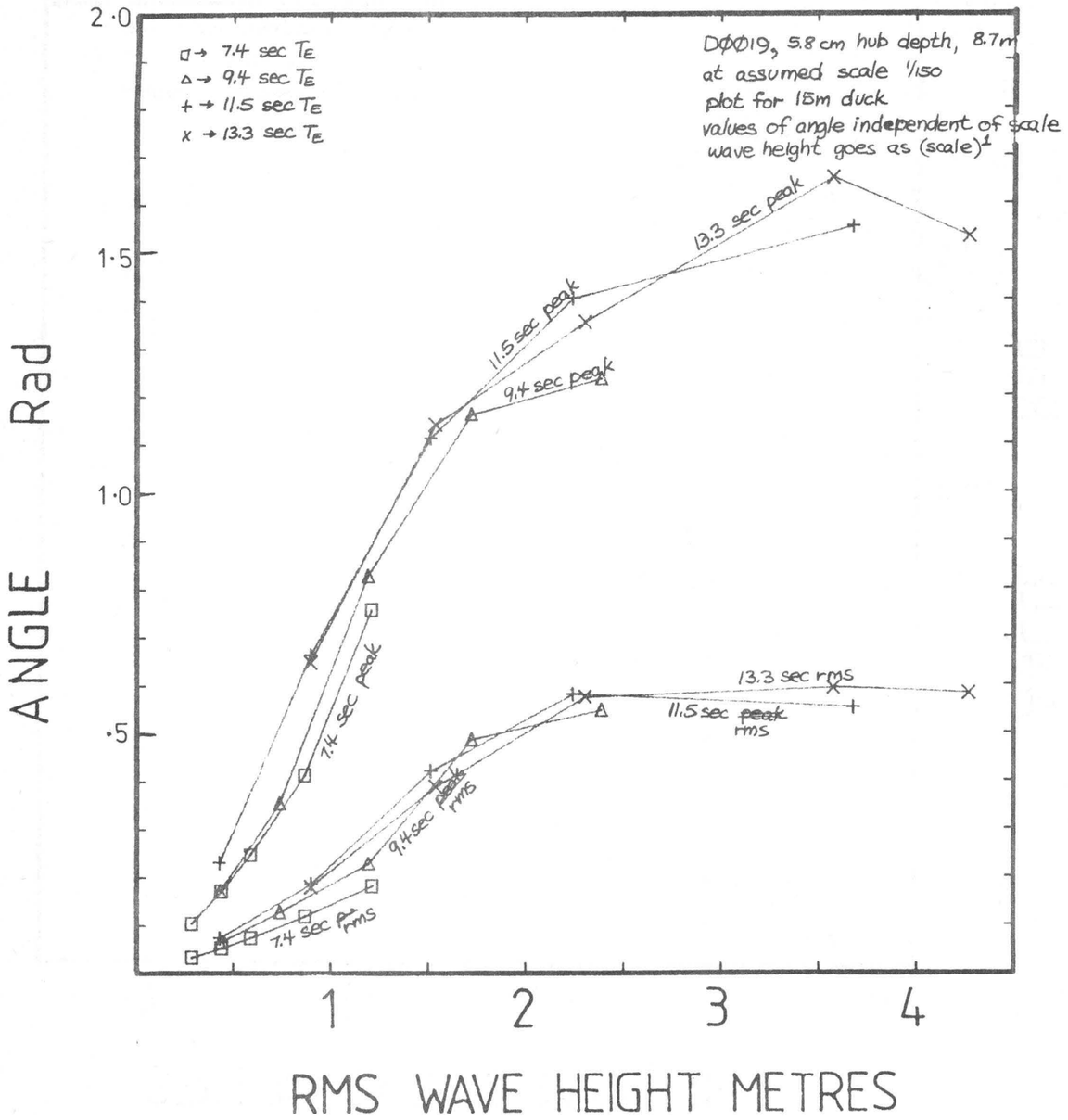

Scatter Diagram Tests

DUCK ANGLE, FIXED RIG, 1MNm/m TORQUE LIMIT

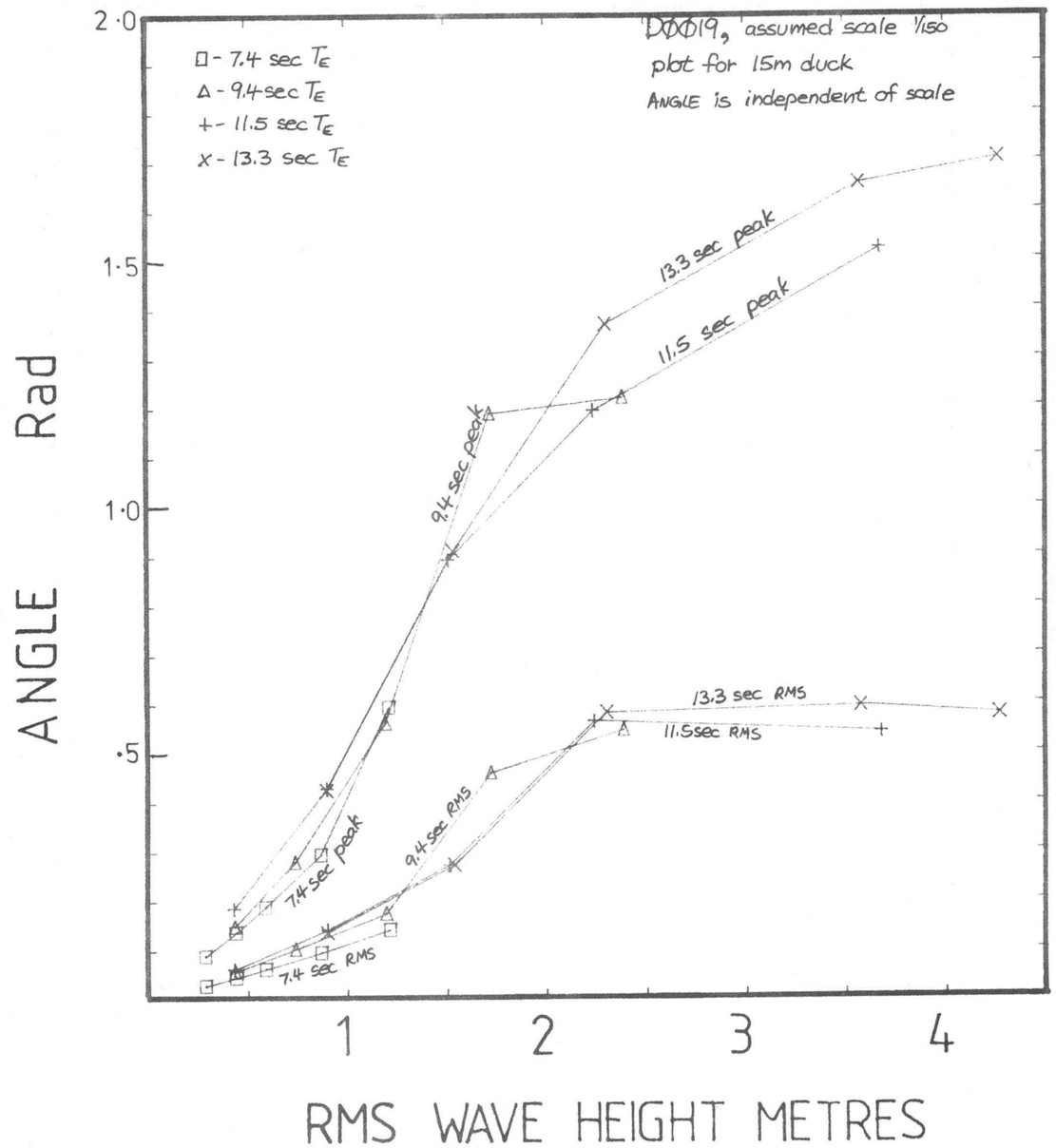

Scatter Diagram Tests

DUCK ANGLE, FIXED RIG, 2MNm/m TORQUE LIMIT

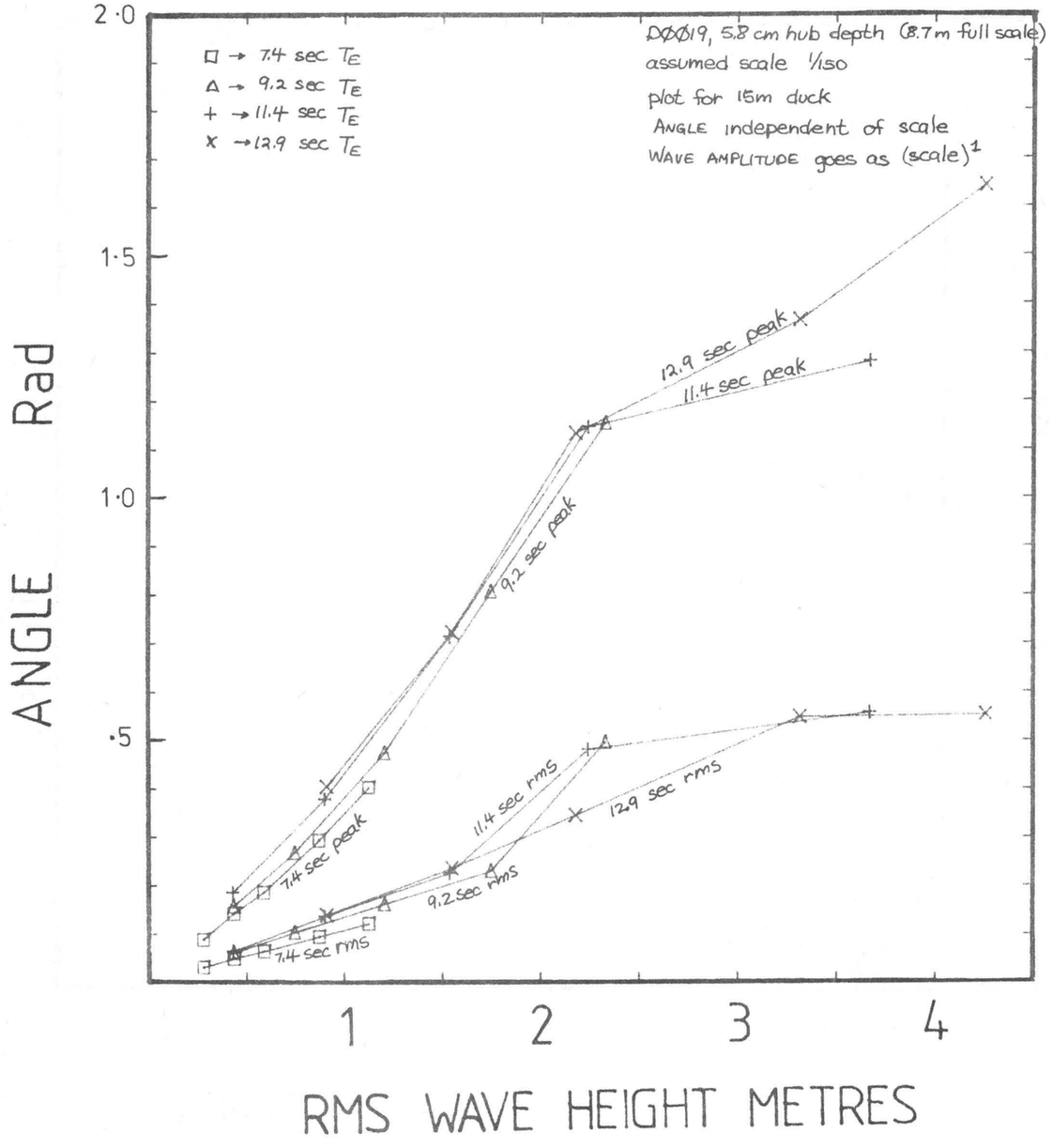

Scatter Diagram Tests

DUCK ANGLE, FIXED RIG, 3MNm/m TORQUE LIMIT

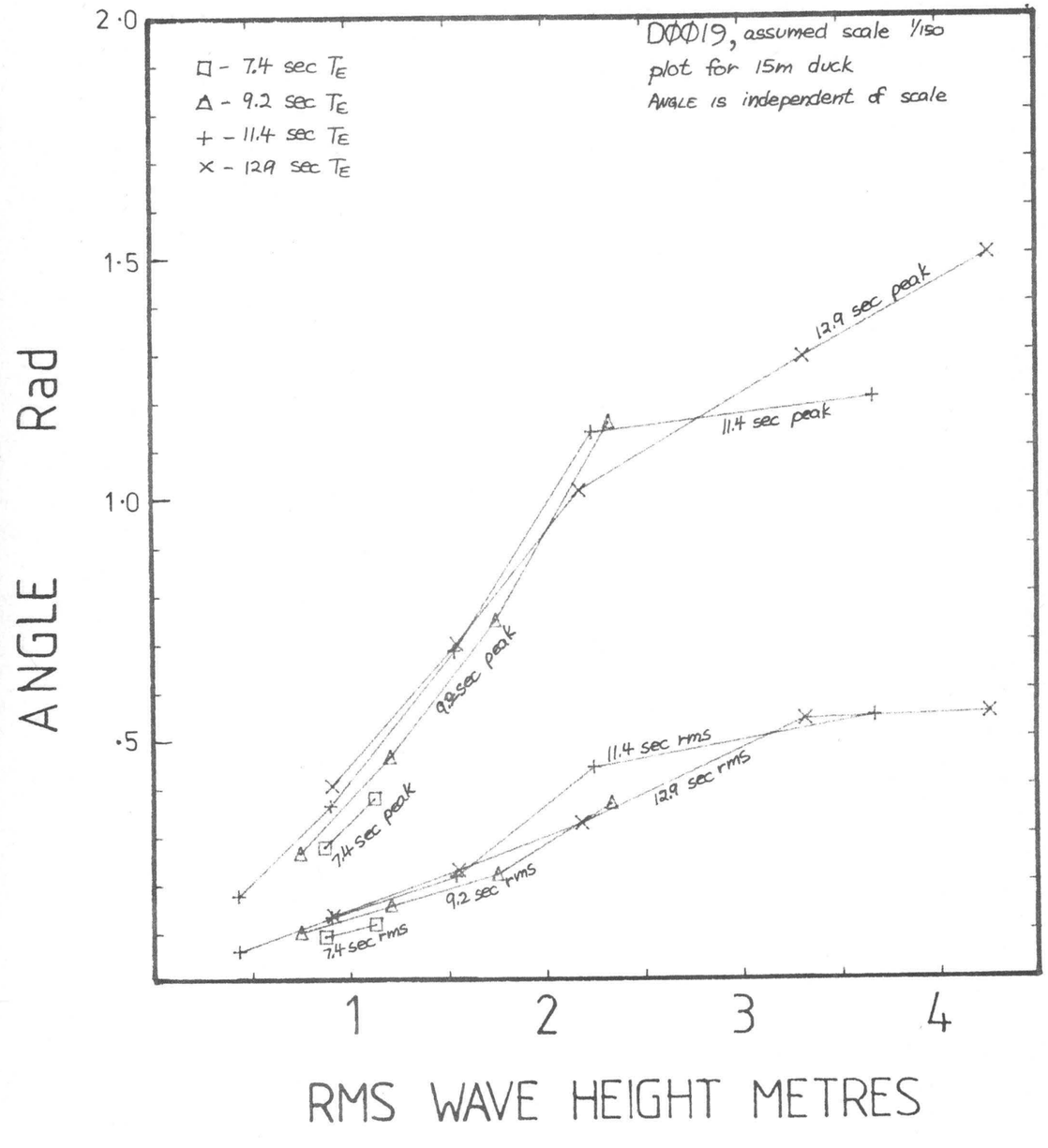

Scatter Diagram Tests
DUCK ANGLE, FIXED RIG

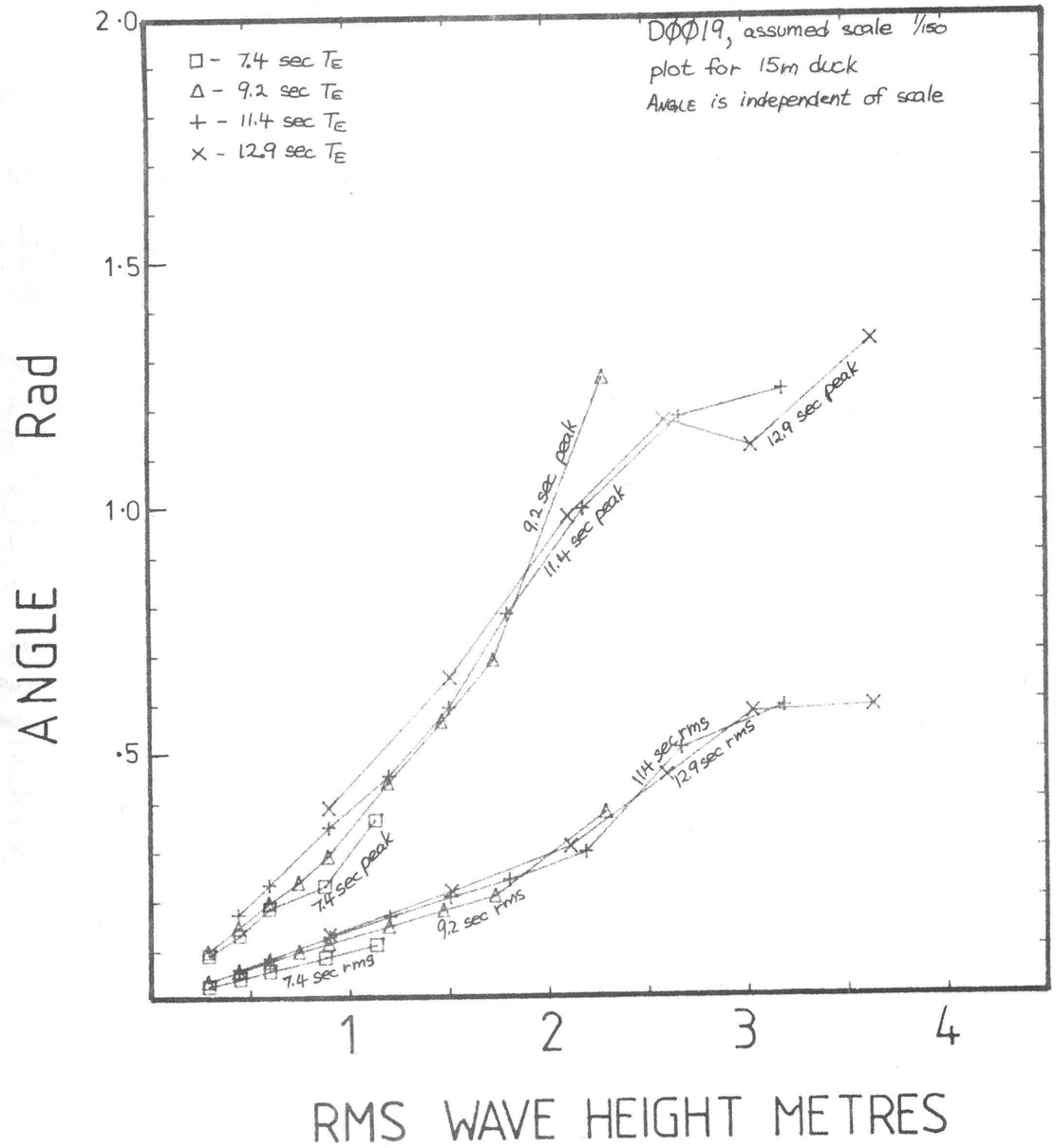

DUCK ANGULAR VELOCITY

Angular velocity is almost completely independent of energy period, with the RMS values lying very nearly on the same line. The RMS values for a torque limit of 4 MNm/m are only about 20% lower than those for 0.5 MNm/m, and the RMS moving rig values are indistinguishable from the fixed rig ones with the same torque limit.

The RMS angular velocities level off in the large seas, but the knee is softer than for the angle measurements.

The peak angular velocities are more reliable than the peak angles since the transducer is likely to be in the middle of its range when the peaks occur. The duck angle is obtained by integrating the angular velocity signal, using the same transducer.

The maximum angular velocities are indicated in the following table:

TORQUE LIMIT MNm/m	MAX. ANG. VEL. rads/sec
0.5	0.78
1	0.75
2	0.74
3	0.65
4	0.52

The peak of about 0.8 radians/second is fairly constant until a torque limit of 3 KNm/m when it drops to below 0.7. At the lowest torque limit the peak is reached at a lower wave height. Moving rig peaks are on average about 20% lower than fixed rig ones with the same torque limit.

Scatter Diagram Tests

DUCK ANGULAR VELOCITY, MOVING RIG 1MNm/m TORQUE LIMIT

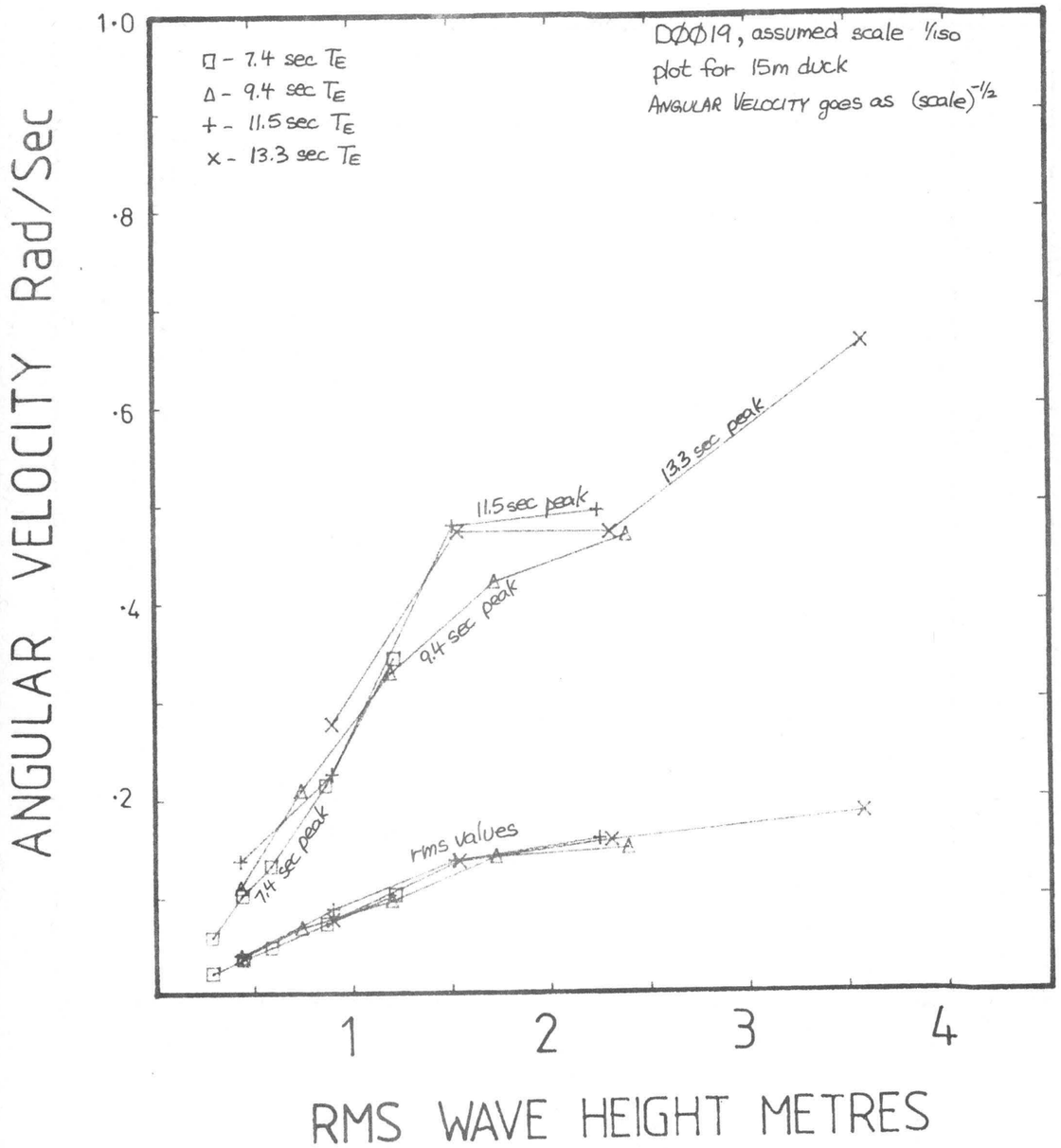

Scatter Diagram Tests

DUCK ANGULAR VELOCITY, FIXED RIG, ·5MNm/m TORQUE LIMIT

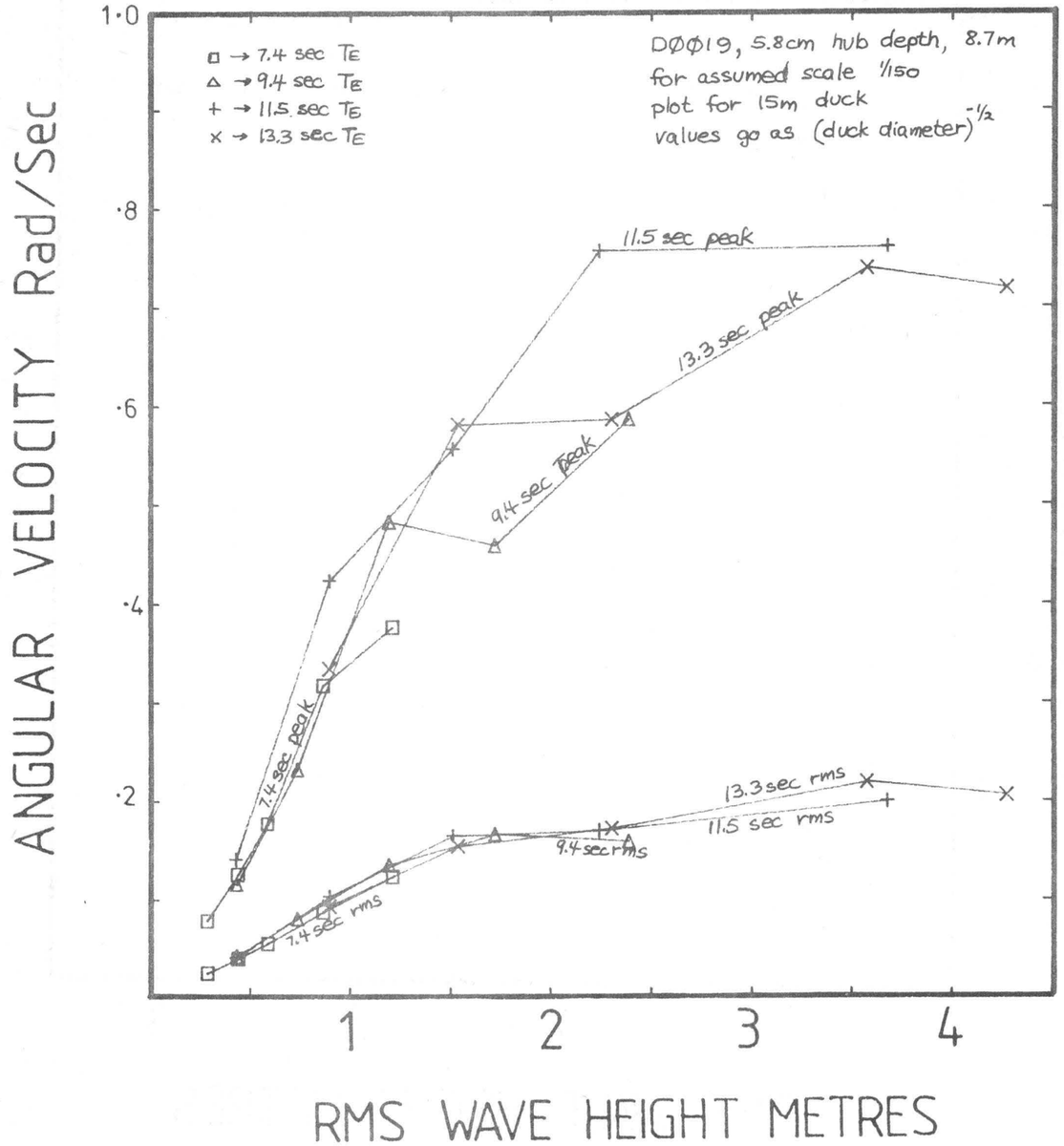

Scatter Diagram Tests

DUCK ANGULAR VELOCITY, FIXED RIG, 1MNm/m TORQUE LIMIT

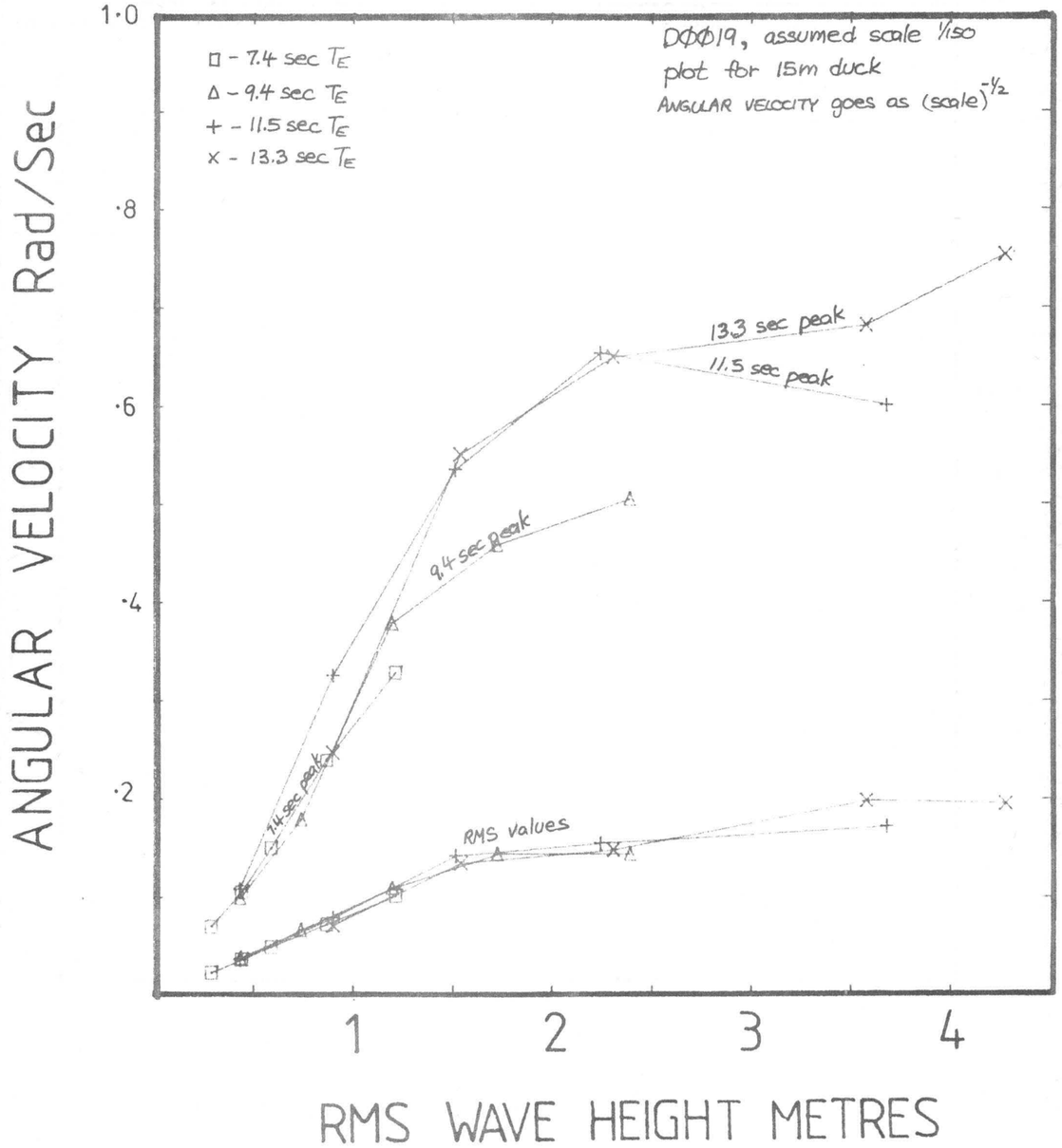

Scatter Diagram Tests

DUCK ANGULAR VELOCITY, FIXED RIG, 2MNm/m TORQUE LIMIT

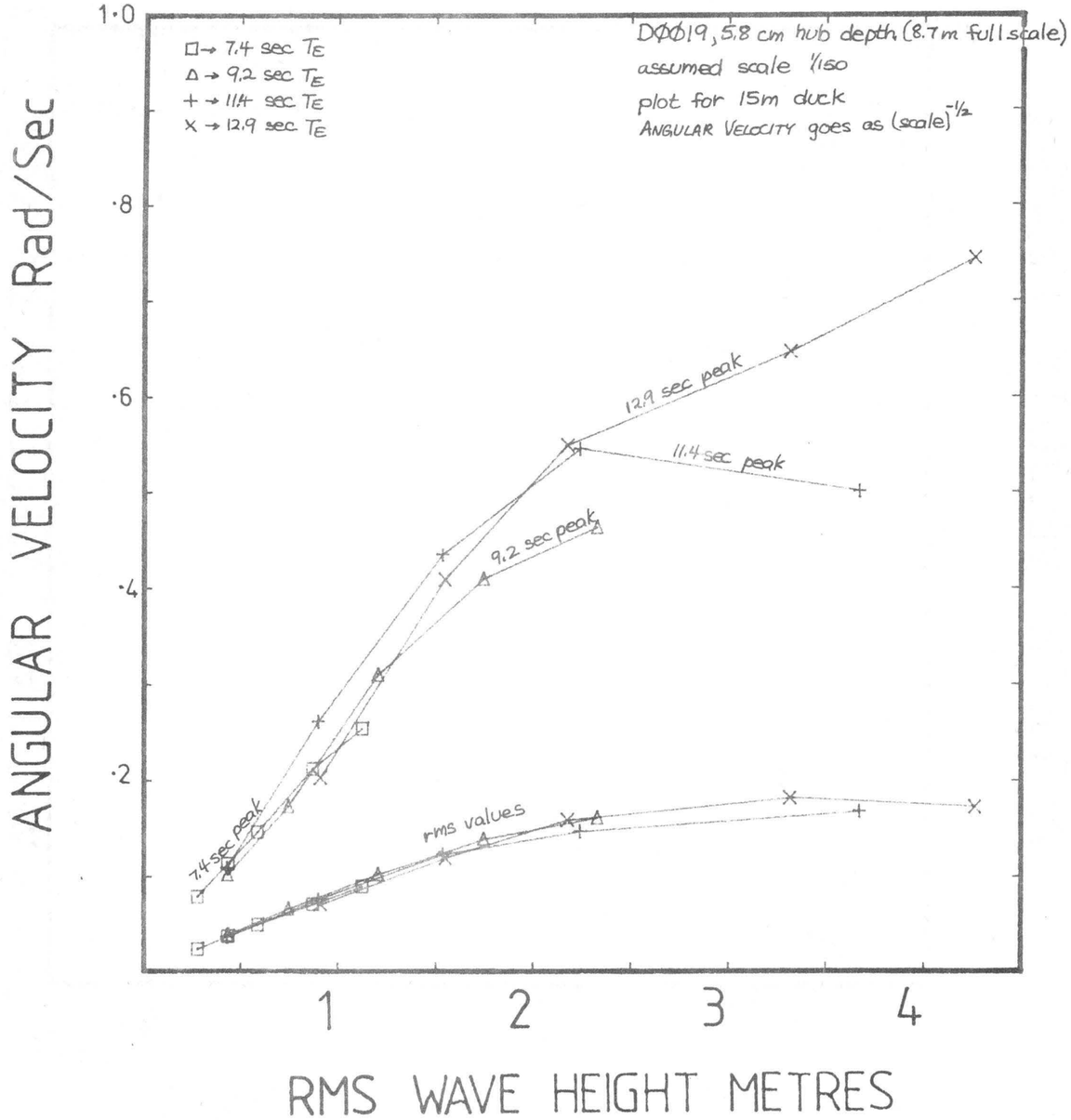

Scatter Diagram Tests

DUCK ANGULAR VELOCITY, FIXED RIG, 3MNm/m TORQUE LIMIT

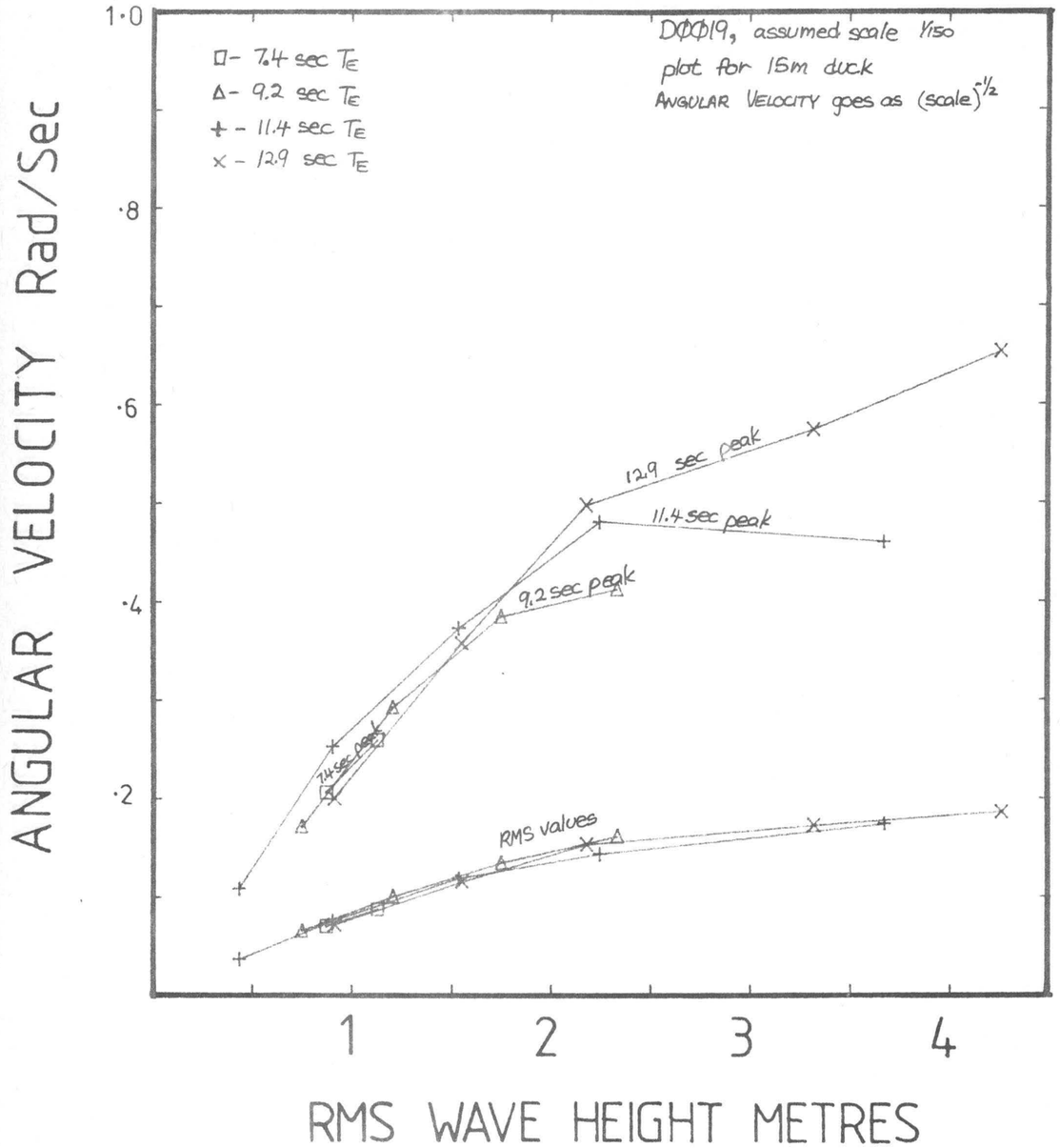

Scatter Diagram Tests

DUCK ANGULAR VELOCITY, FIXED RIG

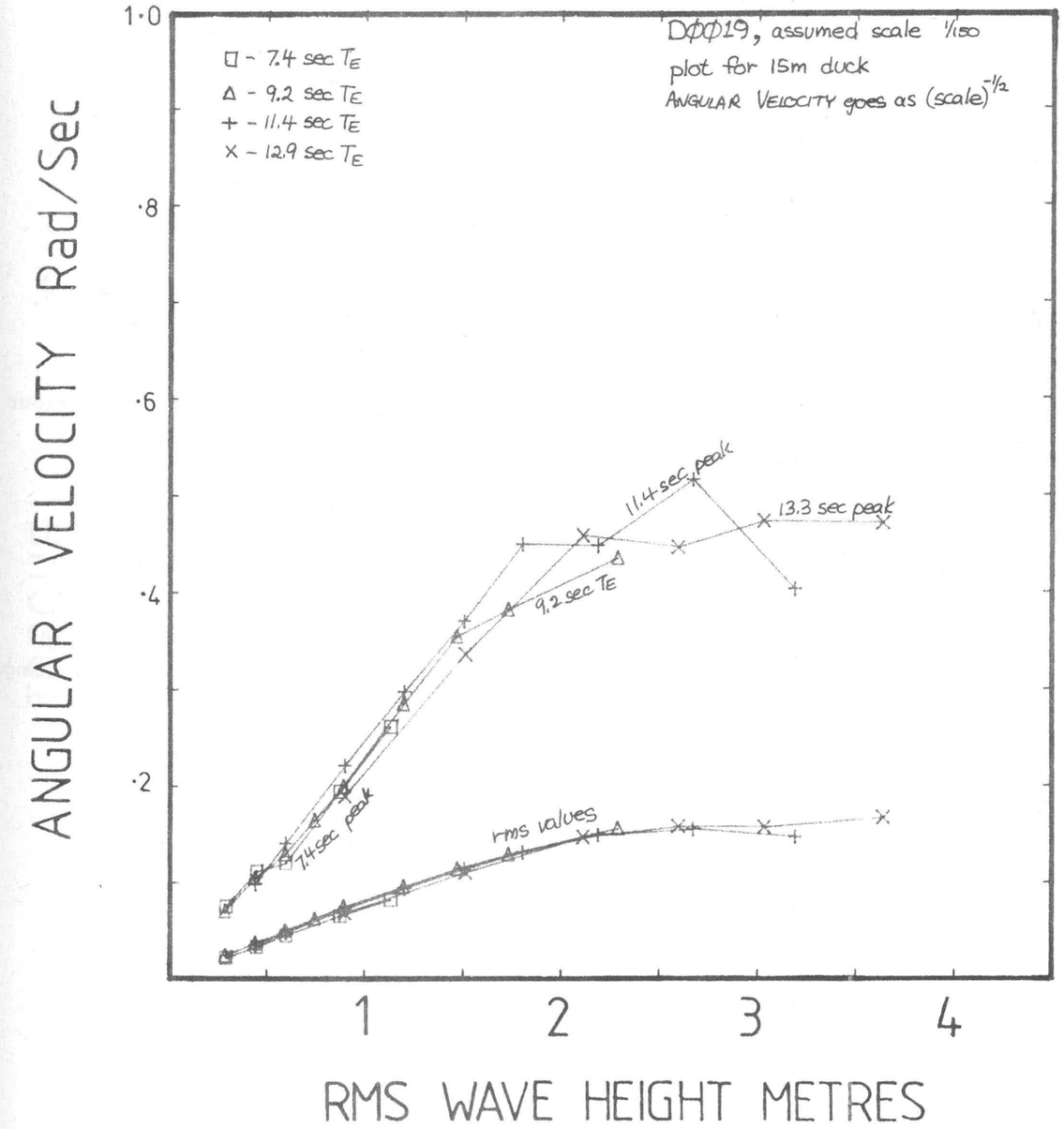

DUCK TORQUE

As torque is directly proportional to angular velocity, it is no surprise to find that it too is nearly independent of energy period. The RMS value goes up approximately linearly at 0.6 MNm/m per RMS metre of wave amplitude until the torque limit is reached. Then the RMS torque becomes fairly constant. These are the values for the various torque limits:

TORQUE LIMIT (MNm/m)	RMS TORQUE PLATEAU (MNm/m)	RMS WAVE FOR PLATEAU CORNER (m)
0.5	0.4	1.2
1	0.7	1.5
2	1.2	2.2
3	1.3	3.5

The highest torque tested (about 4 MNm/m) was limited by the torque transducer in our duck. It showed similar behaviour to the 3 MNm/m tests.

The moving rig behaviour was nearly identical to the fixed rig behaviour at the same torque limit except for large 13 second seas, where the RMS values rose to be nearly as high as the peak values.

The capital cost of pumps is proportional to torque rather than power. If no greater value is placed on high power levels in winter, then we advise a torque limit of 1 MNm/m of duck for the India wave climate. But it would be sensible to choose designs which could allow higher torque limits to be used in the same devices if policy on the relation of summer to winter prices should change.

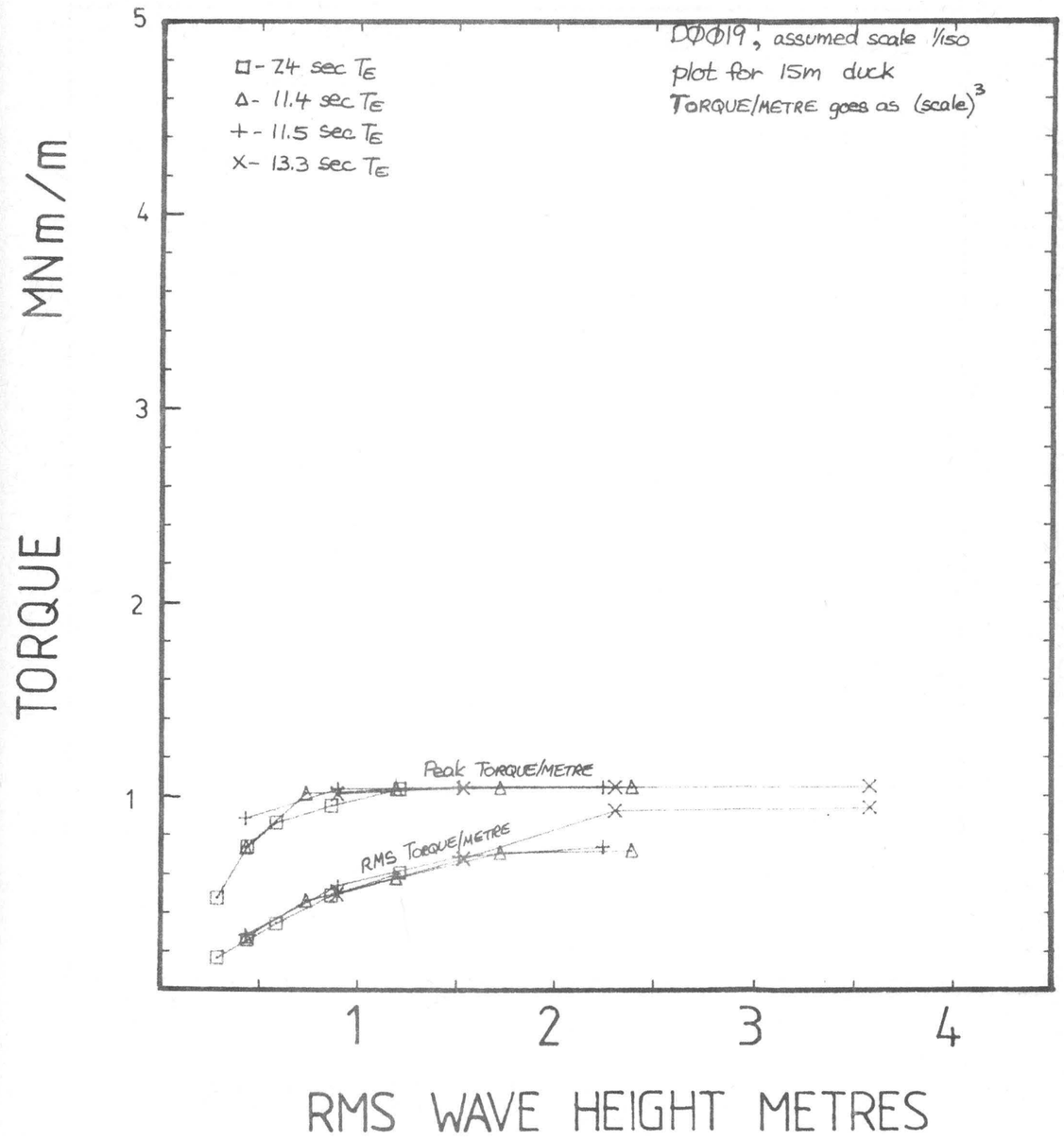

Scatter Diagram Tests

DUCK TORQUE, FIXED RIG, .5MNm/m TORQUE LIMIT

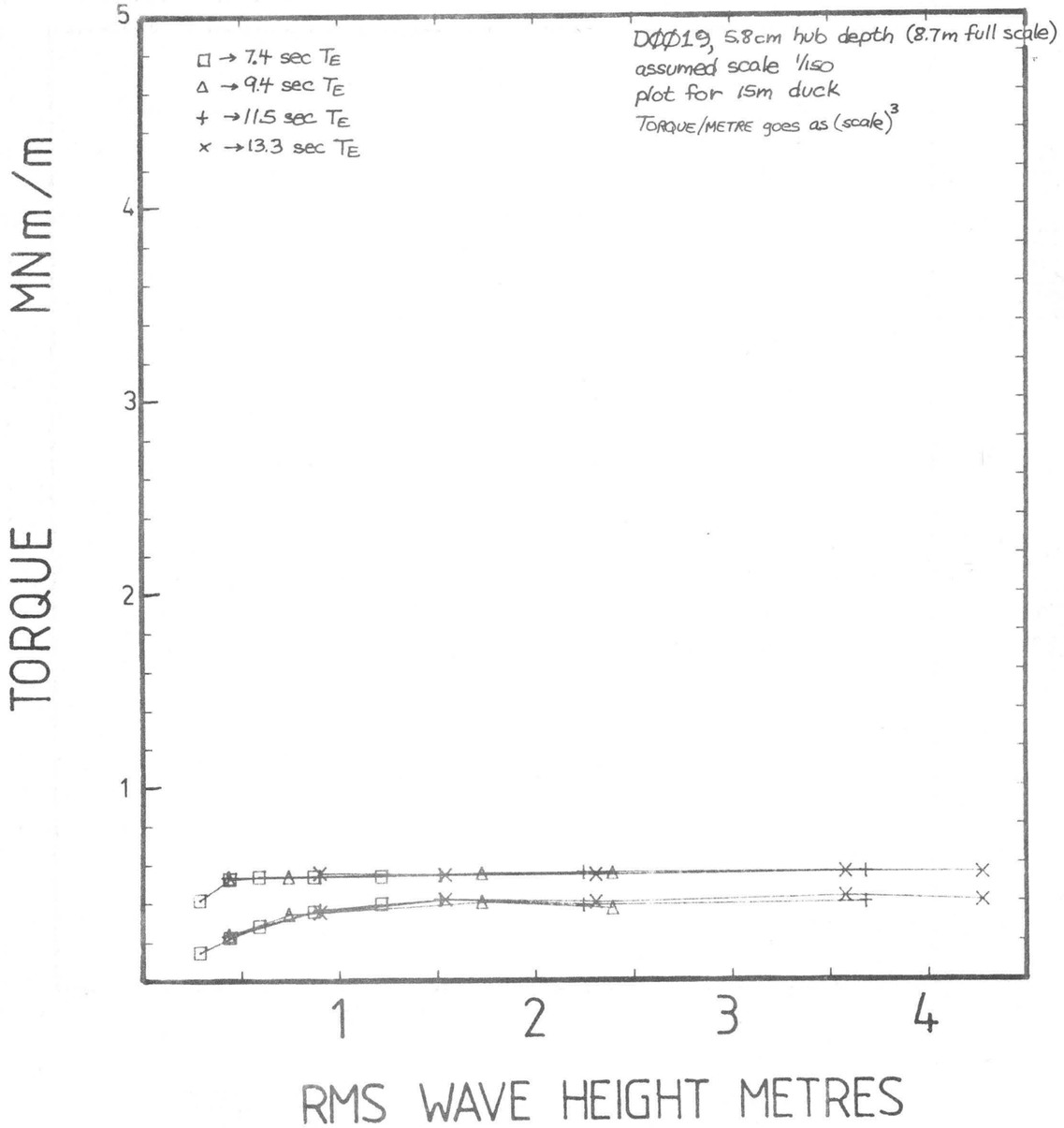

Scatter Diagram Tests

DUCK TORQUE, FIXED RIG, 1MNm/m TORQUE LIMIT

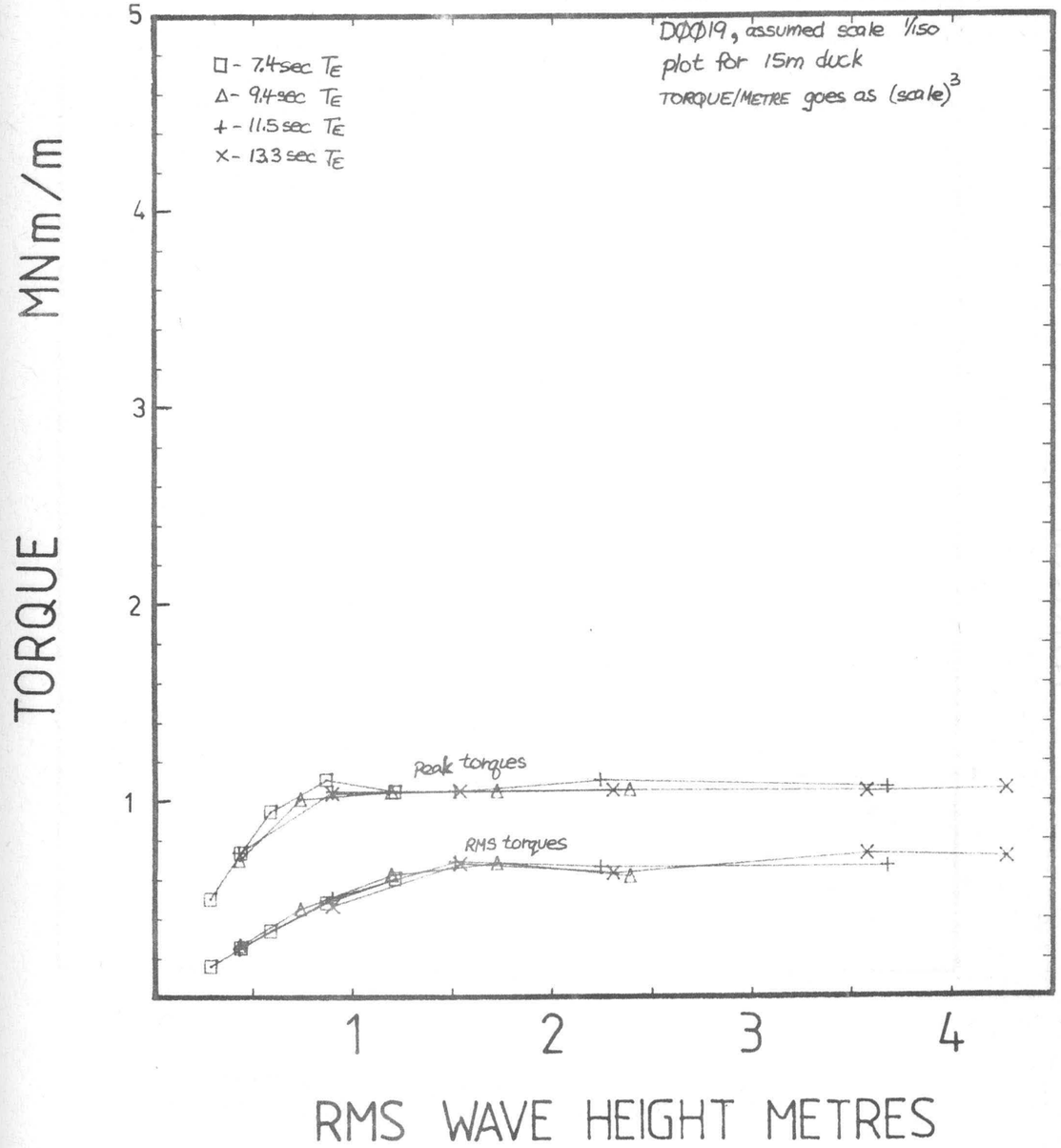

Scatter Diagram Tests

DUCK TORQUE, FIXED RIG, 2MNm/m TORQUE LIMIT

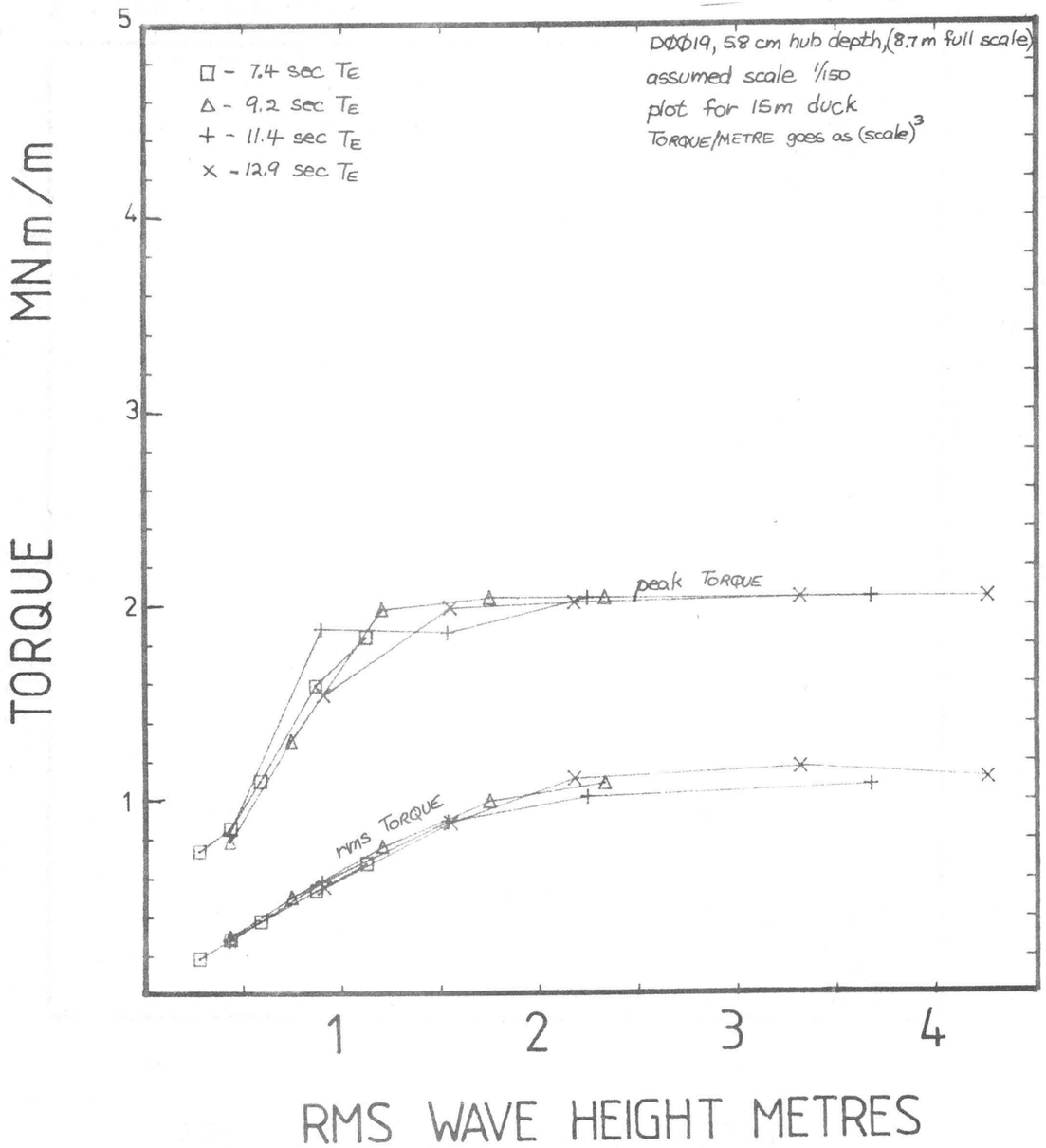

Scatter Diagram Tests

DUCK TORQUE, FIXED RIG, 3MNm/m TORQUE LIMIT

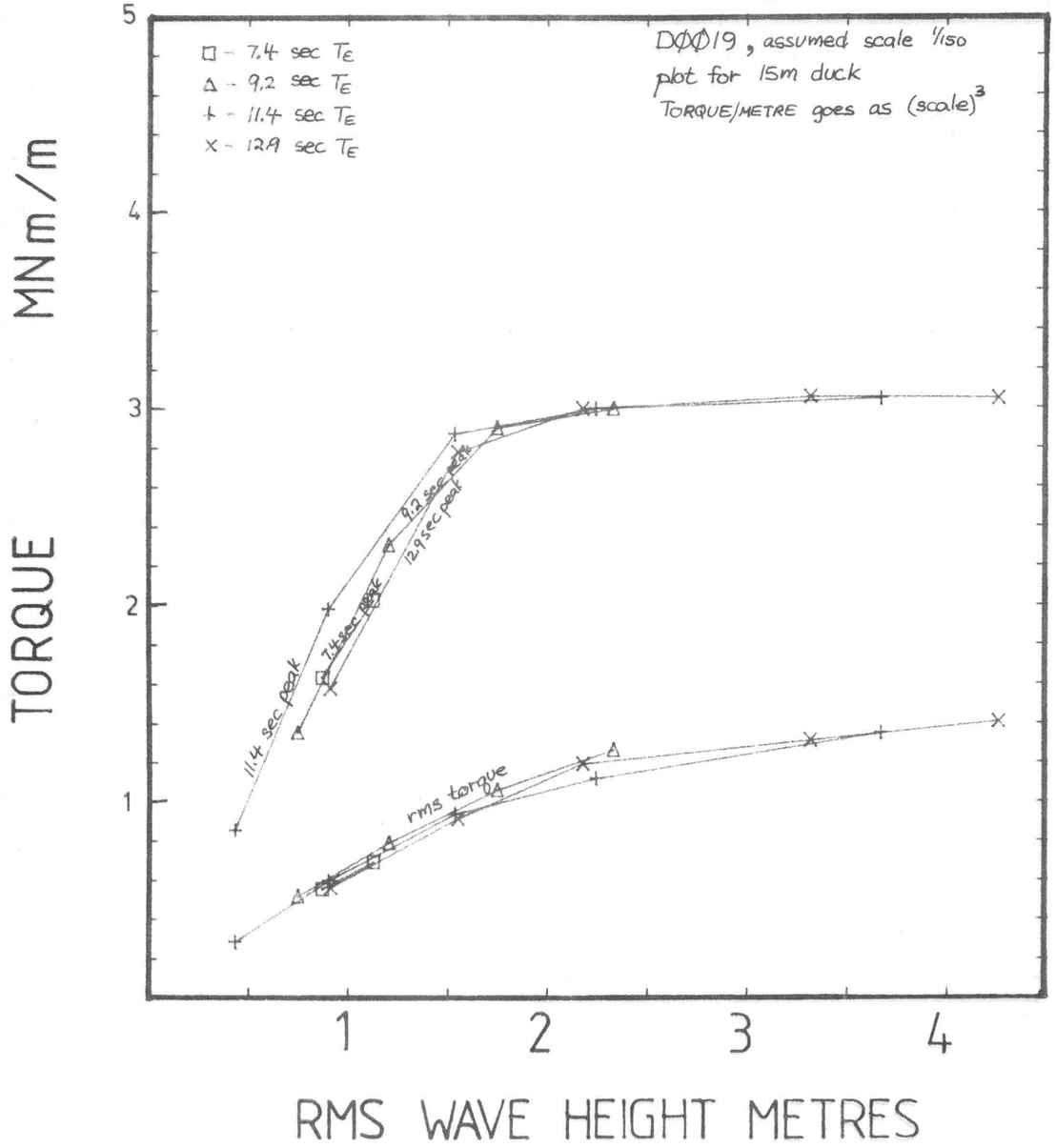

Scatter Diagram Tests

DUCK TORQUE, FIXED RIG

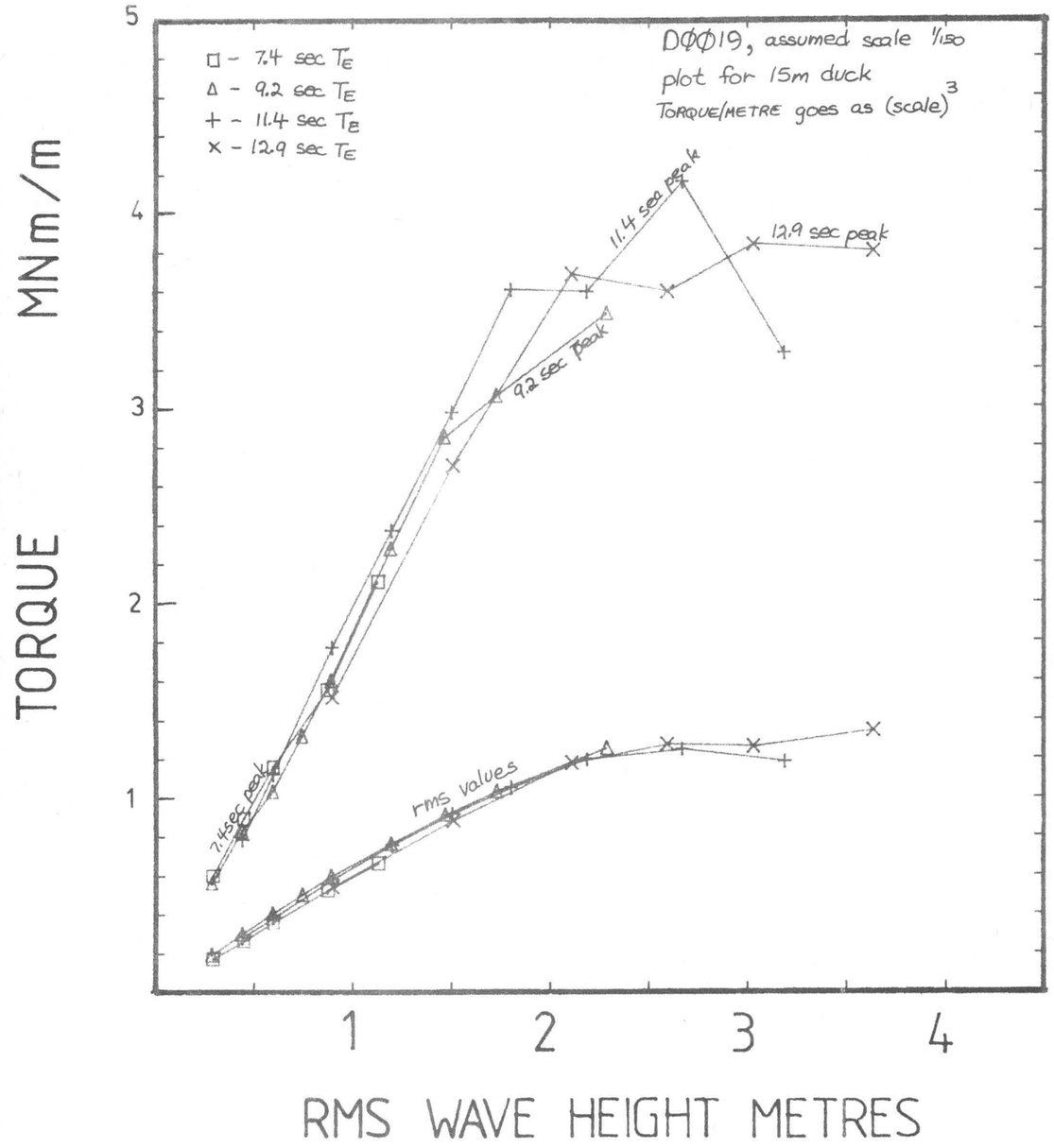

SURGE FORCE

Both the peak and RMS surge forces on the fixed rig show a nearly linear rise with wave amplitude, with slight levelling off at high amplitudes. The forces are very nearly independent of both energy period and torque limit. Therefore they can be predicted well using a force coefficient (see page 6.13). Force coefficients for the test series are given on page 2.58 . The fixed rig tests show RMS-derived coefficients of about 0.4 (500 KN/m at H_{rms} = 4.5 metres). The 7 second sea forces are about 20% lower. Peak forces are about three times the RMS.

Scatter Diagram Tests

SURGE FORCE, MOVING RIG, 1MNm/m TORQUE LIMIT

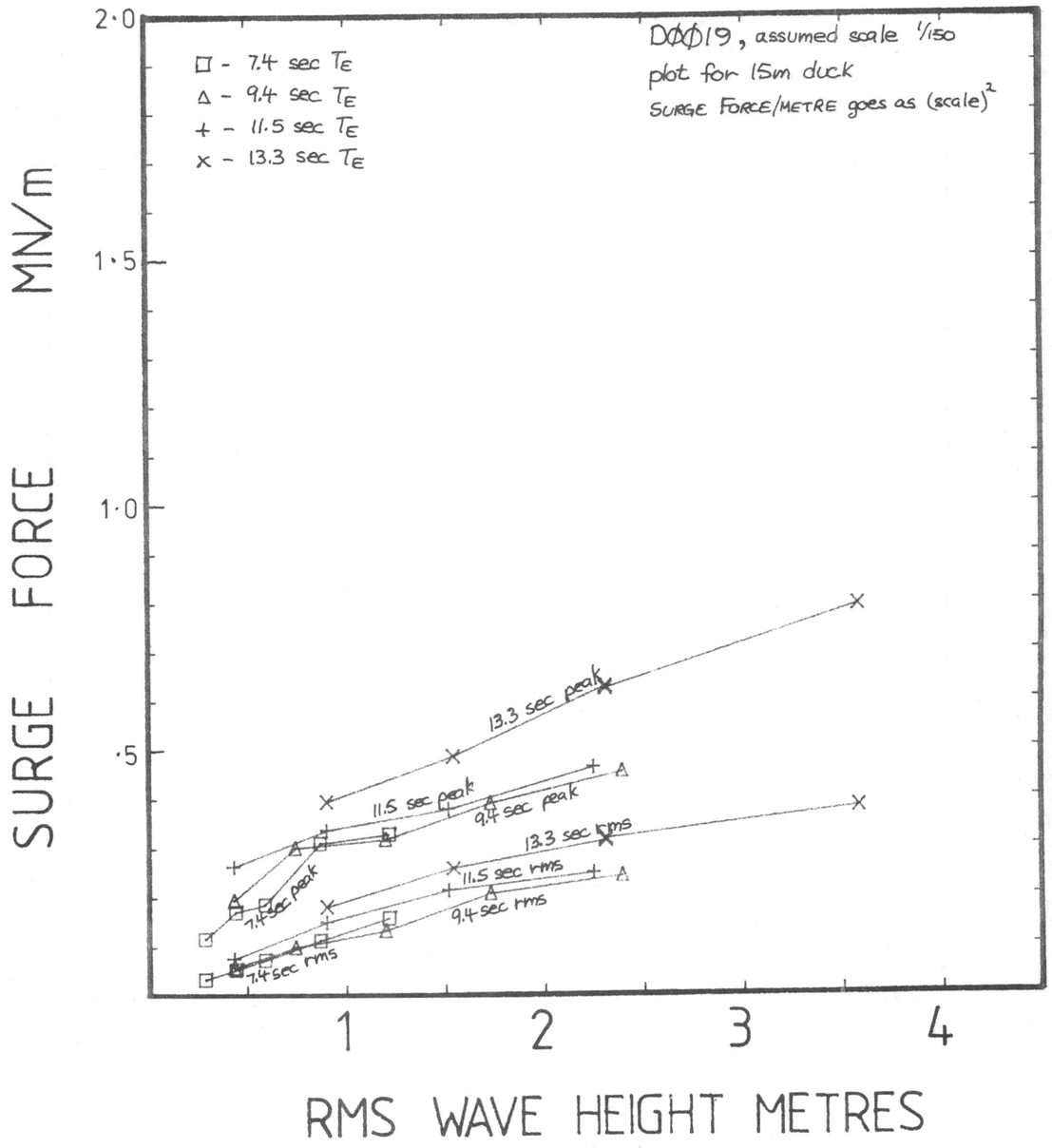

Scatter Diagram Tests

SURGE FORCE, FIXED RIG, ·5MNm/m TORQUE LIMIT

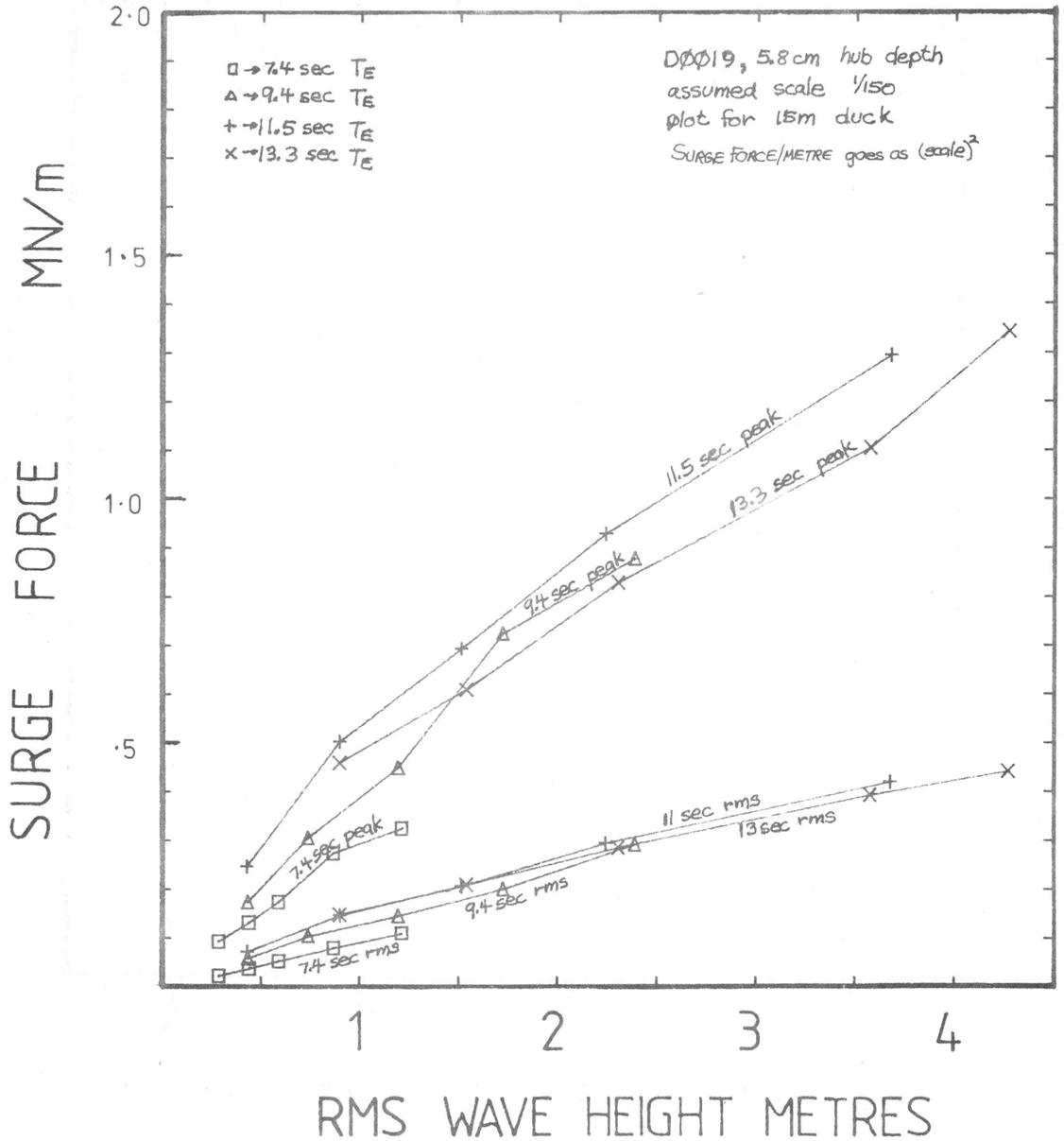

Scatter Diagram Tests

SURGE FORCE, FIXED RIG, 1MNm/m TORQUE LIMIT

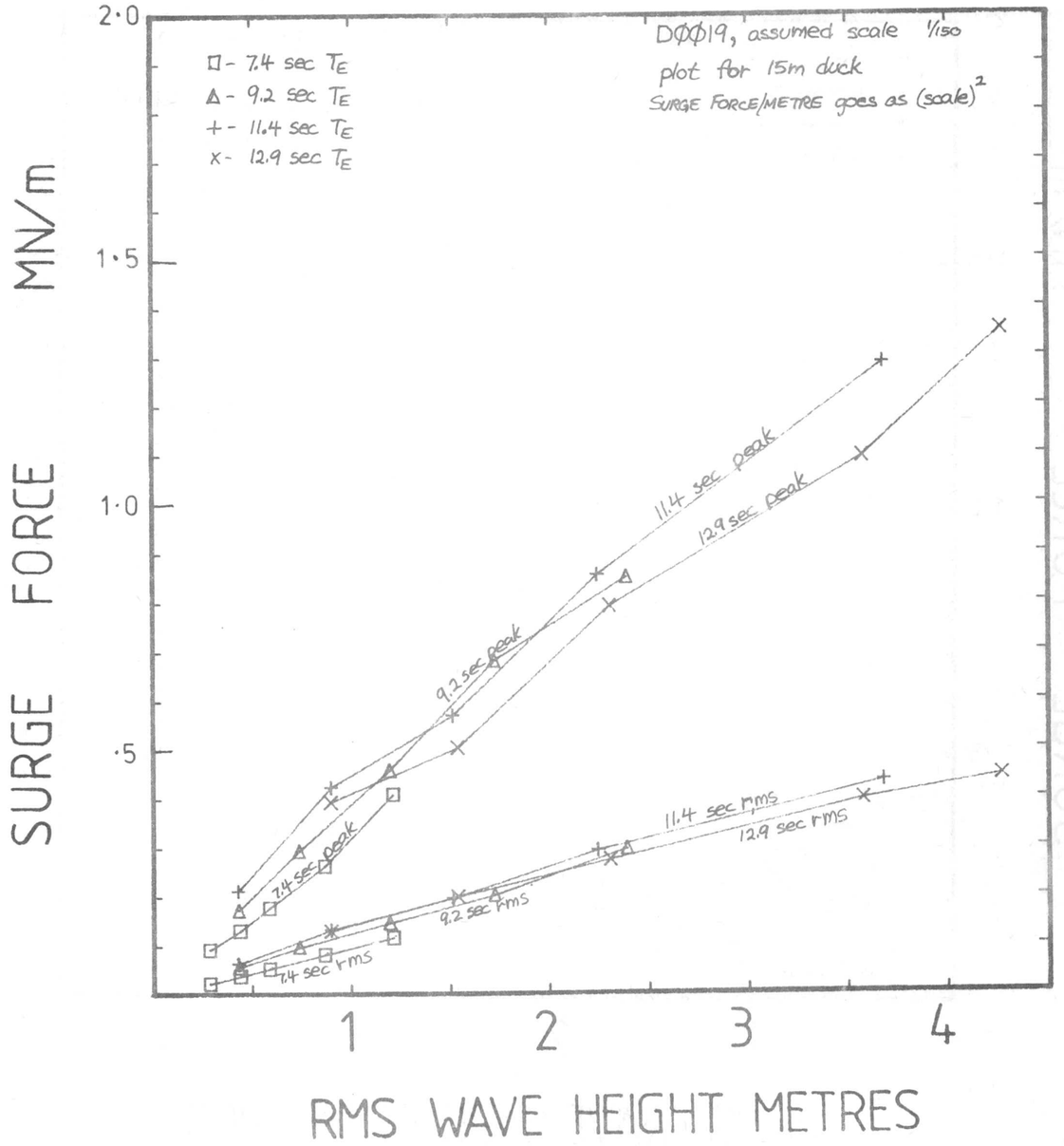

Scatter Diagram Tests

SURGE FORCE, FIXED RIG, 2MNm/m TORQUE LIMIT

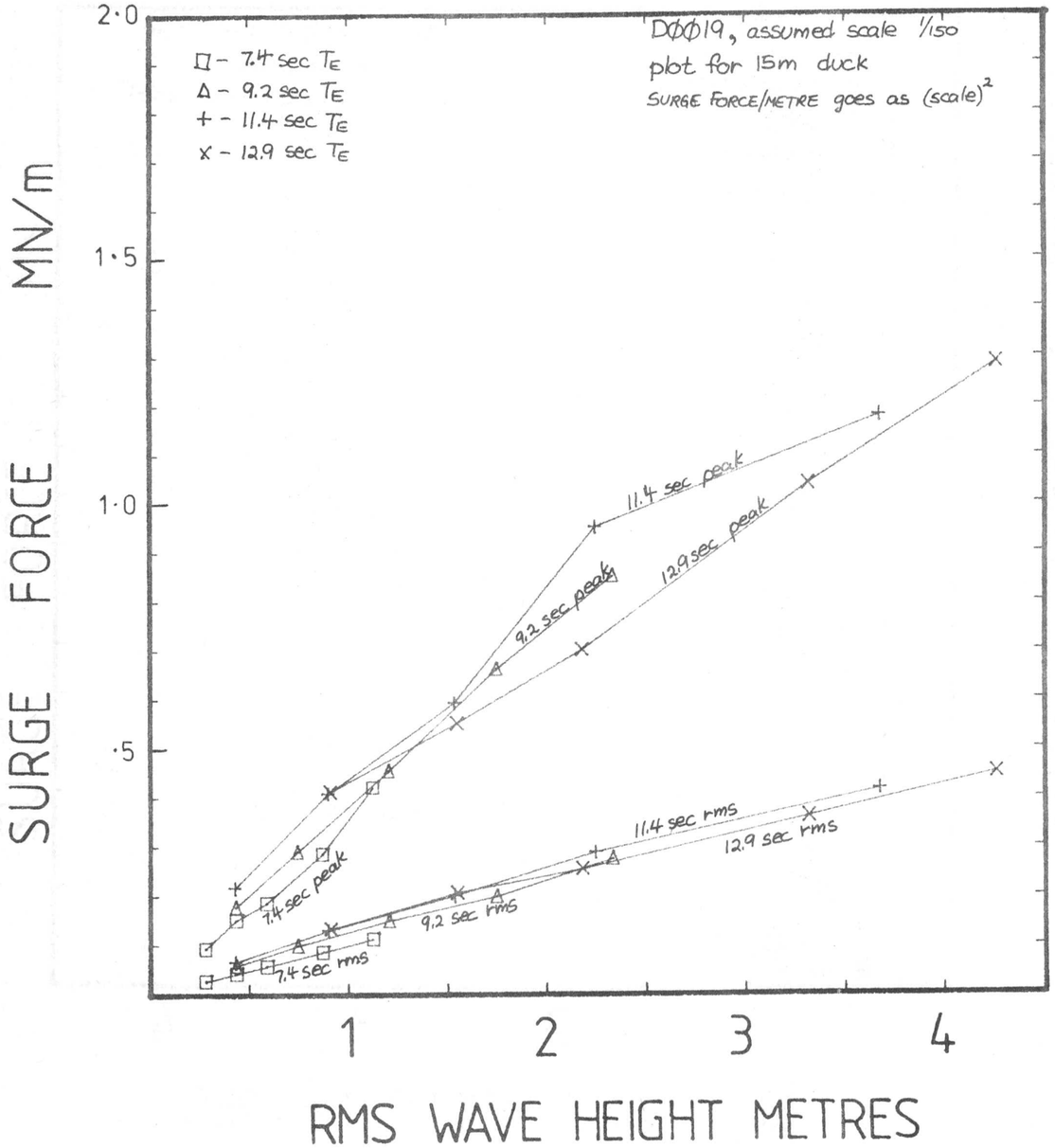

Scatter Diagram Tests

SURGE FORCE, FIXED RIG, 3MNm/m TORQUE LIMIT

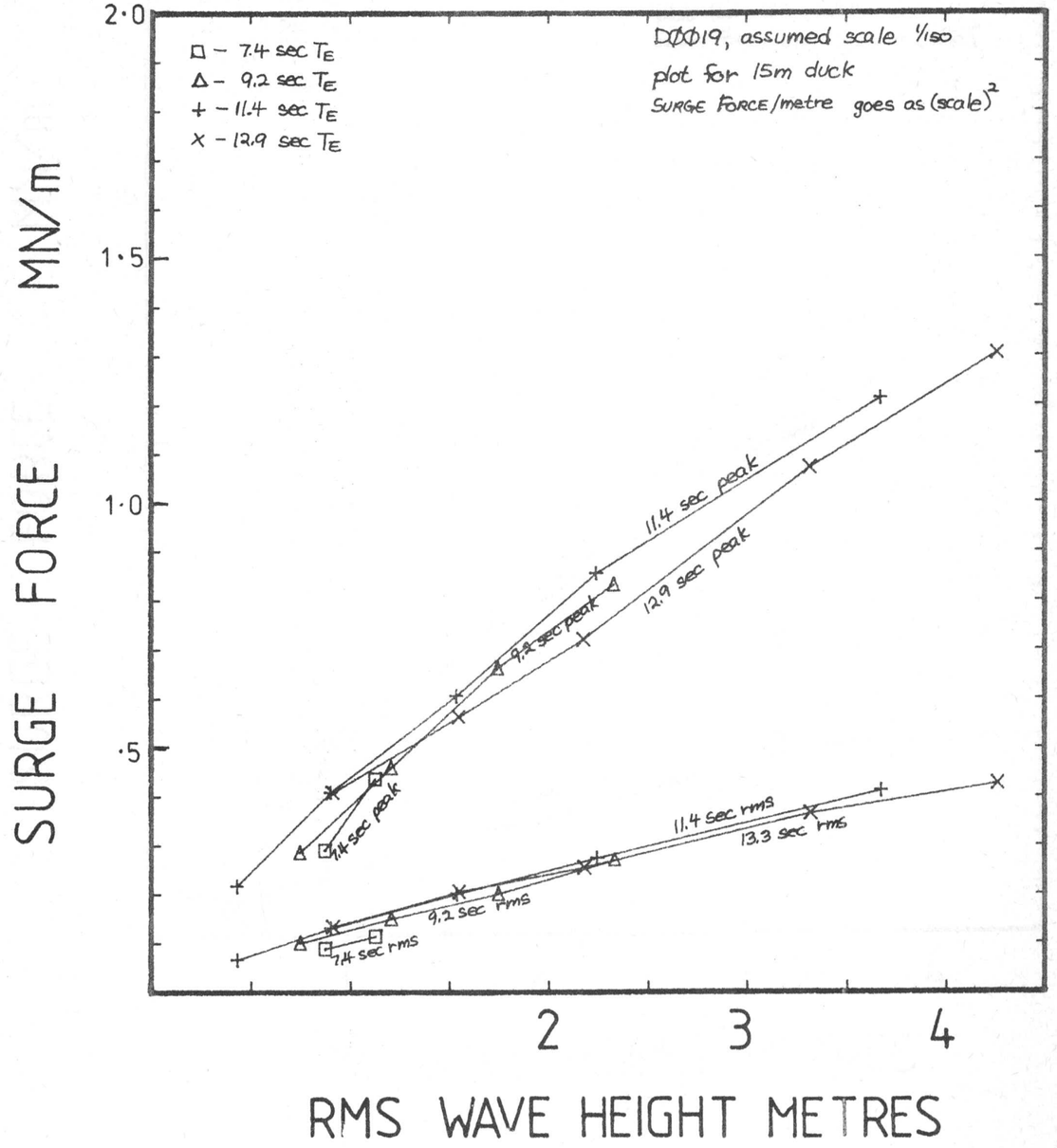

Scatter Diagram Tests

SURGE FORCE, FIXED RIG

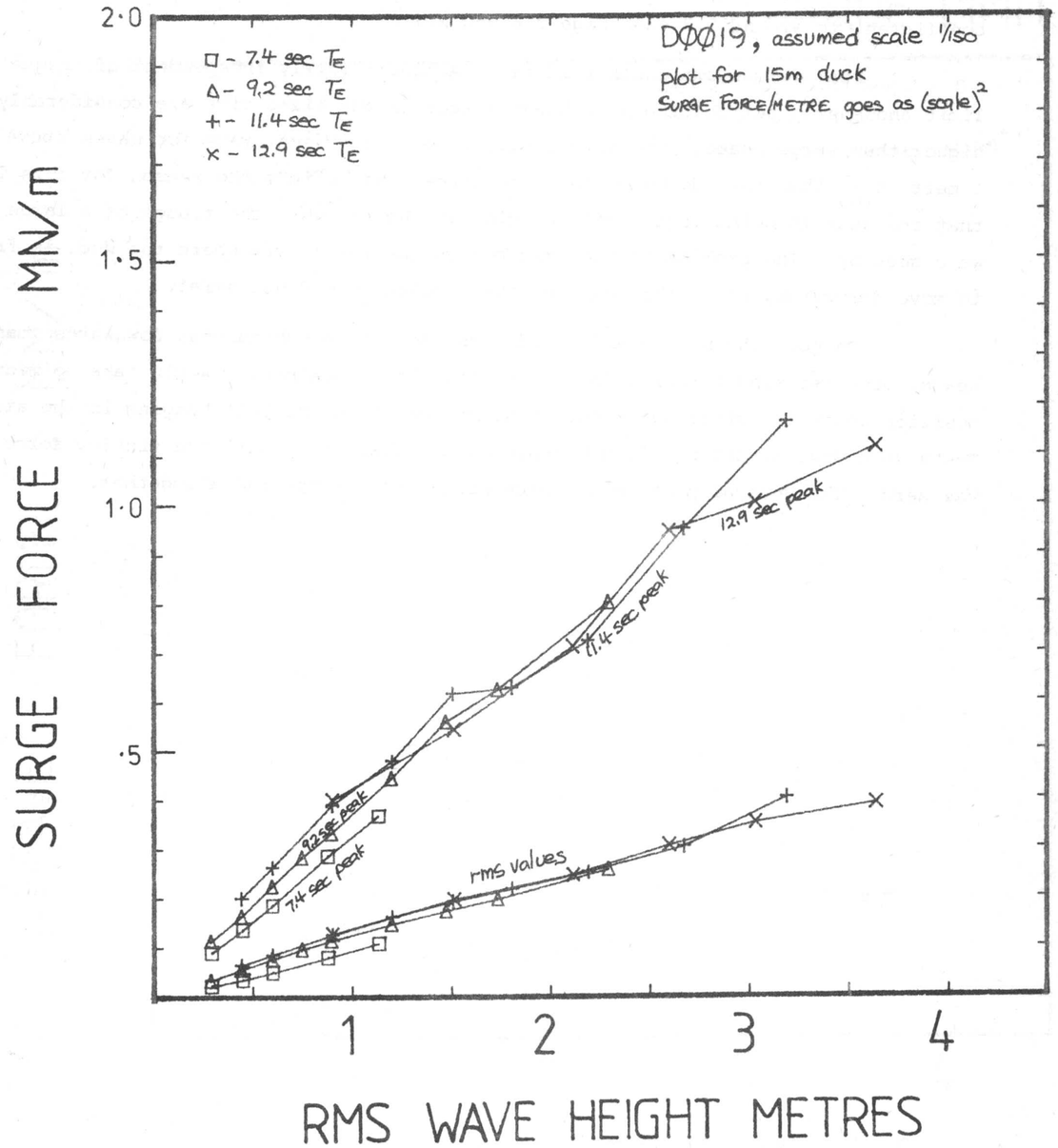

HEAVE FORCE

RMS heave forces are well-behaved and linear, showing very little variation with energy period, torque limit or mounting. The RMS-derived force coefficient is around 0.3 (see page 2.6 and 2.7).

Peak forces are another matter. Although fairly independent of torque limit and energy period, the peak heave forces on the fixed rigs are considerably higher than surge peaks. The forces also rise at a steeper rate for waves above 1 metre H_{rms} than they do below this amplitude. We believe the reason for this is that the duck is being left partly hanging in the air when the trough of a large wave goes by. The problem is much reduced on the moving rig where the duck is free to move downwards, so in the real sea the problem should not exist.

On both the moving and fixed rigs there is a substantial downwards mean heave force (sinking force). In the sea the whole duck string would take up mean position below its still water position, and would not be left hanging in the air. Tests were done adjusting the hub depth on the fixed rig until the sinking force was zero. The unusual peak heave force behaviour disappeared altogether.

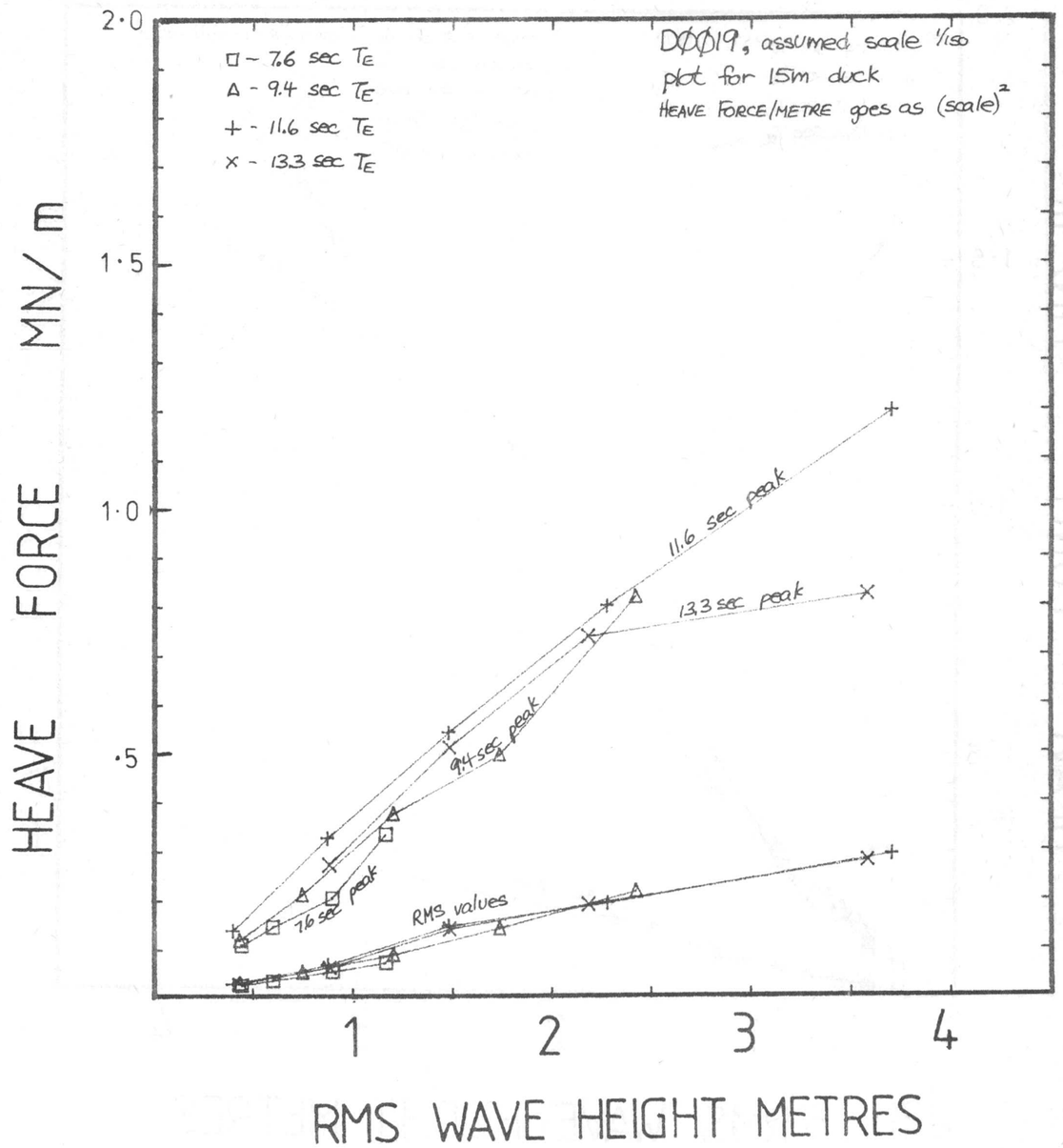

Scatter Diagram Tests

HEAVE FORCE, FIXED RIG, 5MNm/m TORQUE LIMIT

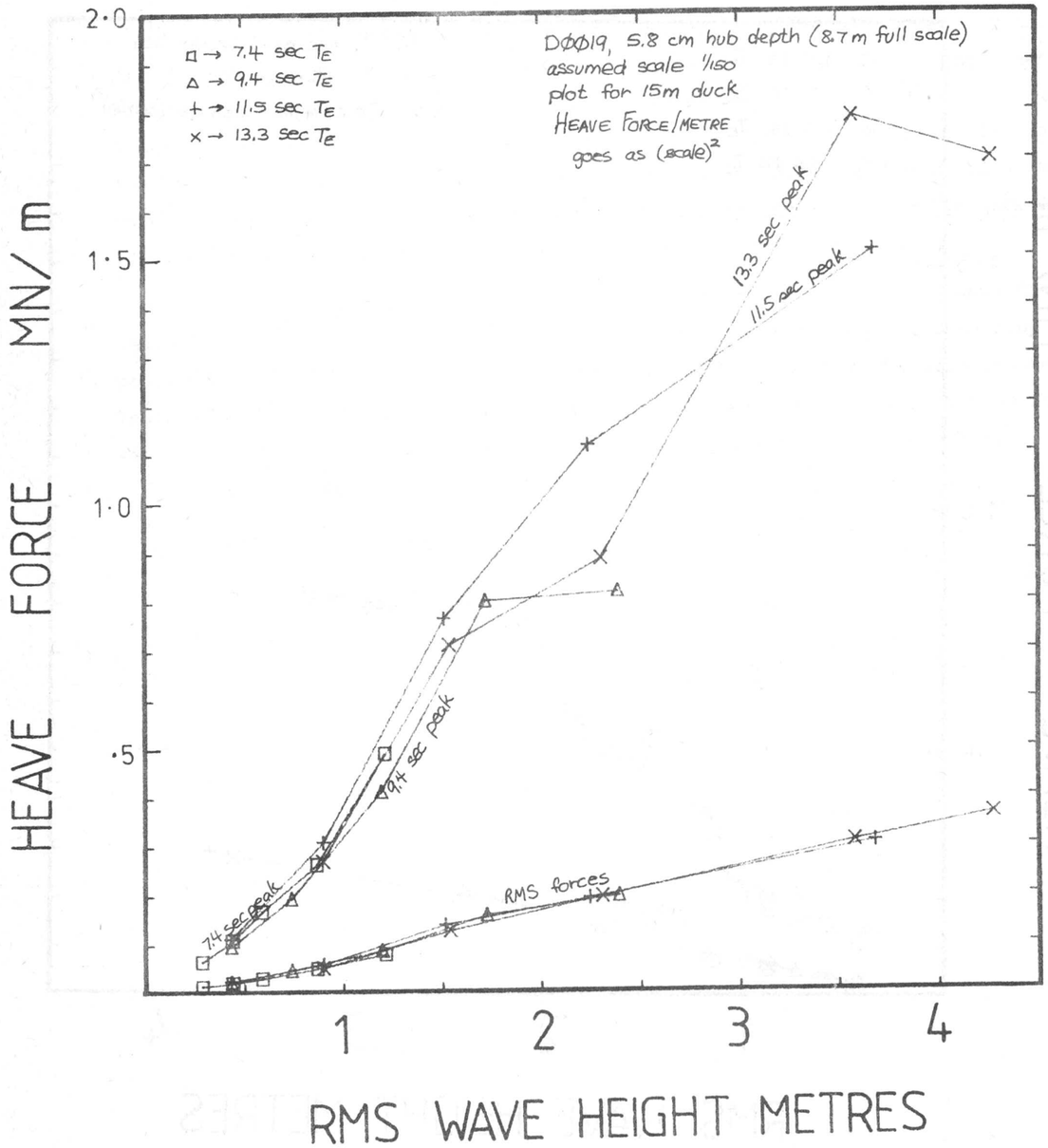

Scatter Diagram Tests

HEAVE FORCE, FIXED RIG, 1MNm/m TORQUE LIMIT

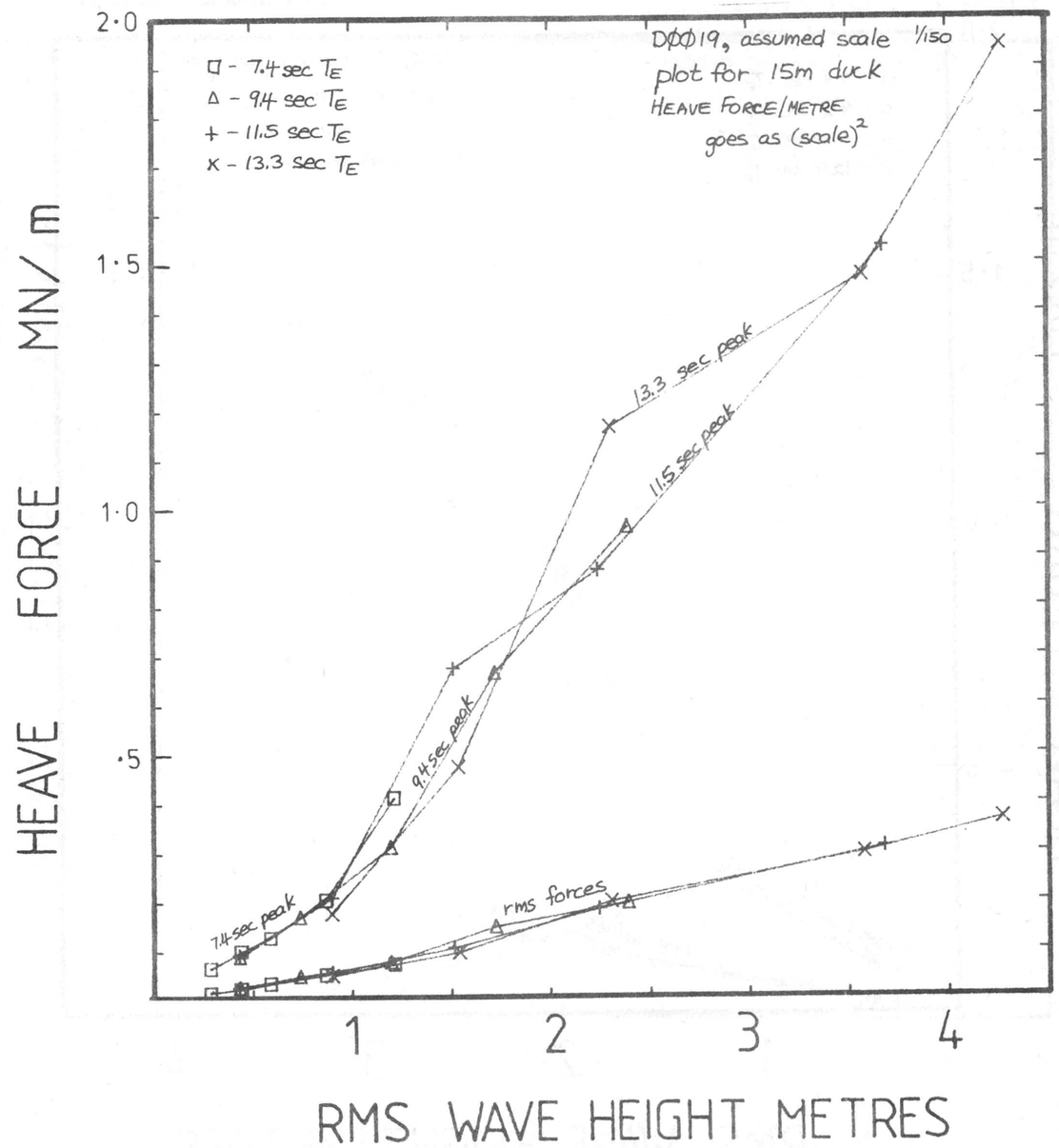

Scatter Diagram Tests

HEAVE FORCE, FIXED RIG, 2MNm/m TORQUE LIMIT

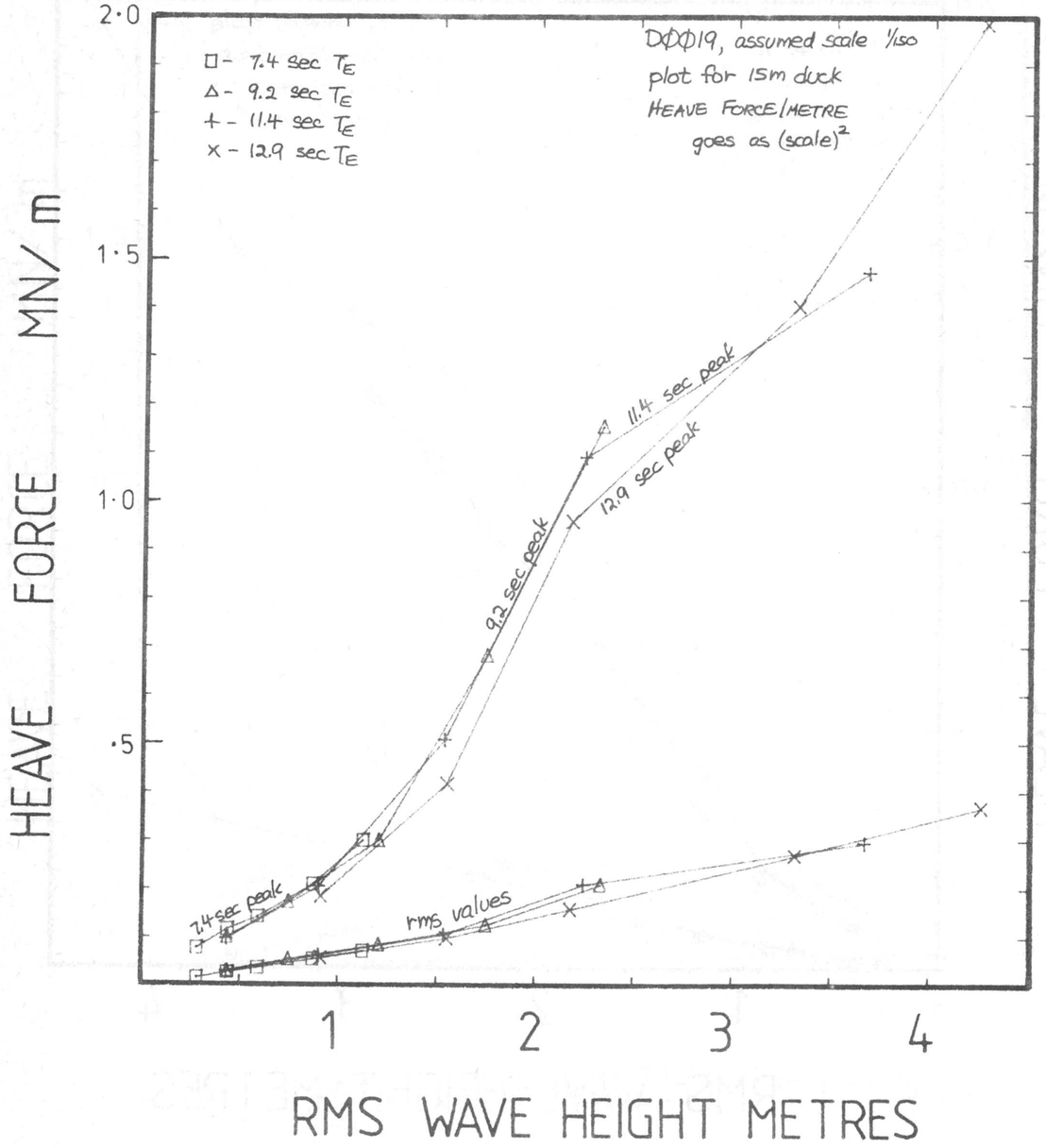

Scatter Diagram Tests

HEAVE FORCE, FIXED RIG, 3MNm/m TORQUE LIMIT

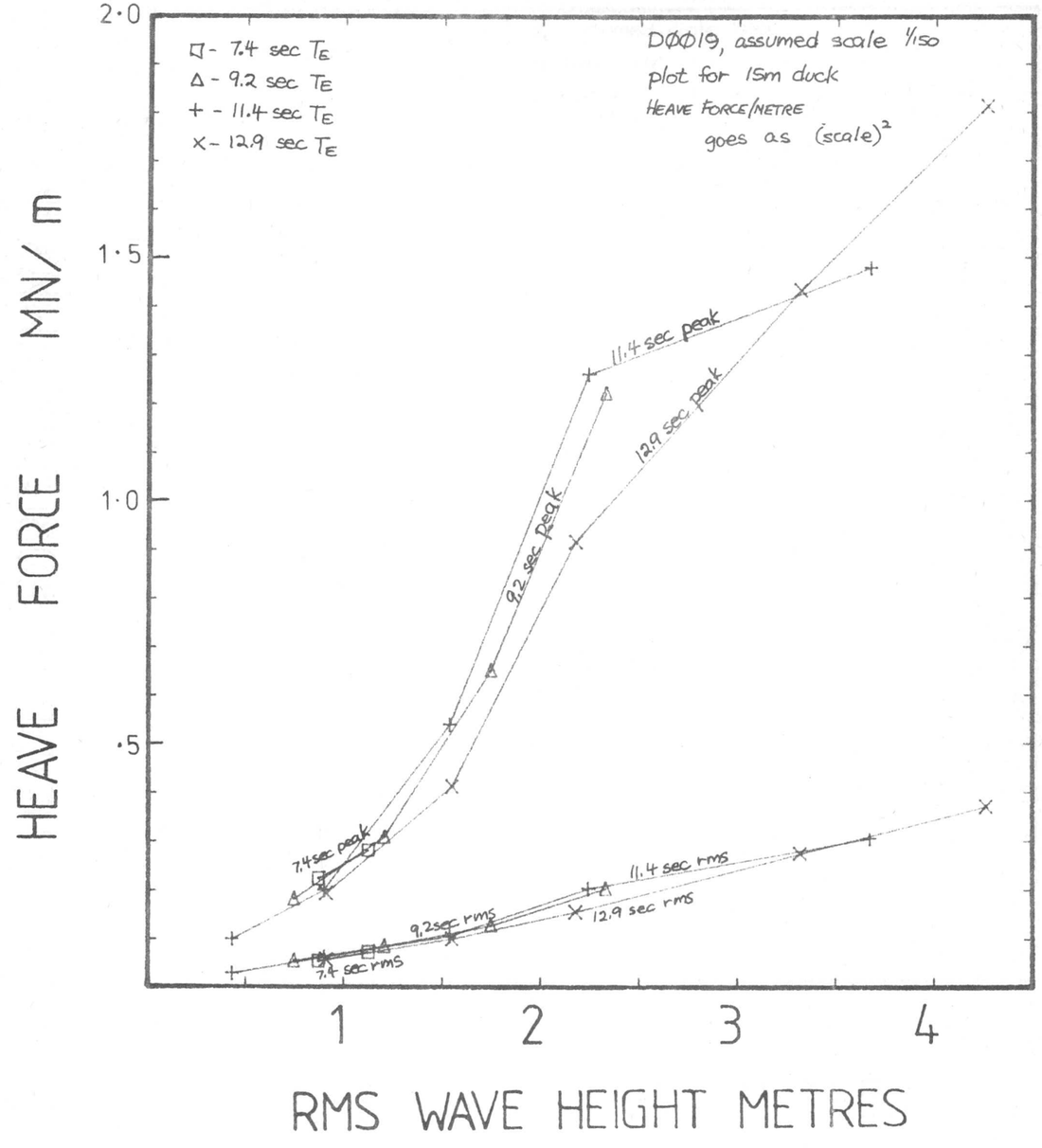

Scatter Diagram Tests
HEAVE FORCE, FIXED RIG

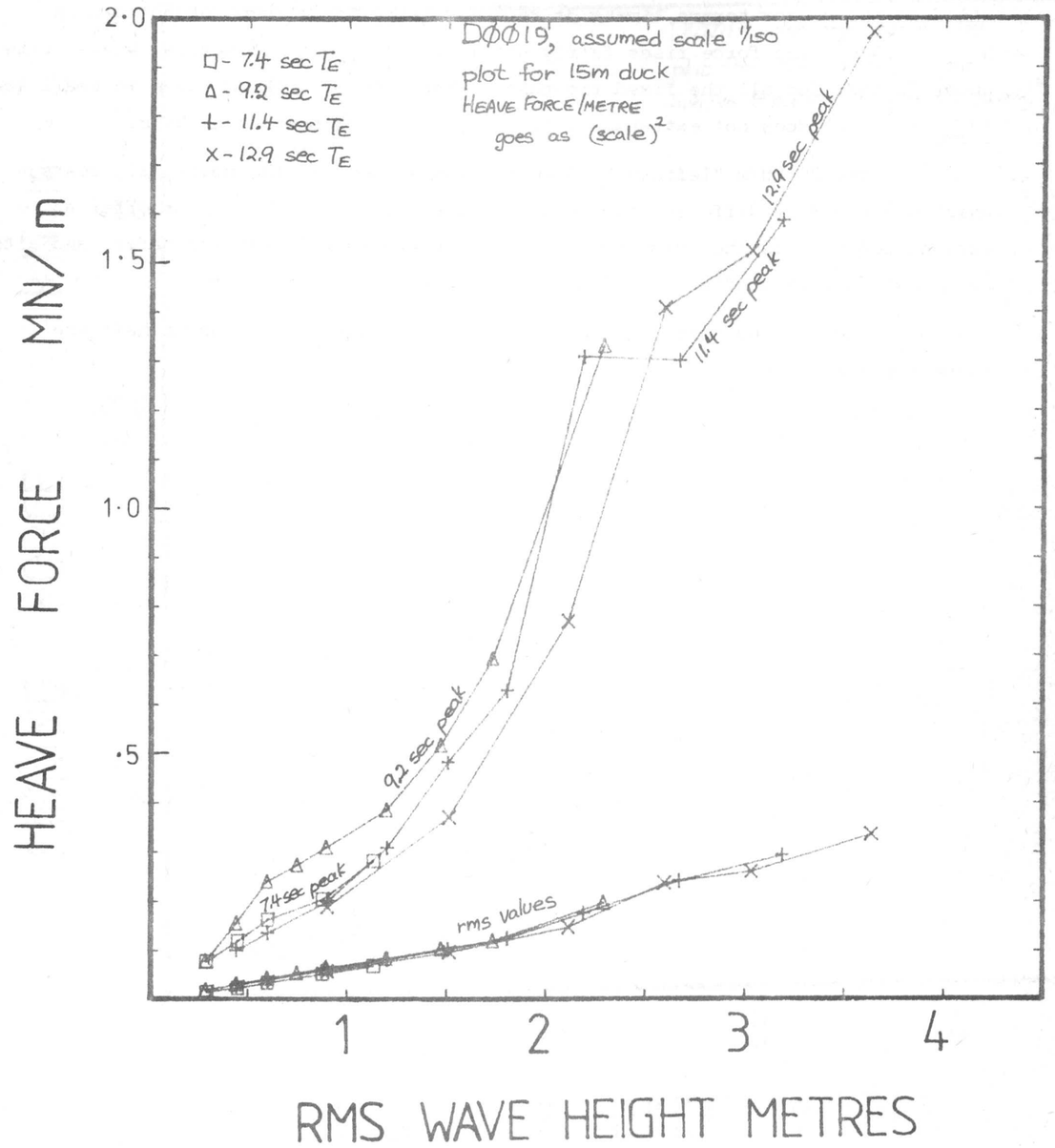

SINKING FORCE

Sinking force, the mean heave force, is another parameter which depends very little on the energy period. It is not strongly dependent on torque limit, although the higher torque limits do reduce sinking force by about 30% around H_{rms} = 2.5 m. The force rises fairly slowly up to H_{rms} = 1.5 metres, where it is about 70 kN/m for all the fixed rig tests. The line of sinking force in small seas (H_{rms} = 0.5 m) does not extrapolate to zero, but towards about 20 kN/m.

The 20 kN/m "leftover" force is also evident in the moving rig tests which use entirely different transducers and electronics. We cannot offer an explanation but, as the force-measuring strain gauges were checked before and after each test, we are confident that there was no experimental error.

The sinking force on the moving rig in large seas is about half the value for the fixed rig.

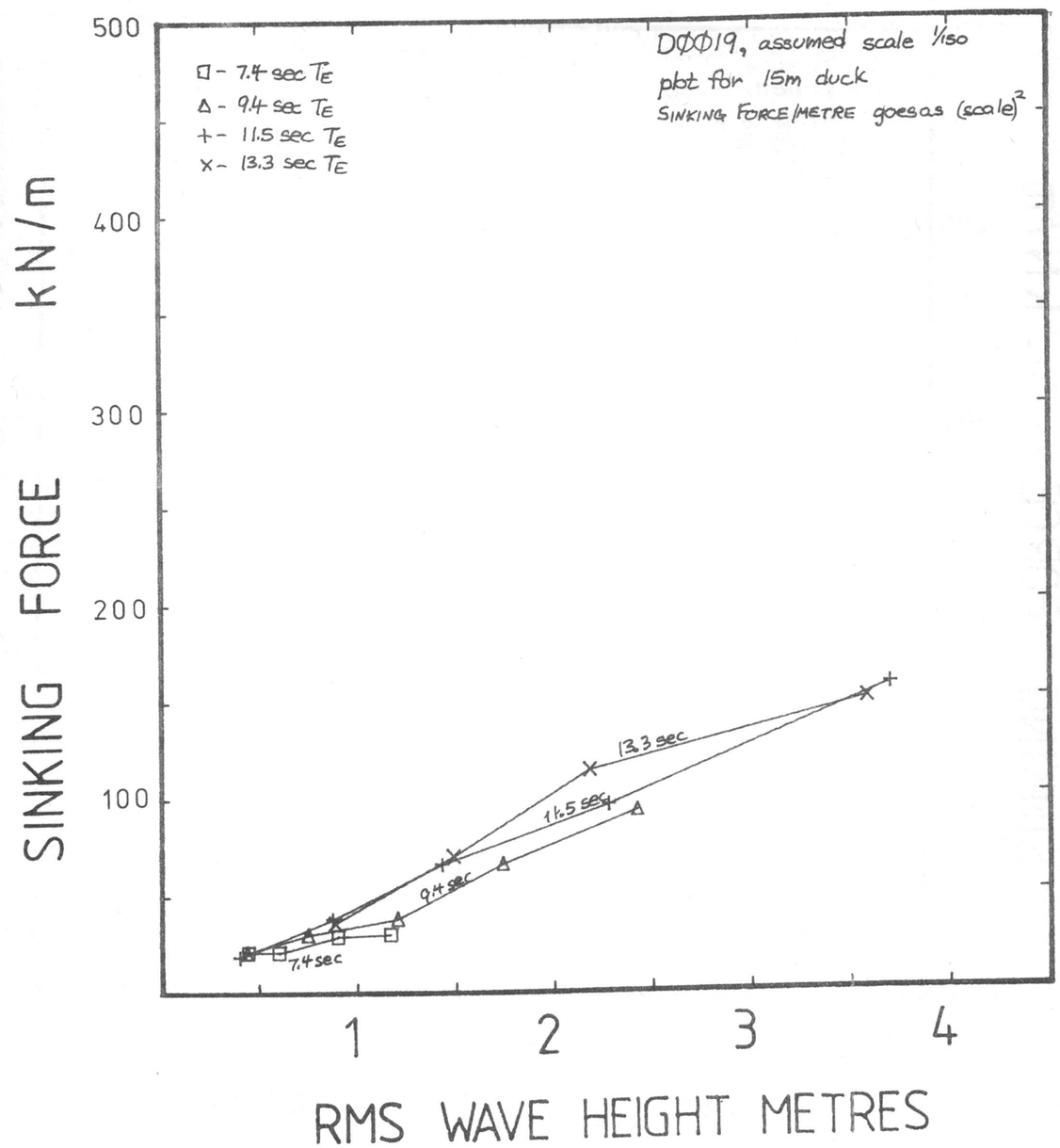

Scatter Diagram Tests

SINKING FORCE, FIXED RIG, ·5MNm/m TORQUE LIMIT

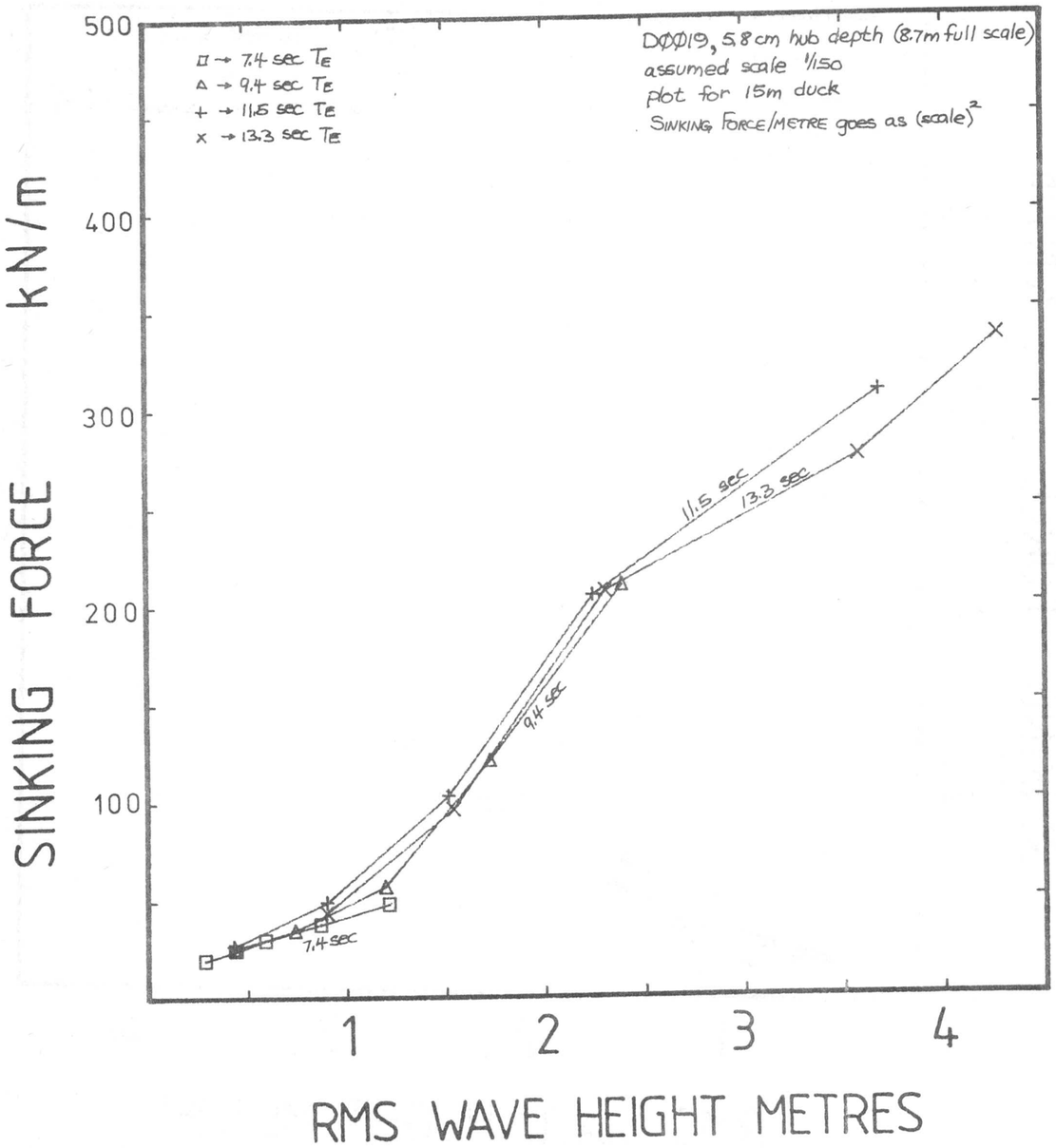

Scatter Diagram Tests

SINKING FORCE, FIXED RIG, 1MNm/m TORQUE LIMIT

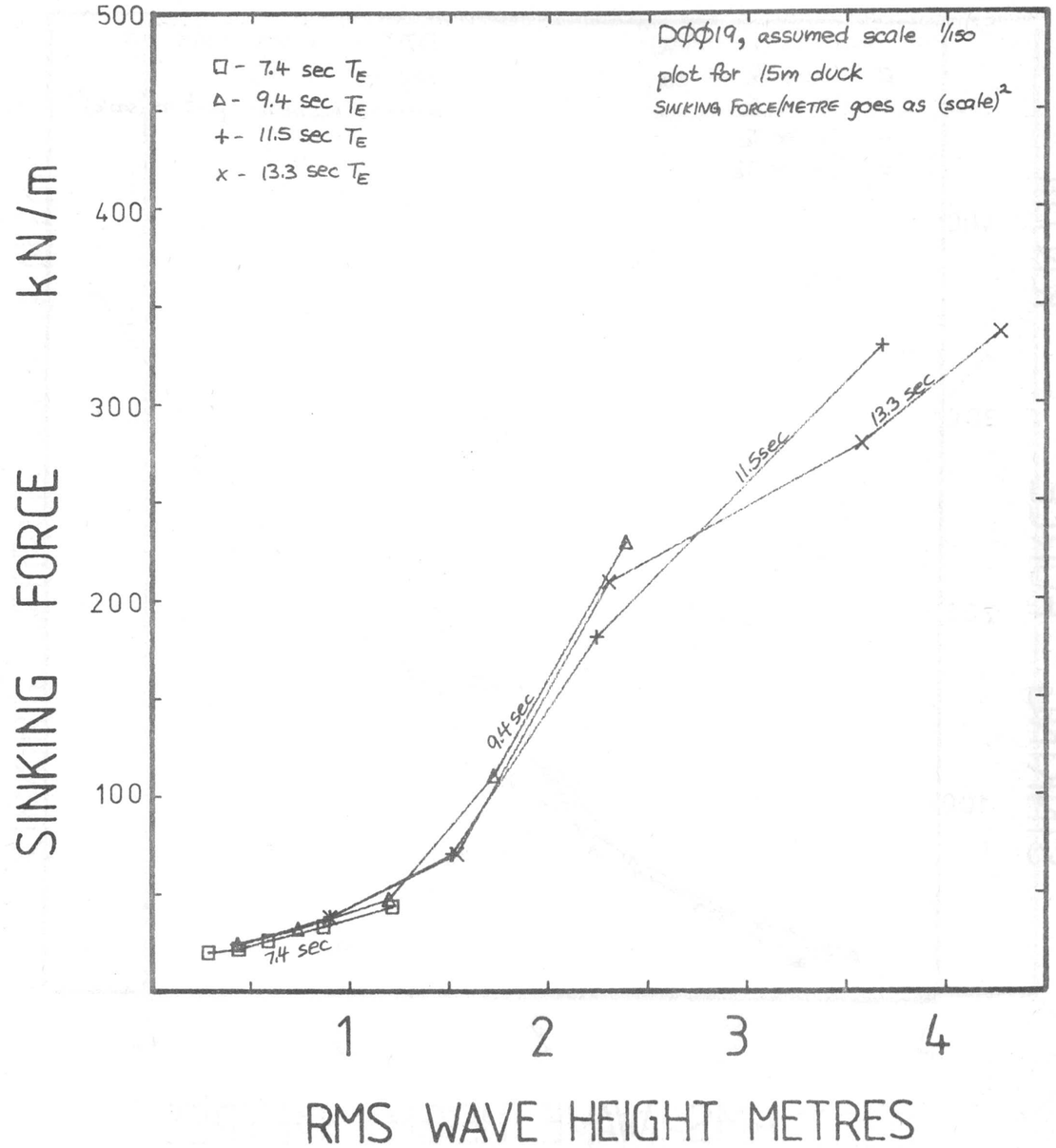

Scatter Diagram Tests

SINKING FORCE, FIXED RIG, 2MNm/m TORQUE LIMIT

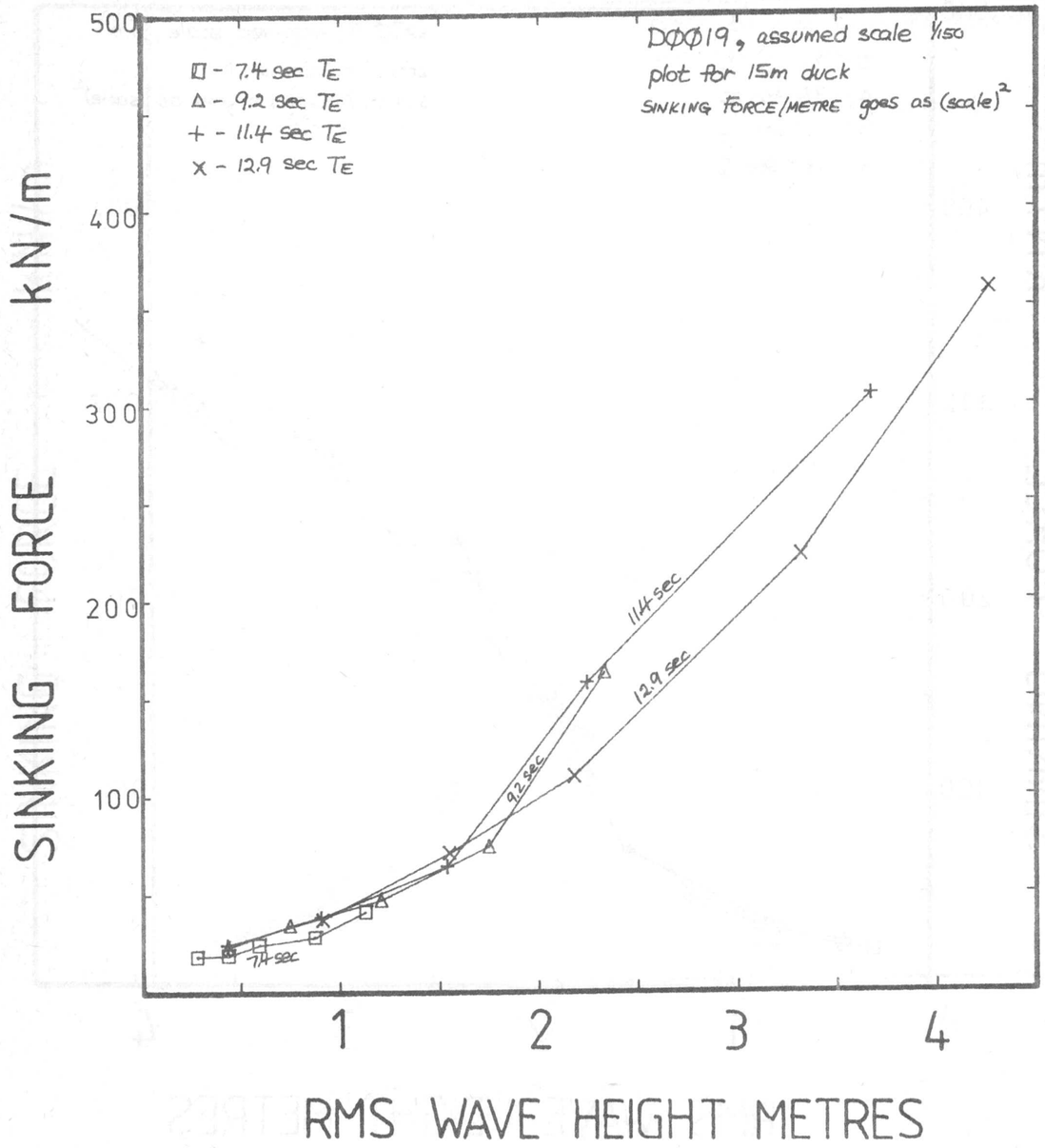

Scatter Diagram Tests

SINKING FORCE, FIXED RIG, 3MNm/m TORQUE LIMIT

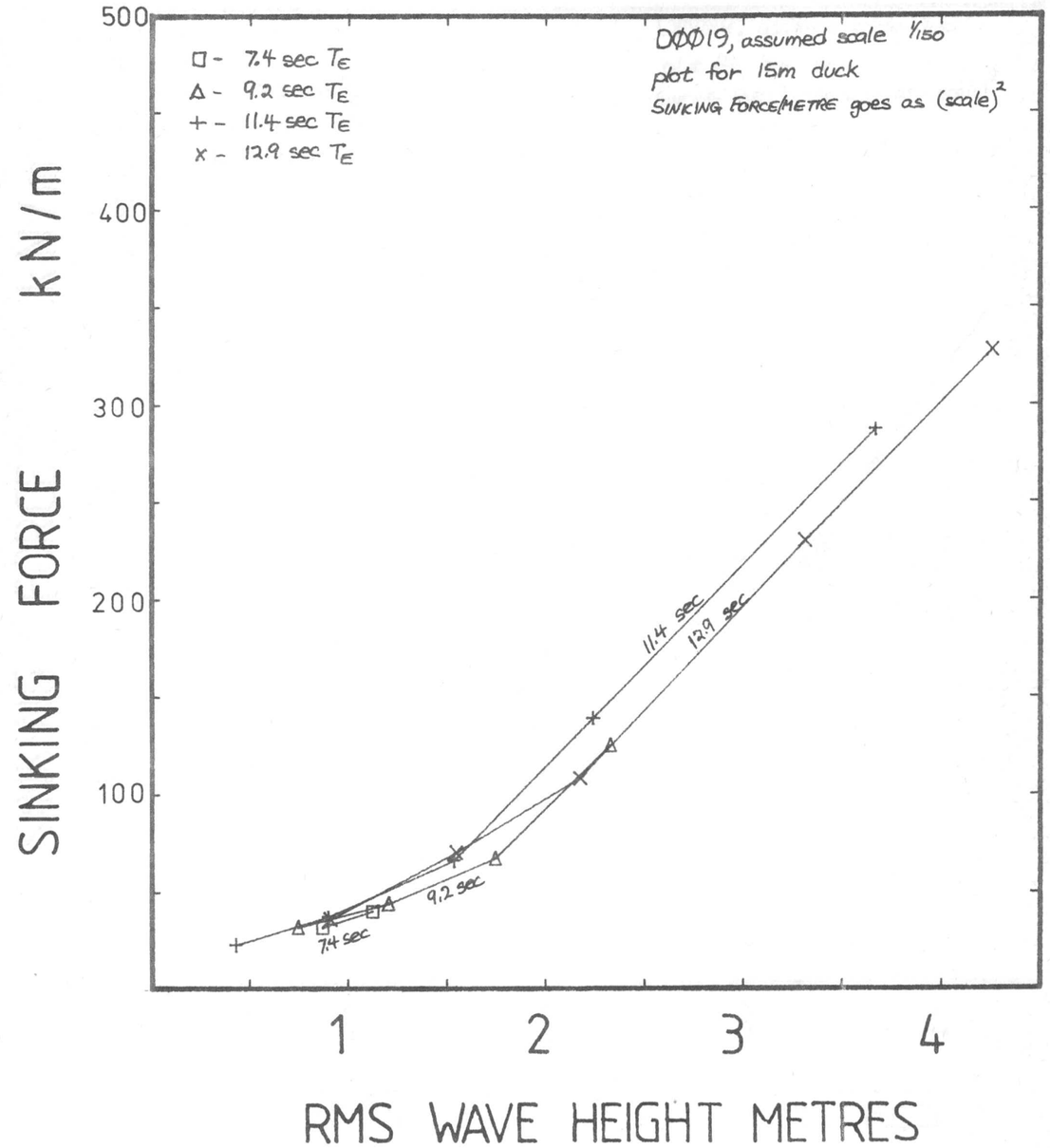

Scatter Diagram Tests
SINKING FORCE, FIXED RIG

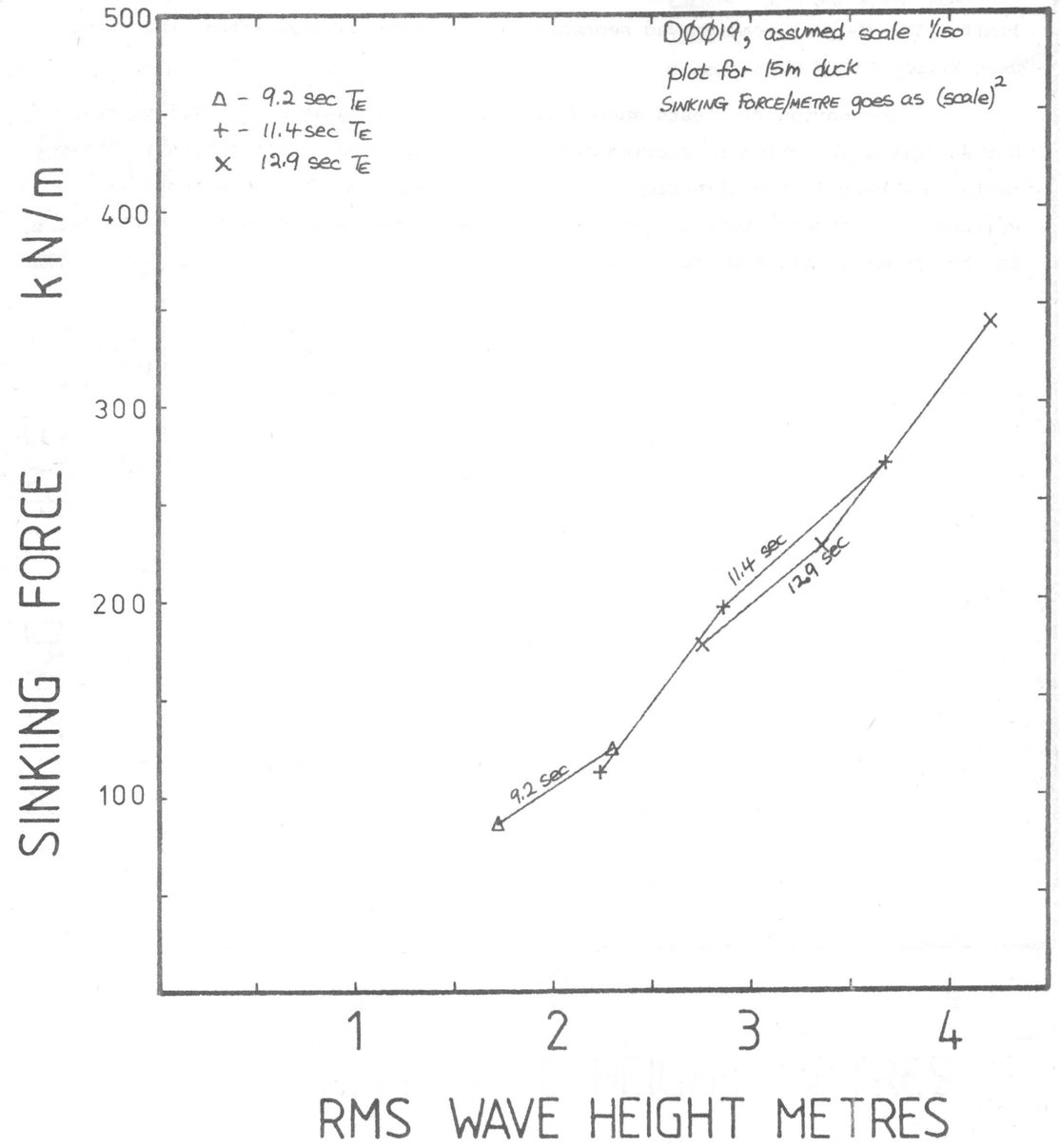

MOORING FORCE

Mooring force, the mean force in the surge direction, is much smaller than the sinking force. Like the sinking force, is has a "leftover" force of 20 kN/m at small wave amplitudes. Mooring forces are fairly independent of torque limit. The shorter seas showed somewhat greater mooring forces than the longer seas.

The moving rig tests showed similar results up to H_{rms} = 1,5 metres, but an actual reduction in mooring force above this level. All forces in these tests have been in the direction of the wave propagation, but some tests on cylinders and observations in our wide tank have shown that mean forces can be in the opposite direction to the wave travel.

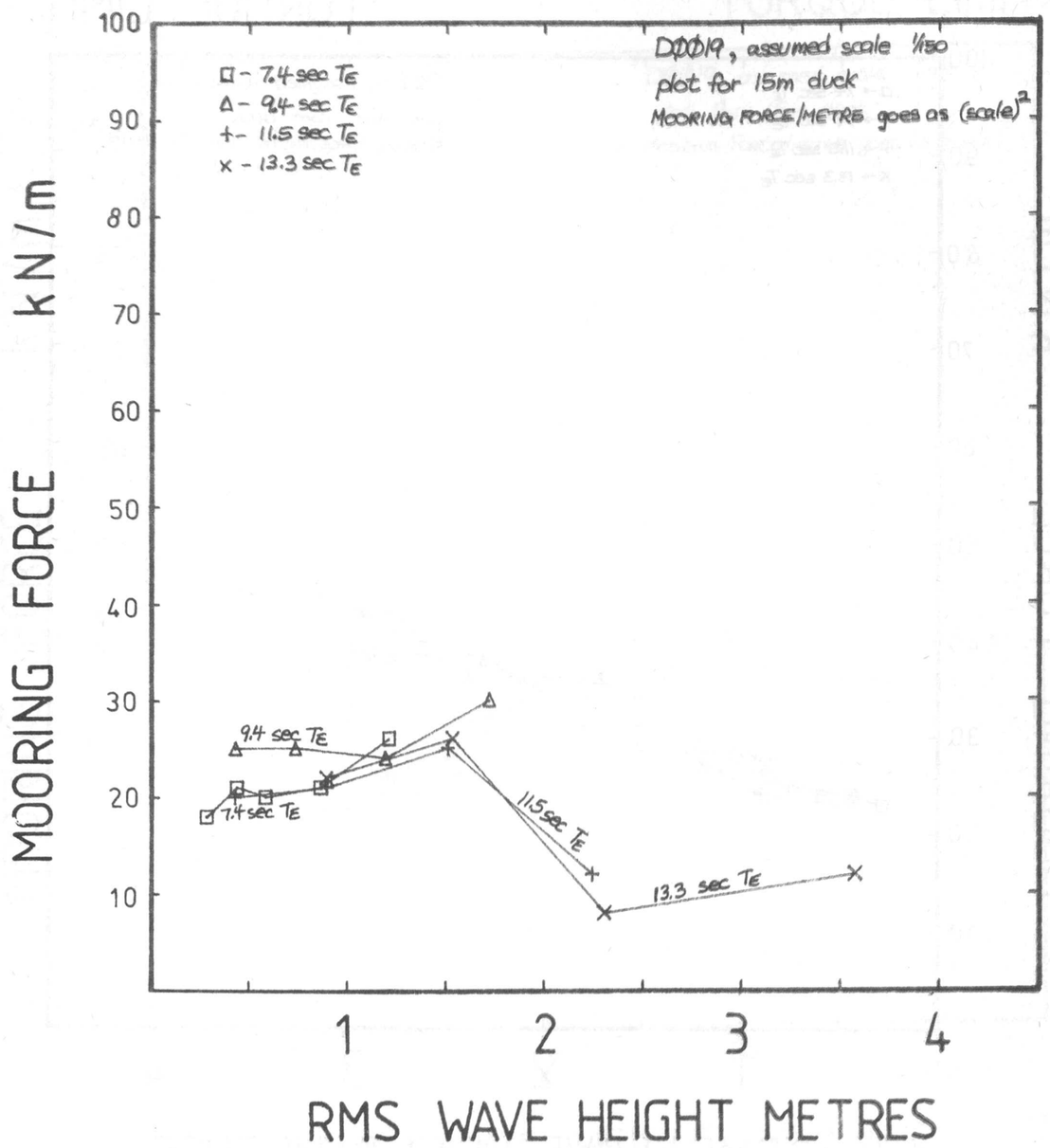

Scatter Diagram Tests

MOORING FORCE, FIXED RIG, 5MNm/m TORQUE LIMIT

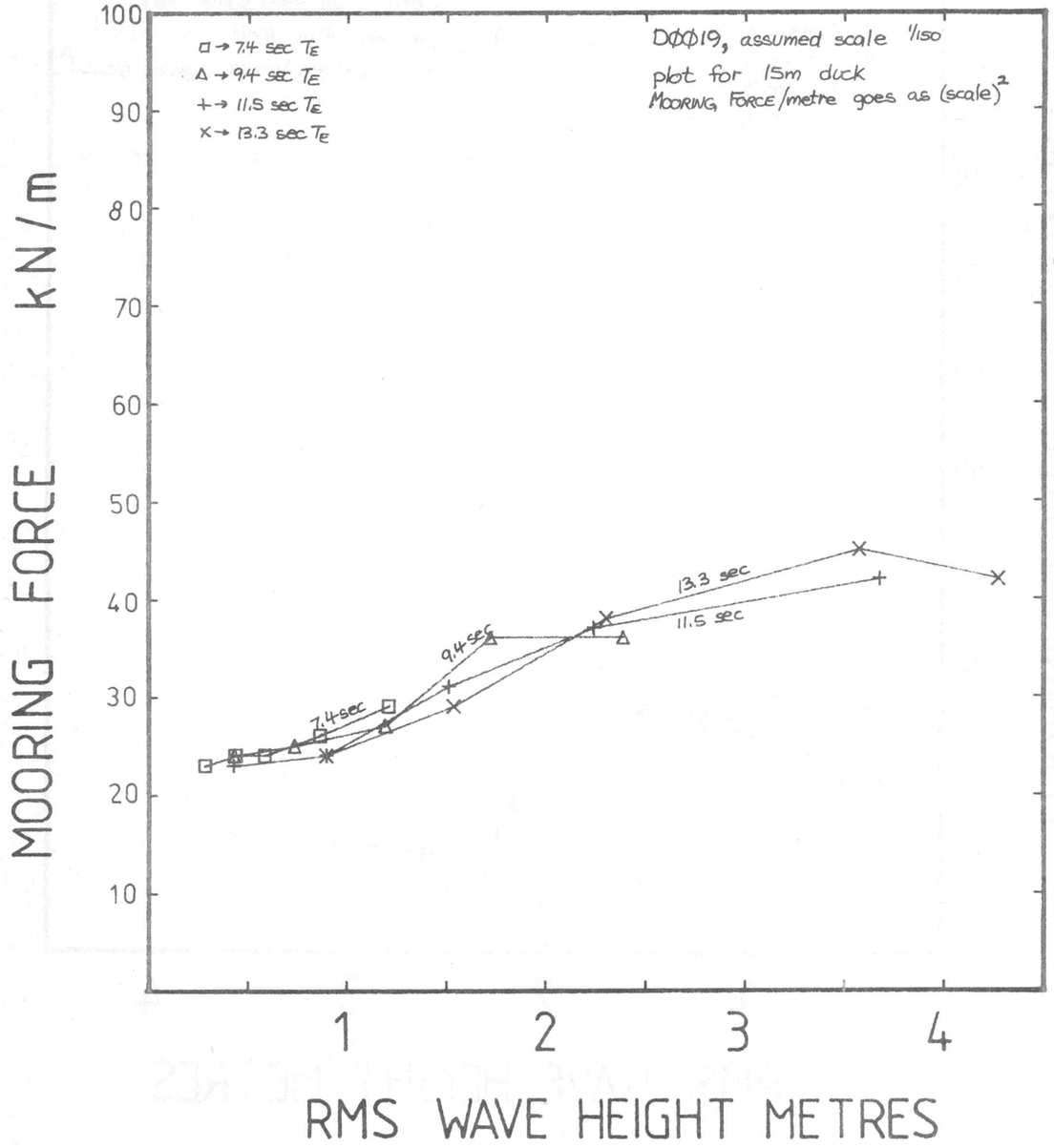

Scatter Diagram Tests

MOORING FORCE, FIXED RIG, 1MNm/m TORQUE LIMIT

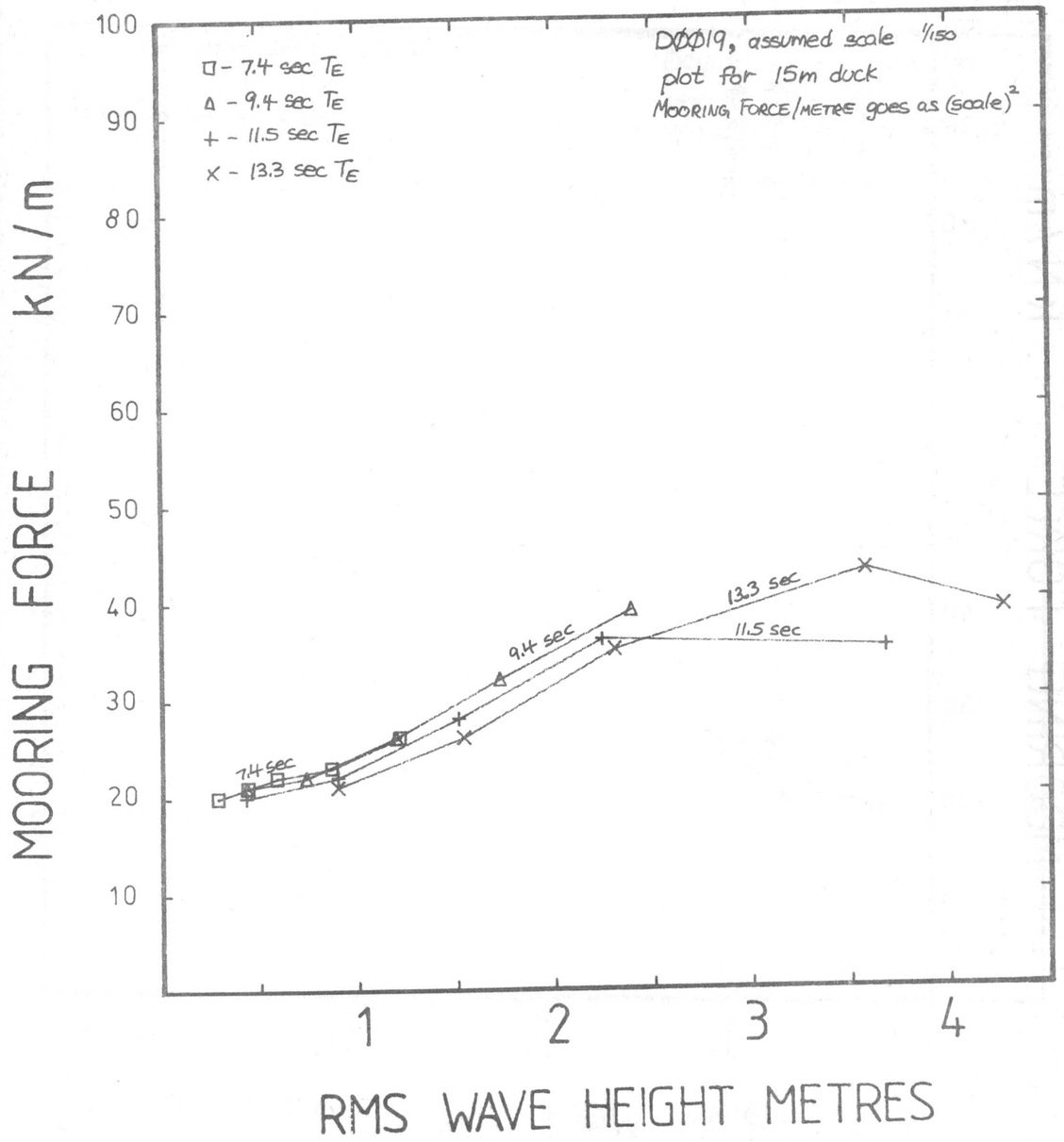

Scatter Diagram Tests

MOORING FORCE, FIXED RIG, 2MNm/m TORQUE LIMIT

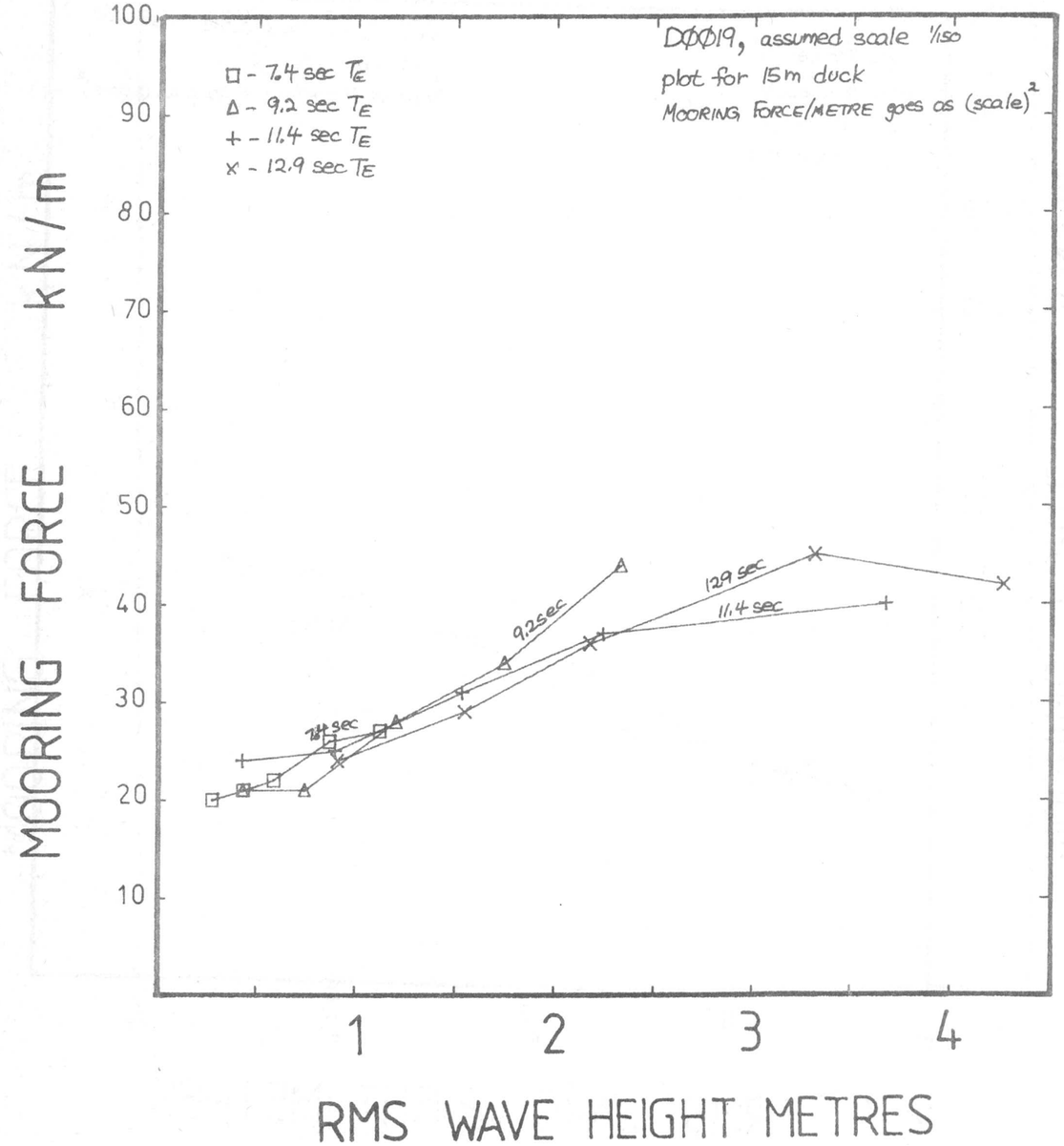

Scatter Diagram Tests

MOORING FORCE, FIXED RIG, 3MNm/m TORQUE LIMIT

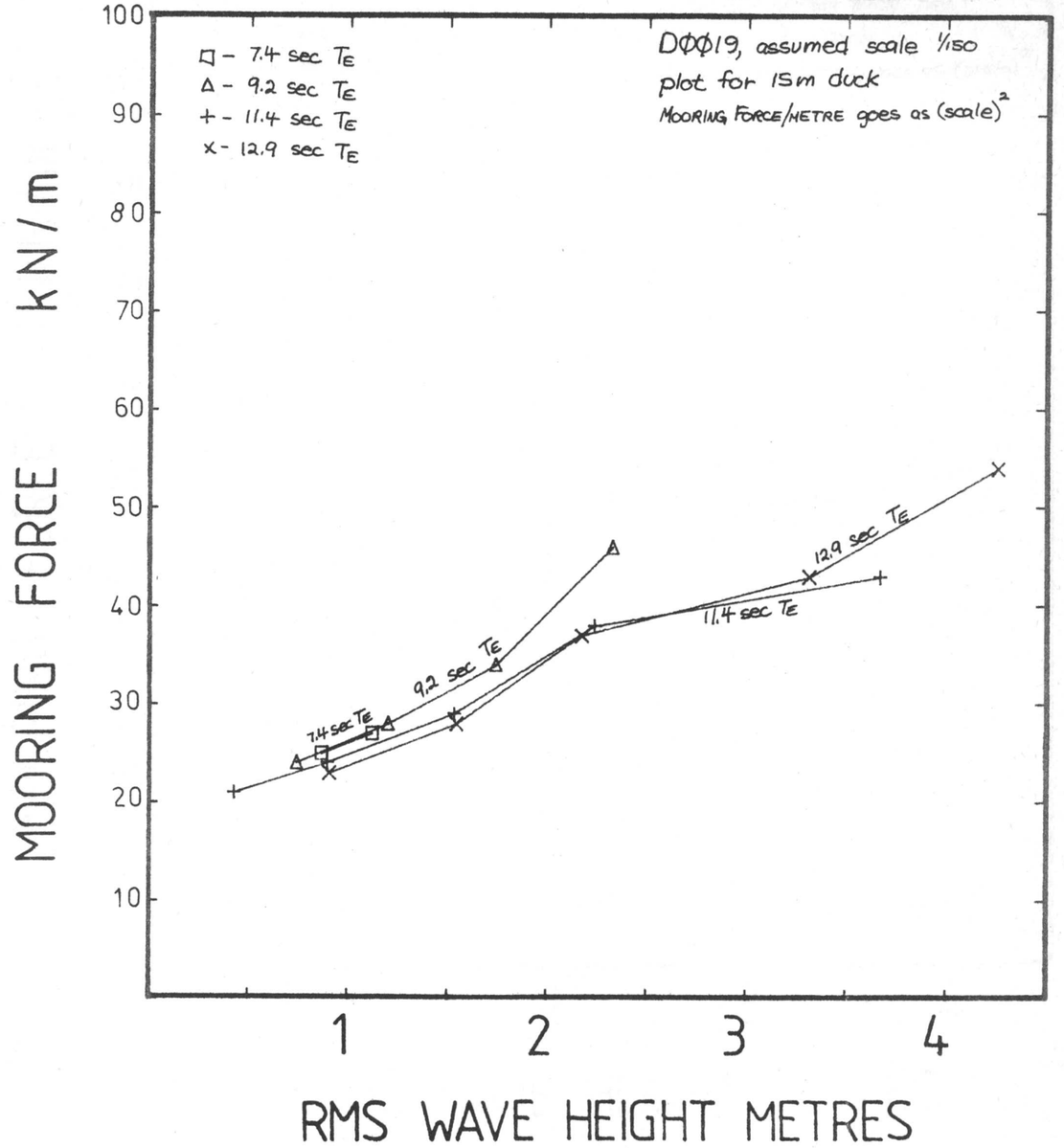

Scatter Diagram Tests

MOORING FORCE, FIXED RIG

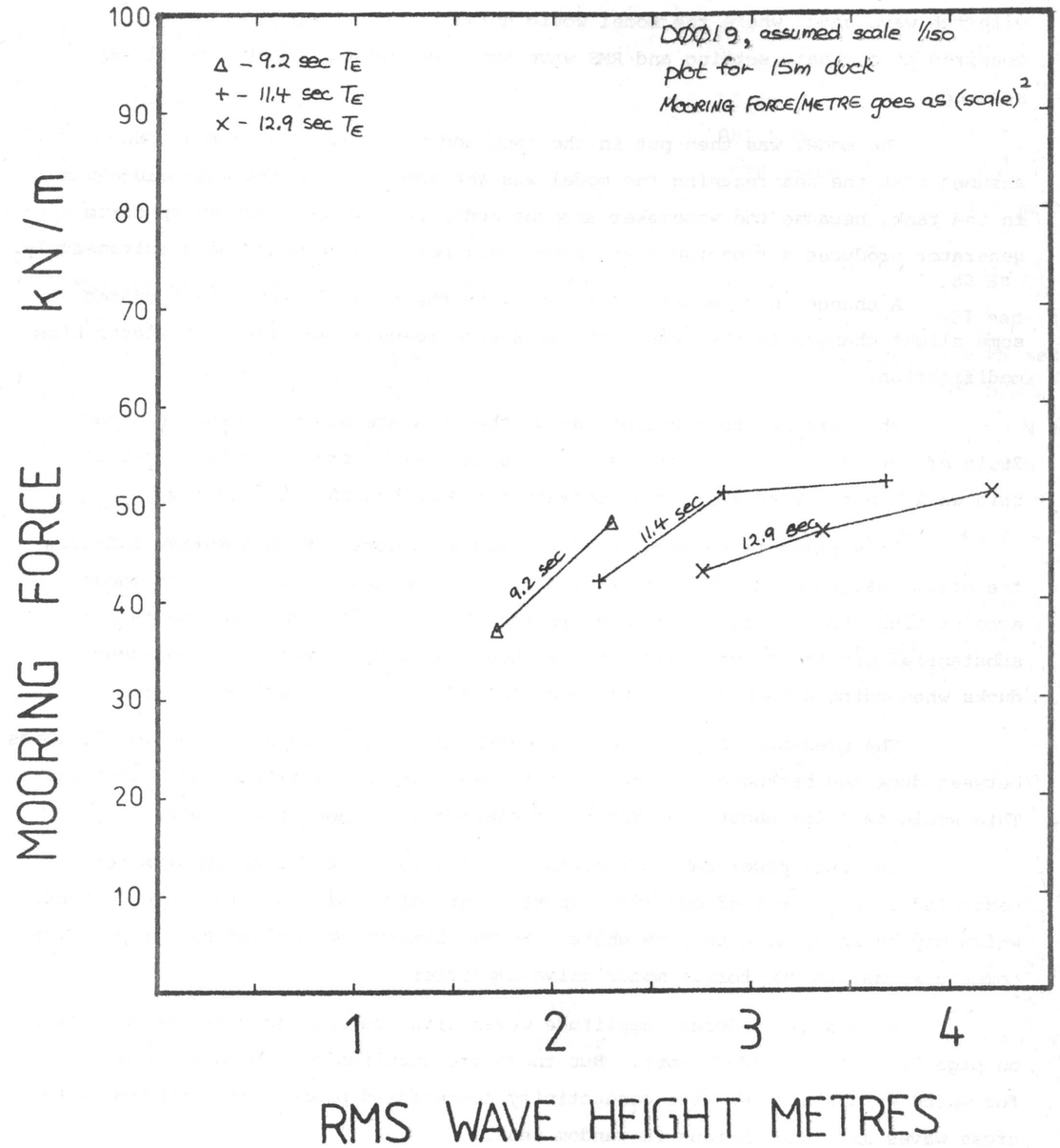

TESTING PROCEDURE

Since most of the parameters studied are not a strong function of energy period, we used only four values of T_e. We computed discrete spectra to approximate Pierson-Moskowitz spectra and measured the seas in the tank with the wave gauge where the model would normally be. Energy period was measured at one gain setting and RMS wave amplitude measured for several gain settings.

The model was then put in the tank and the seas were re-run. We assumed that the sea reaching the model was the same as when the wave gauge was in the tank, because the wavemaker absorbs model reflections and the spectrum generator produces a repeatable sequence. Parameters were measured simultaneously.

A change in wavemaker electronics in the middle of the tests caused some slight changes in the seas. The seas were re-measured after the electronics modification.

Photographs and descriptions of the rigs are given on page 26.3 and 26.15 of our 1976 report. Force sensing is done with torque strain gauges on thin wall tubes. They are fitted between the duck bearing and the rig.

This presents no problems for fixed axis work. With a moving axis rig the strain gauges sense the forces needed to accelerate the rig but not those accelerating the section of backbone inside the duck. The rig inertia is substantial but it is not clear how one should apportion inertia of adjacent ducks when using a backbone of intermediate and nonlinear compliance.

The presence of joints betwen backbone sections does not remove all loads between duck and backbone. We may have to deal with accelerations of ½ g or so. This would call for about 700 kN/m to accelerate a 13.5 metre backbone.

The duck power take-off mechanism is a force feed-back dynamometer described on page 26.1 of our 1976 report. This gives an angular velocity signal which may be integrated to give angle. Torque limits are applied by clipping the command signal to the torque motor drive amplifier.

We measure moderate amplitude waves with heaving float gauges as shown on page 26.7 of our 1976 report. But these are unsuitable in breaking waves for which we use a three-wire conductivity compensated probe. The problems with cross waves are less obvious in random seas.

TEST PARAMETERS & ACCURACIES

The model was ballasted as shown on page 3.2.

	MODEL SCALE	15 m SCALE
AXIS DEPTH IN CALM WATER	5.8 cm	8.8 m
TANK WIDTH	30 cm	
WATER DEPTH	60 cm	80 m
EDINBURGH GRAVITATIONAL ACCELERATION	981.5 cm/sec^2	
TANK WATER DENSITY	.998 gm/cm^3	
ASSUMED SEA WATER DENSITY		1.027 gm/cm^3
WAIT-TIME BEFORE MEASURMENT	30 sec	
SAMPLING RATE (SYNCHRONISED WITH SEA GENERATION)	10 Hz	.82 Hz
SAMPLING TIME	51.2 sec	627 sec
DYNAMOMETER DAMPING COEFFICIENT	5.4 Ncm sec/rad	7.6 MN sec/rad
MOVING RIG STIFFNESS (both axes)	2000 N/m	10^6 N/m^2
DAMPING	20 N sec/m	125000 N sec/m^2
FORCE LIMIT	3 N	230 kN/m
ACCURACIES:		
RMS WAVE MEASUREMENT	± 2% < 2 cm RMS	< 3 m
	± 5% > 2 cm RMS	> 3 m
PEAK WAVE MEASUREMENT	± 10% < 2 cm RMS	< 3 m
	± 20% > 2 cm RMS	> 3 m
TORQUE	± 3% < .5 rad	
	± 10% > 1 rad	
ANGLE (Max. trustworthy measurements +1.4, -1 rad)	± 3% < .5 rad	
RMS FORCE MEASUREMENTS	± 5%	
PEAK FORCE MEASUREMENTS	± 10%	
AVERAGE FIXED RIG FORCE ZERO STABILITY OVER TEST	± .02 N	1.4 x 10^3 kN/m
AVERAGE MOVING RIG FORCE ZERO STABILITY OVER TEST	± .05 N	3.8 x 10^3 kN/m
MAXIMUM FORCE RANGE	± 100 N	7.7 x 10^6 N/m
MAX. FORCE ZERO DRIFT FOR USE OF MEAN FORCE	± .1 N	7.1 x 10^3 N/m
MAX. FORCE ZERO DRIFT FOR USE OF ANY FORCES	± .3 N	23 x 10^3 N/m

CHARACTERISTICS AND DRAWING OF MEDIUM-BEAKED DUCK D0019

The hump-backed duck design is the result of tests in big waves. The humps have no effect in small waves so that efficiency is kept high when we need it. But as soon as we have generated more power than the transmission system can absorb it is desirable to dump the surplus by making waves astern. This has the useful effect of reducing the mooring forces. Indeed, the tests shown on page 2.73 show that mooring forces can get lower at high wave amplitudes.

The drawing on page 3.2 shows D0019 as ballasted for most of the tests in this report. The moving-magnet dynamometer which is necessary for the high torque limit tests is overweight. It lies across the nod axis inside the space reserved for backbone. Its presence has much more effect on the radial distance of the centre of gravity than on the moment of inertia or the pendulum behaviour of the duck. There is good agreement between the performance of D0019 and its 1/15th scale version, D0012, tested at Feltham, which had all ballast weights outside the backbone area. We tried extra inertia in D0020 with disappointing results and so we think that any changes should be such as to reduce the nodding inertia.

The important parameter is the angle between the line of profile symmetry and the line joining the CG to the nod axis. This determines whether or not the duck will recover from capsize. We recommend that an intermediate recovery rate is best and this occurs with CG angles of about 10°. We may try a little less for ducks on mountings with high heave compliance. It will also be interesting to try duck profiles with slightly slimmer paunches and fatter humps. However, the symmetrical version has the advantage for mid-ocean use that a very small ballast movement will let it take waves from astern. This will be a useful feature for stations in mid-ocean and north of Orkney.

The ballasting arrangements have not yet been modified for the zero heave stiffness mounting.

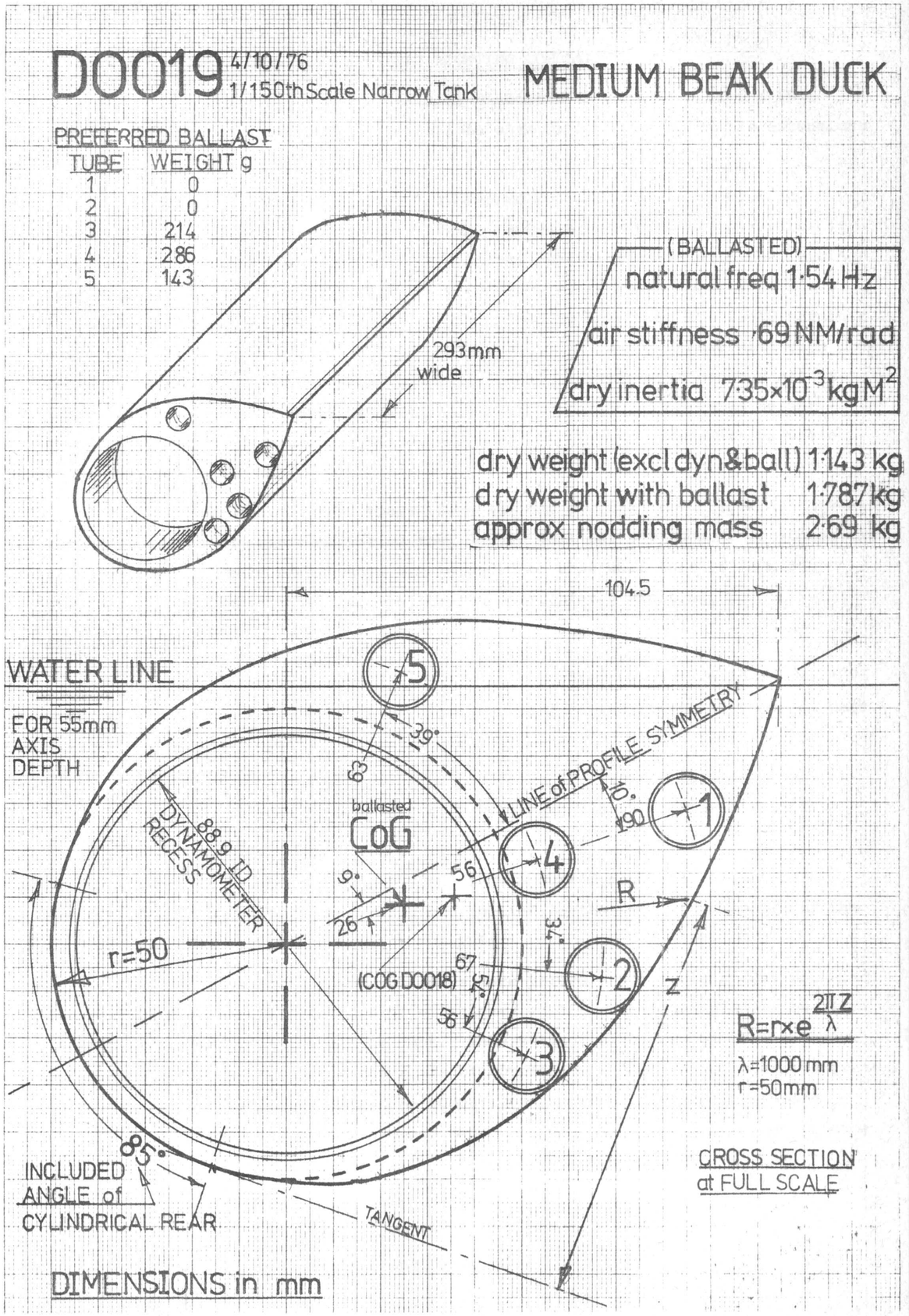

EXPERIMENTS WITH VARIABLE MOUNTING COMPLIANCE

The background to these tests is discussed on page 25.6 of the 1976 report. The idea started during discussions with David Evans about his extensions to Ogilvie's work.

Ogilvie[1] has shown that a submerged cylinder rotating about an eccentric axis makes waves on one side only. Evans predicted that in reverse it would make an excellent wave absorber and he has demonstrated it with the surging/heaving rig. We can understand how the phenomenon arises by arguing as follows. The circular motion of the cylinder could be produced by giving it simple harmonic motions in the heave and surge directions which are 90^{o} out of phase with each other. The waves produced by the heave motion alone would be symmetric fore and aft of the cylinder, while the waves produced by the surge motion along would be anti-symmetric. When both motions combine, the waves on one side are additive while those on the other cancel.

Evans[2] emphasized that these ideas are not peculiar to cylinders. Given the correct mounting characteristics they should work for any object, including the back of a duck. These experiments are intended to show what sort of mounting stiffness is desirable. We find the results particularly exciting.

APPARATUS

We used the surge/heave/pitch rig as described on page 26.15 of our 1976 report. The duck was D0019 with waterline and ballast conditions as shown on page 3.1 and 3.2 of this report. These had been optimised for best performance at 10^{6} N/m^{2} stiffness density.

Tests were made in regular waves with wave length to diameter ratio = 8.00, 10.8, 15.6, 19.3 and 21.6.

At first we used simple damping in the duck dynamometer with torque proportional to velocity. No damping was applied to the rig. The inertia of the rig was reduced to the minimum value possible.

Both heave and surge compliances were varied and efficiency was measured. The results are shown as contours of efficiency in the compliance plane with all parameters scaled up as for a 15 m duck. Interesting things happen at high heave compliance and so we have made the scale of compliance in that axis ten times greater than for surge in all the graphs. As comparisons between different tests are particularly important, we have grouped miniature graphs on the same pages to show the effects of:

(1) wave length
(2) extra inertia
(3) negative spring in nod

EXPERIMENTS WITH VARIABLE MOUNTING COMPLIANCE

(1) WAVELENGTH & COMPLIANCE

All the graphs show two regions of high efficiency which are separated by a valley, running parallel to the surge compliance axis, in which the efficiency is under 20%. No tests were done below 20% but it was almost as if one could tune for zero efficiency.

As wavelength increases

(a) the two high efficiency regions move towards the high surge compliance direction and keep fairly well abreast

(b) contours separate towards the high heave compliance direction.

It is reasonable to expect that long period waves would have greater crest length. This would make the ducks think that they were on more compliant mountings, so behaviour with wavelength appears to be particularly fortunate. It is an unexpected bonus comparable with the wavelength behaviour of added inertia which keeps ducks in tune.

If rigidity costs money and compliance is cheap, the area of high heave compliance is very attractive.

DUCK EFFICIENCY on COMPLIANT AXIS

5 Wavelengths

dynamometer: DAMPING ONLY

WAVELENGTH INCREASING ↓

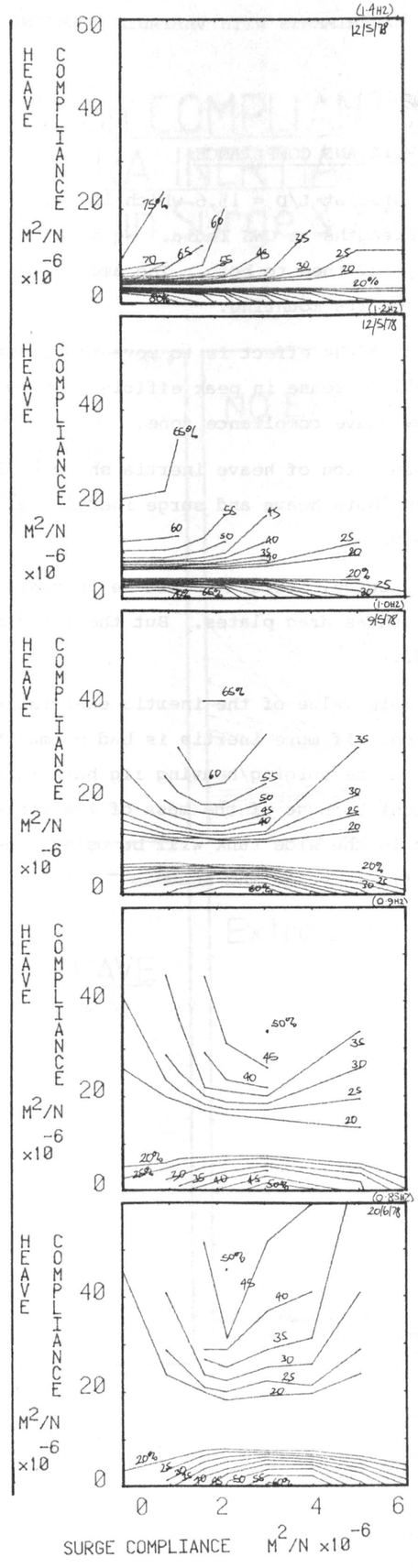

L/d=8·0 see p 4·10

L/d=10·8 see p 4·11

L/d=15·6 see p 4·12

L/d=19·3 see p 4·13

L/d=21·6 see p 4·14

(2) EXTRA INERTIA AND COMPLIANCE

We tested at L/D = 15.6 which is the centre of the commercially attractive wavelengths at OWS India. We added inertia to the heave axis only, surge axis only and then to both. The amount added roughly doubled the inertia of a dry duck and its mounting.

In surge the effect is to move the right-hand contours towards the left. There is a small increase in peak efficiency from 60% to 70% but only over a small area in the low heave compliance zone.

The addition of heave inertia shows a similar crushing in the heave direction. When both heave and surge inertia values are increased, crushing in both axes occurs.

In practice, inertia could be increased by the addition of appendages to the spine such as drag plates. But these tests suggest that it would be a bad thing to do.

The main value of the inertia exercise comes from the doubtful practice of extrapolation. If more inertia is bad we may hope that less inertia will be good. Models on the surging/heaving rig have inertia values higher than the simple duck displacement because of the mass of the linkage and dynamometer. The free-floating ducks in the wide tank will be using a new dynamometer design which will have less inertia in surge and heave.

DUCK EFFICIENCY on COMPLIANT AXIS
the effect of EXTRA INERTIA, in Surge & Heave

L/d=15·6

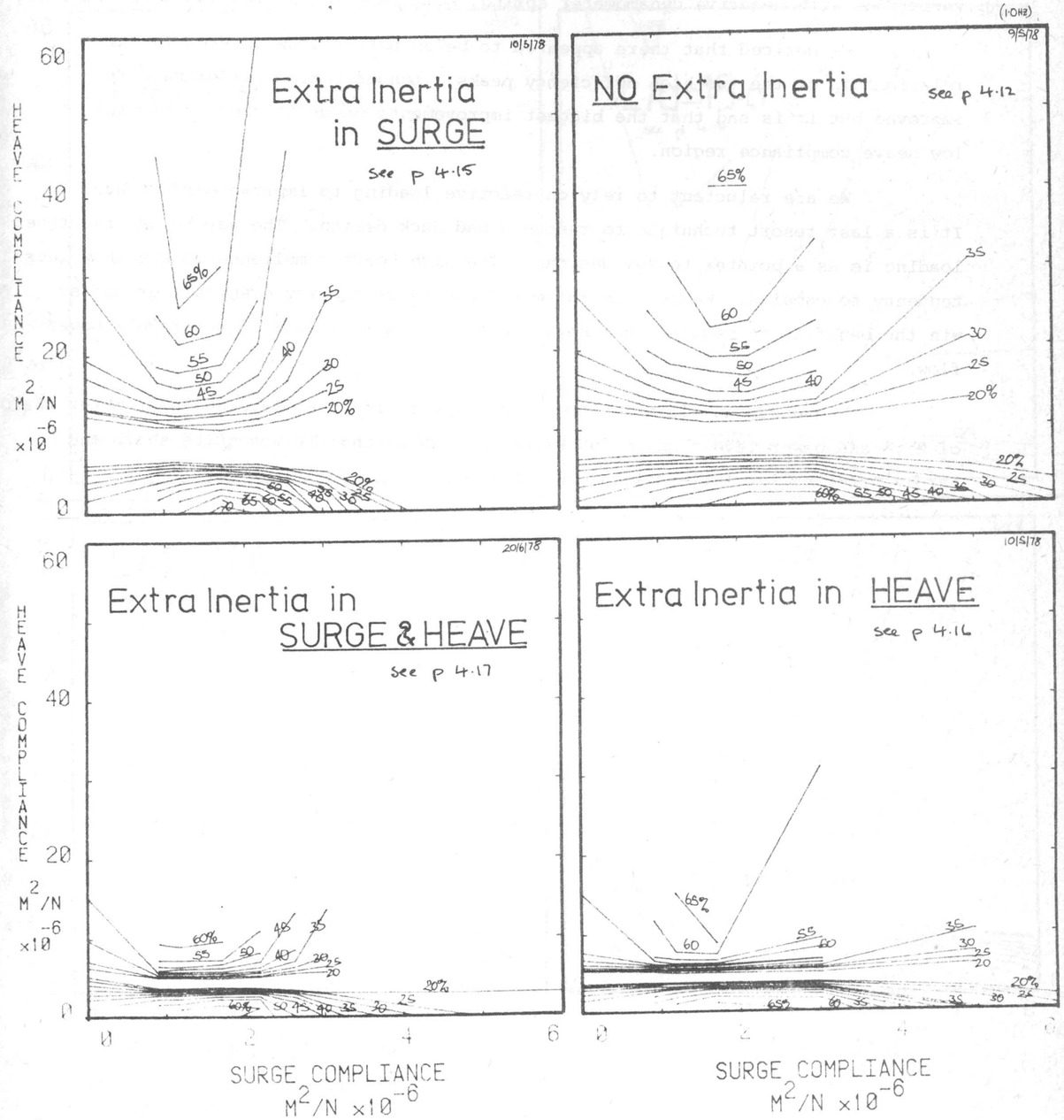

(3) NOD SPRING AND COMPLIANCE

The ballasting for D0019 was optimised for good capsize recovery in extreme waves. We were also trying to maintain wideband performance without smart power take-off (see page 41, 1975 Report). But when we combined compliance variations with negative dynamometer spring, some interesting results were obtained.

We noticed that there appeared to be an anti-clockwise skew in the relationship of the two high efficiency peaks. Longer period performance is improved but it is sad that the biggest improvements occur to the peak in the low heave compliance region.

We are reluctant to rely on reactive loading to improve performance. It is a last resort technique to rescue a bad duck design. The way to use reactive loading is as a pointer to new designs. The high heave compliance models show less tendency to capsize. We hope to raise the centre of gravity even further and so win the benefits of negative spring without the complications of reversible power flow.

There was an all-time record of 73% efficiency at wavelength/diameter ratio of 21.6 and power levels up to 100 kw/metre. This pinnacle was quite sharp and hardly practical at full-scale.

DUCK EFFICIENCY on COMPLIANT AXIS
the effect of negative NOD SPRING at 2 wavelengths

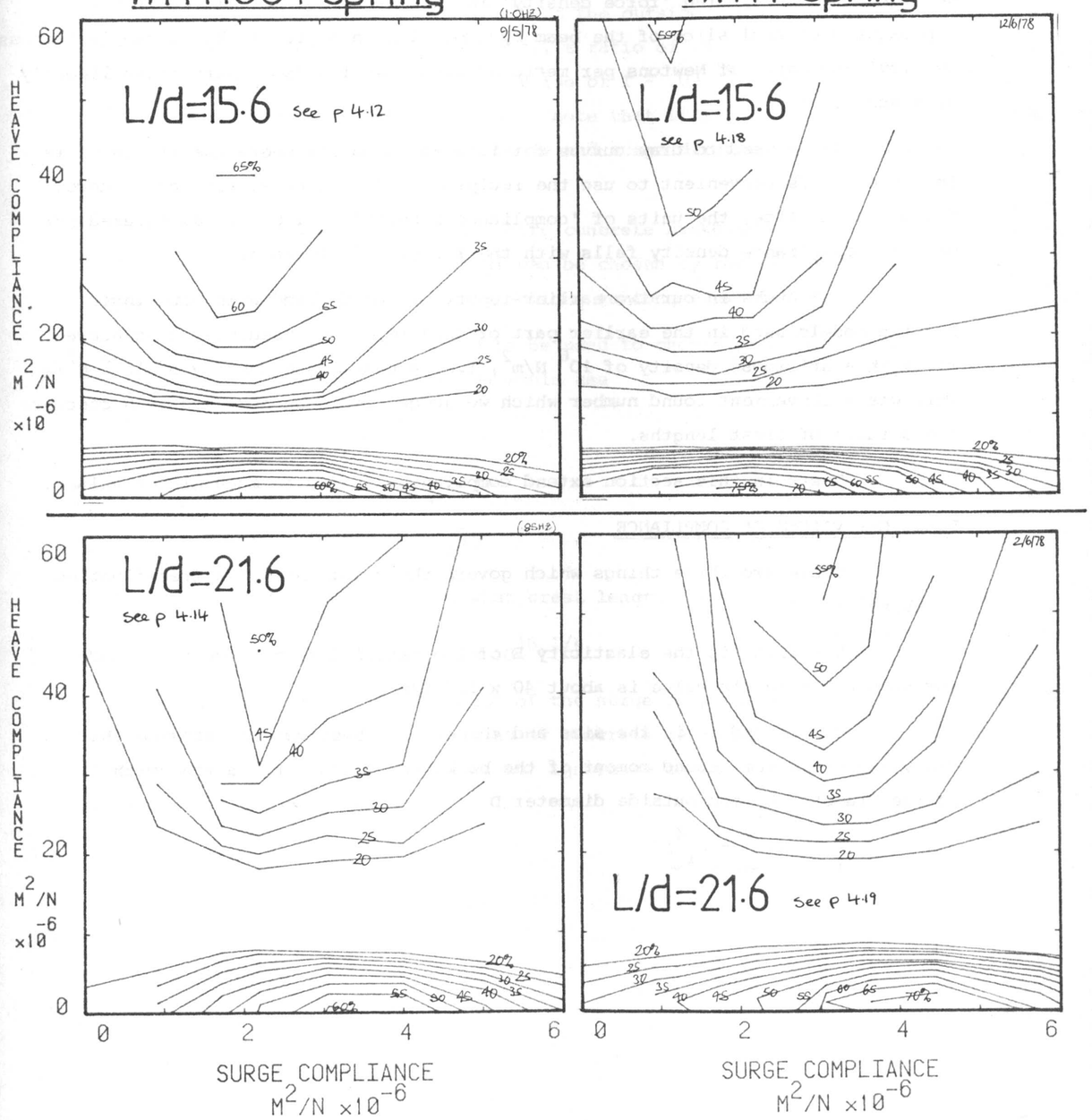

UNITS OF COMPLIANCE

If a force is applied to a spring and the extension observed, we describe the stiffness of the spring by the ratio of force to movement. The units of stiffness are Newtons per metre.

Now consider a distributed force field along the length of a long beam. We talk about an applied 'force density' in Newtons per metre. If we wish to represent a central slice of the beam by a model in a narrow tank, we use 'stiffness density' and units of Newtons per metre squared. Stiffness density rises linearly with scale.

If we need to draw curves for fixed-axis models where the stiffness is infinite, it is convenient to use the reciprocal of stiffness, i.e. compliance. For our beam slice, the units of 'compliance density' will be metres squared per Newton. Compliance density falls with the reciprocal of scale.

For ducks in our two earlier reports we used fixed-axis mountings. For the models used in the earlier part of this report we used the surge/heave rig with a stiffness density of 10^6 N/m^2, i.e. a compliance density of 10^{-6} m^2/N. This was a convenient round number which we judged could be achieved with concrete for a range of crest lengths.

Tests in this section extend compliance density to much higher values.

PRACTICAL VALUES OF COMPLIANCE

There are three things which govern the compliance of a free-floating backbone.

The first is the elasticity E of the material from which it is made. For good concrete its value is about 40×10^9 N/m^2.

The second is the size and shape. The best way to describe this is the value of I, the second moment of the backbone string. For a tube with inside diameter D_i and outside diameter D

$$I = \frac{\pi(D^4 - D_i^4)}{64}$$

If we make an air-filled neutrally buoyant tube out of material with specific gravity γ, then the ratio of the inner to the outer dimension is

$$\frac{Di}{D} = \sqrt{1 - \frac{1}{\gamma}}$$

The value of γ for concrete is about 2.4. This means that the inside diameter of an air-filled tube must be at least .76 of the outside. But to allow for bulkheads, extra machinery, buoyancy material, etc., a ratio of .8 is more probable. This leads to wall thickness of .1 D and a value of $I \simeq .03\ D^4$. The factor .03 will be convenient to remember. (We should also note that if it is not necessary to provide equal strength and rigidity in both heave and surge directions, we can choose I from, say, .01 to .05 D^4.)

The product EI for a 13.5 metre concrete backbone of even wall thickness will be about 4×10^{13} Nm^2. While EI can be chosen by the designer, he cannot control crest length except by lying oblique to long-crested swell.

If static beam theory had to be used to choose compliance values K for model tests in a narrow tank, we would use

$$K = \frac{C^4}{16\pi^4 EI}$$

$$= \frac{C^4}{6.23 \times 10^{16}}$$

Alternatively, if we need to know what crest length our K value represents, we use

$$C = (K \times 6.23 \times 10^{16})^{1/4}$$

In our graphs, the midpoint of the surge compliance axis is 3×10^{-6} m^2/N for which C = 658 metres. It seems as if concrete backbones have more than enough rigidity but it is a great pity that our ignorance on the subject of crest length statistics is so extensive.

DUCK EFFICIENCY on COMPLIANT AXIS

monochromatic sea: T=8·7 sec; L/d=8·0

parameters scaled up to represent 15m dia duck

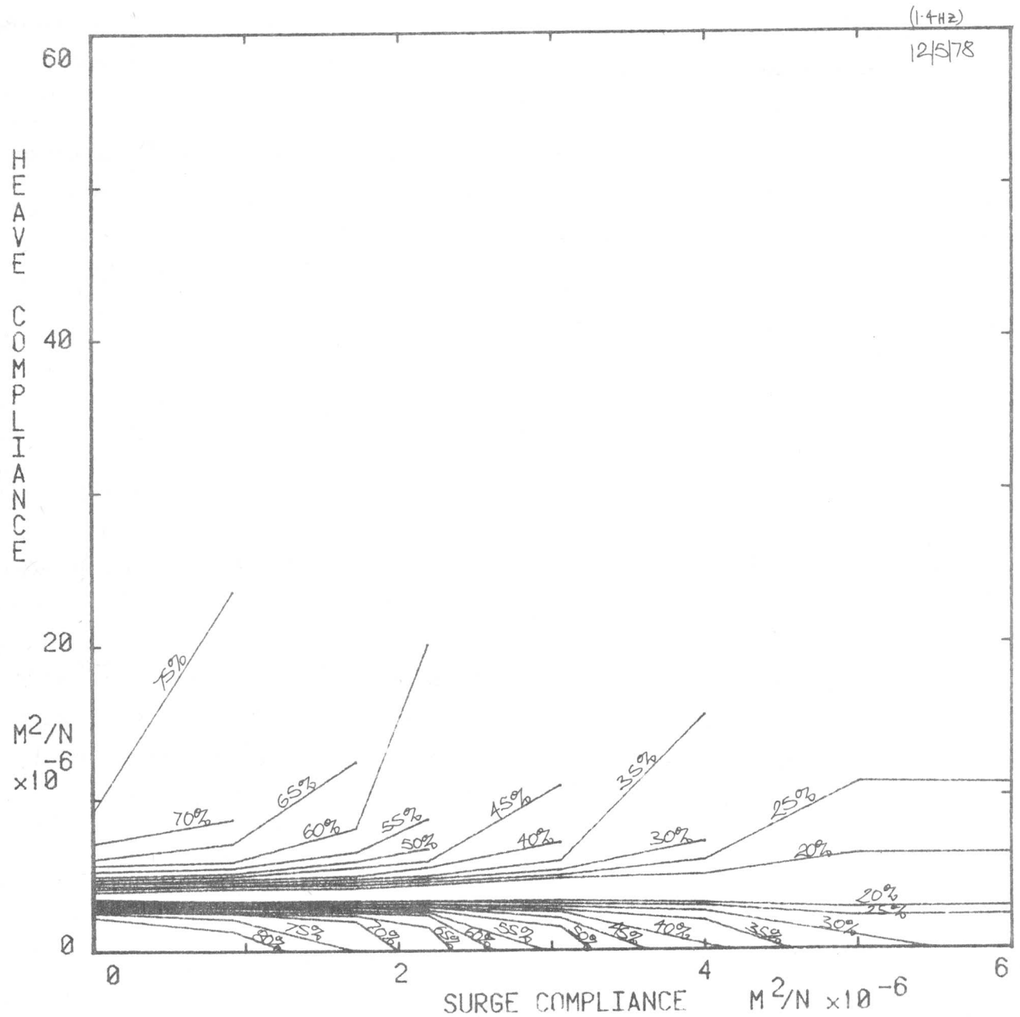

D0019

total surge inertia: 374 tonnes/m total heave inertia: 542 tonnes/m	nod damping: 7·7 MN/rad/s/m

DUCK EFFICIENCY on COMPLIANT AXIS

monochromatic sea: T=10·2sec; L/d=10·8

parameters scaled up to represent 15m dia duck

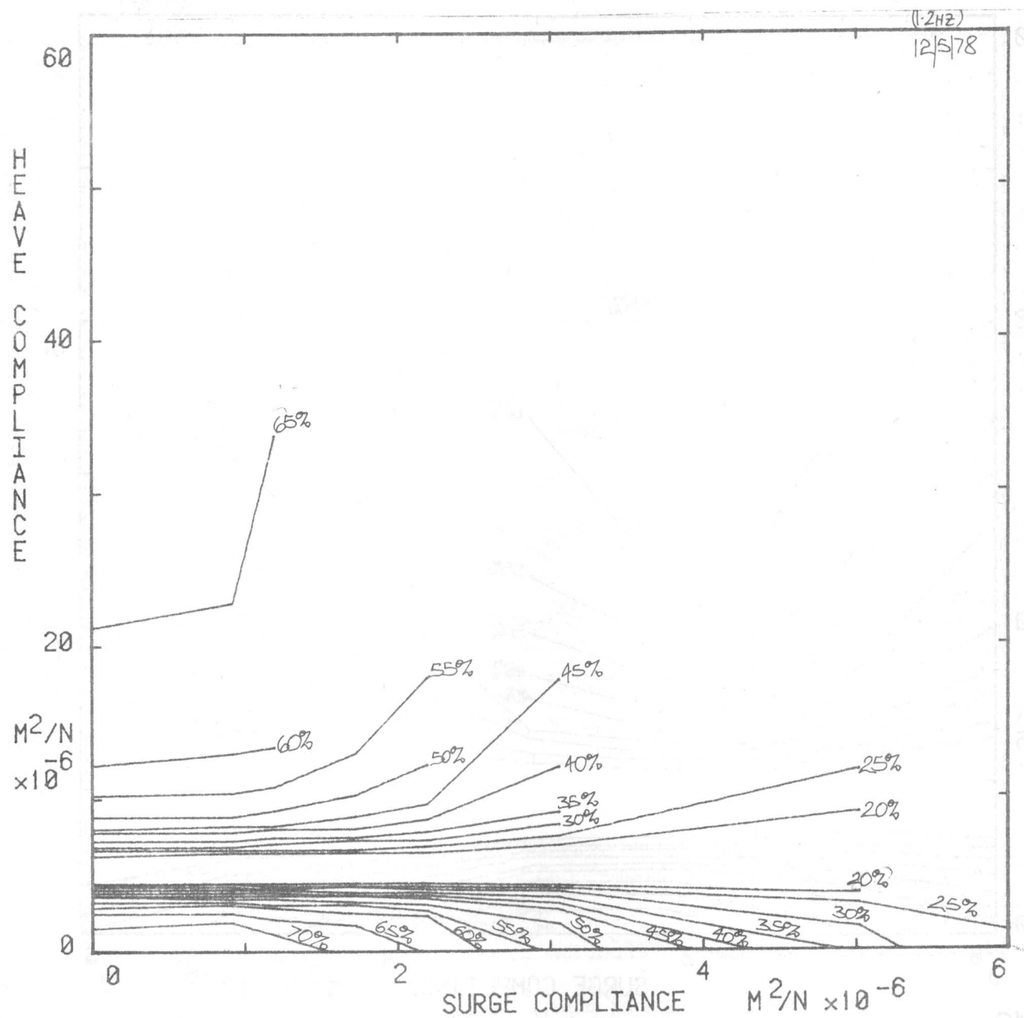

D0019

total surge inertia: 374 tonnes/m total heave inertia: 542 tonnes/m	nod damping: 7·7 MN/rad/s/m

DUCK EFFICIENCY on COMPLIANT AXIS
monochromatic sea: T=12·2 sec; L/d=15·6

parameters scaled up to represent 15m dia duck

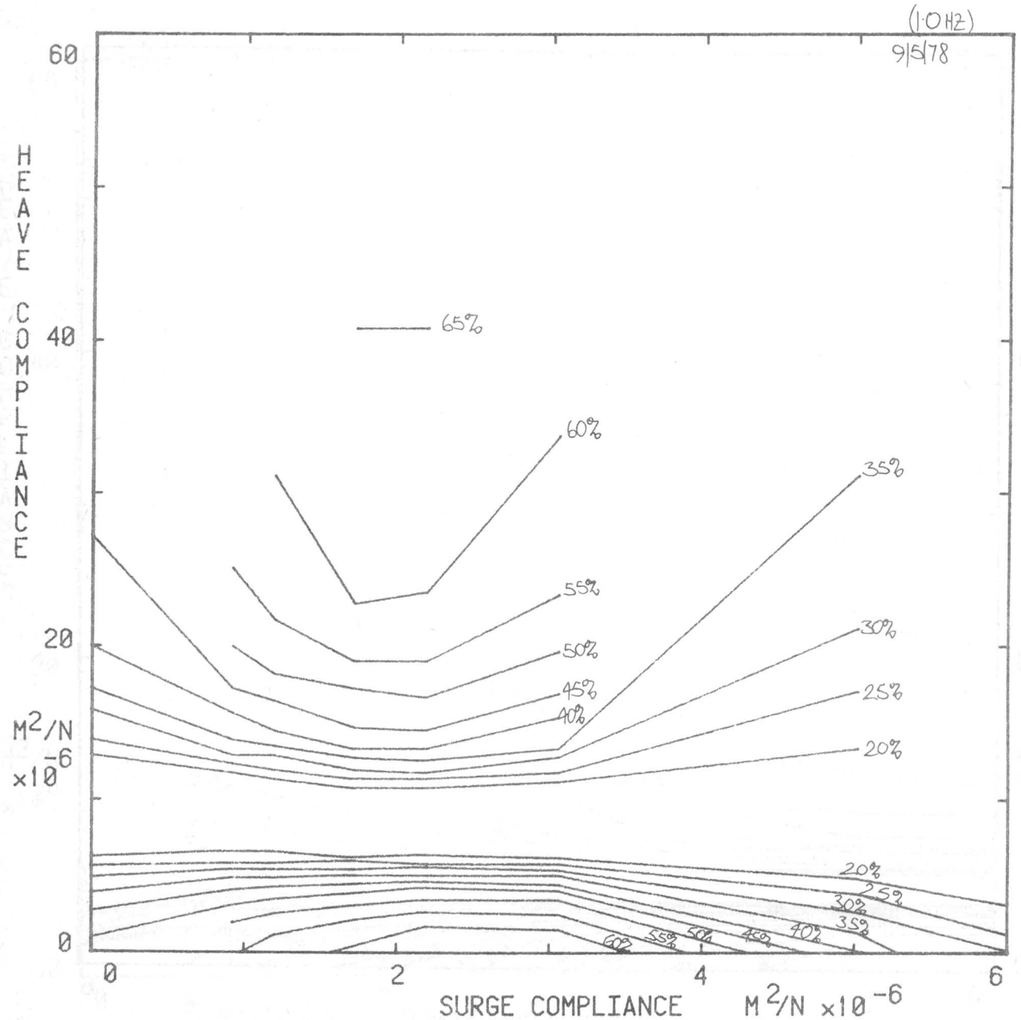

D0019

total surge inertia: 374 tonnes/m total heave inertia: 542 tonnes/m	nod damping: 7·7 MN/rad/s/m

DUCK EFFICIENCY on COMPLIANT AXIS
monochromatic sea: T=13·6 sec; L/d=19·3

parameters scaled up to represent 15m dia duck

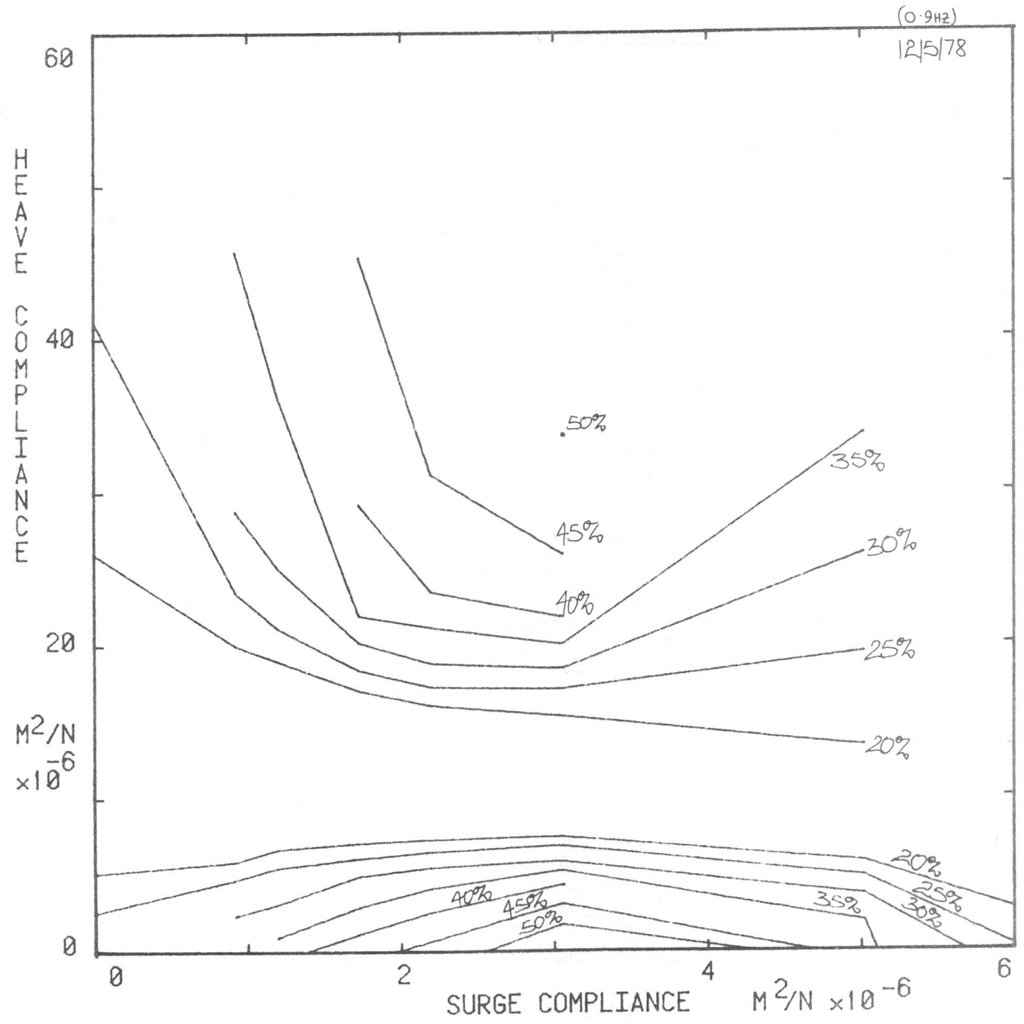

D0019

total surge inertia: 758 tonnes/m total heave inertia: 542 tonnes/m	nod damping: 7·7 MN/rad/s/m

DUCK EFFICIENCY on COMPLIANT AXIS

monochromatic sea: T=14·4sec; L/d=21·6

parameters scaled up to represent 15m dia duck

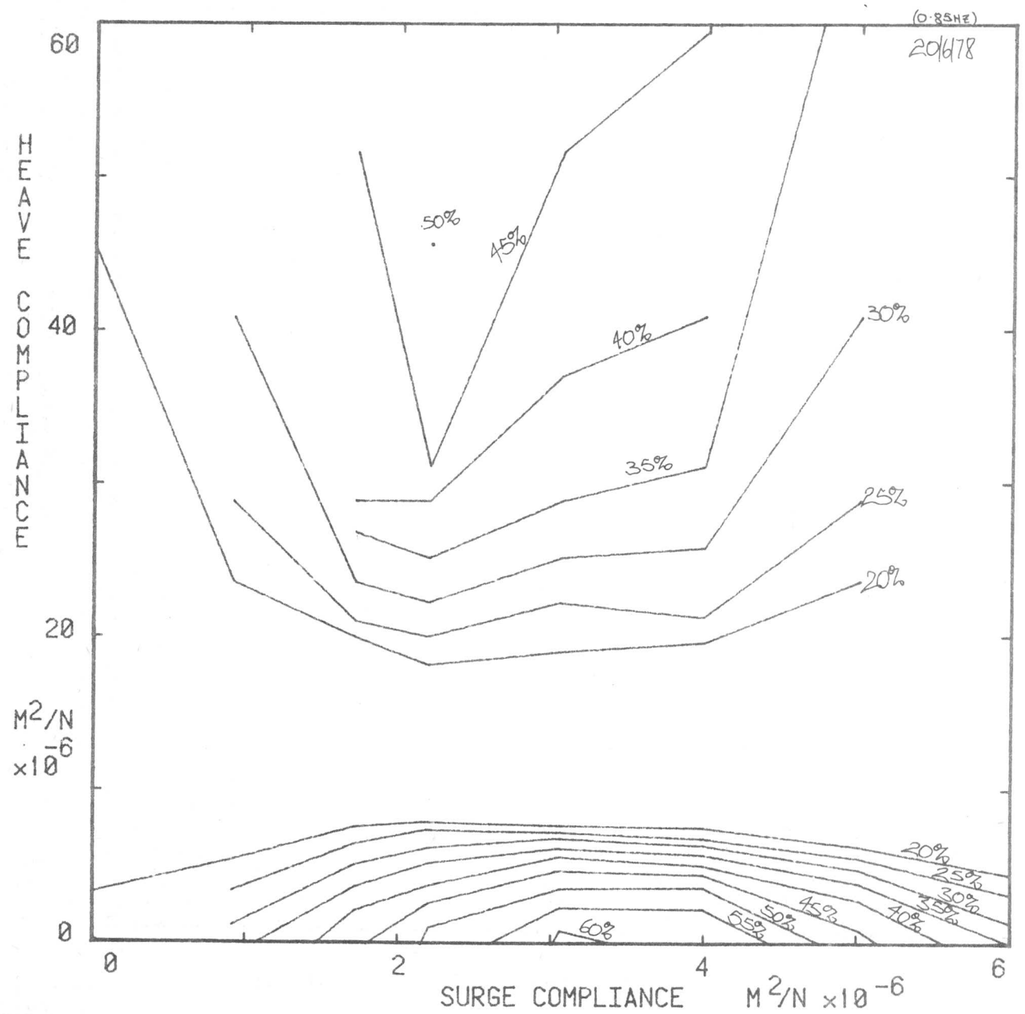

D0019

total surge inertia: 374 tonnes/m total heave inertia: 542 tonnes/m	nod damping: 7·7 MN/rad/s/m

DUCK EFFICIENCY on COMPLIANT AXIS

monochromatic sea: T=12·2sec; L/d=15·6

Added INERTIA in Surge

parameters scaled up to represent 15m dia duck

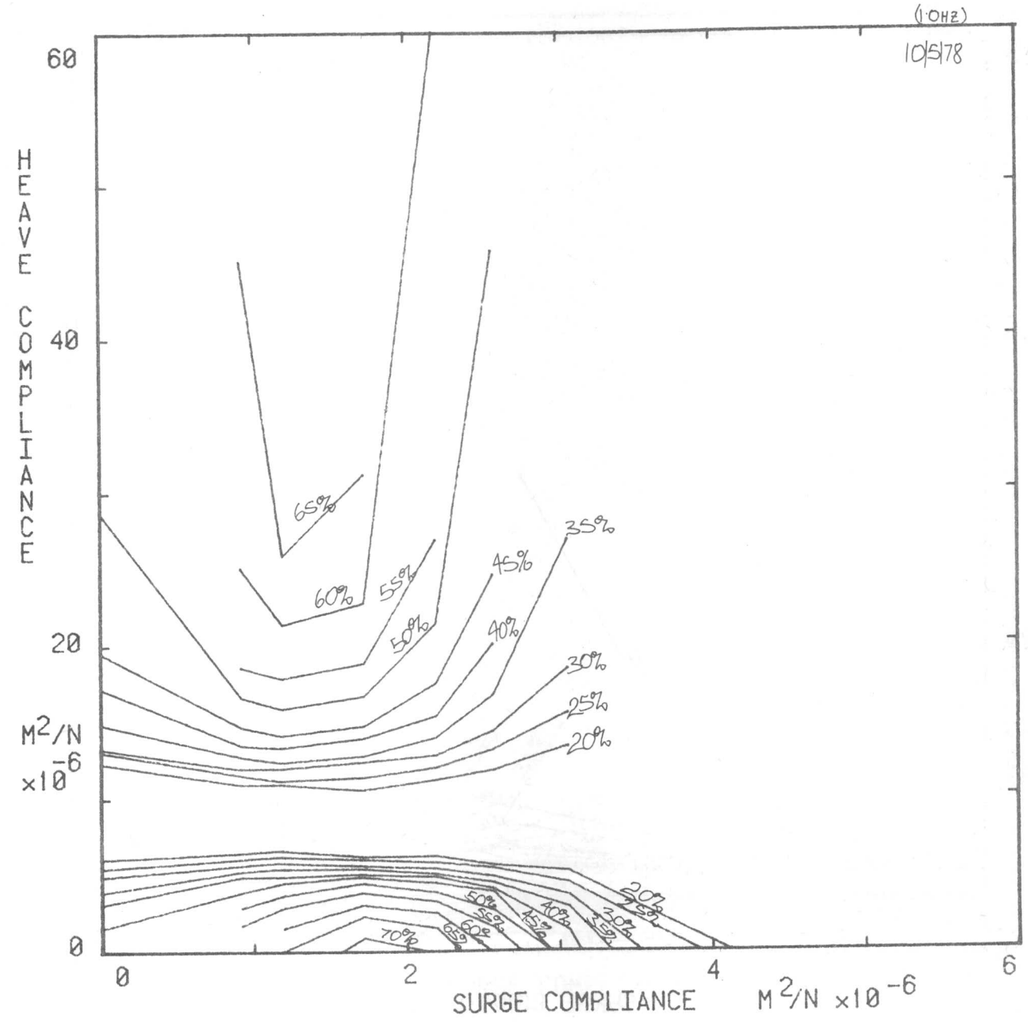

DUCK EFFICIENCY on COMPLIANT AXIS

monochromatic sea: T=12·2sec; L/d=15·6
Added INERTIA in Heave
parameters scaled up to represent 15m dia duck

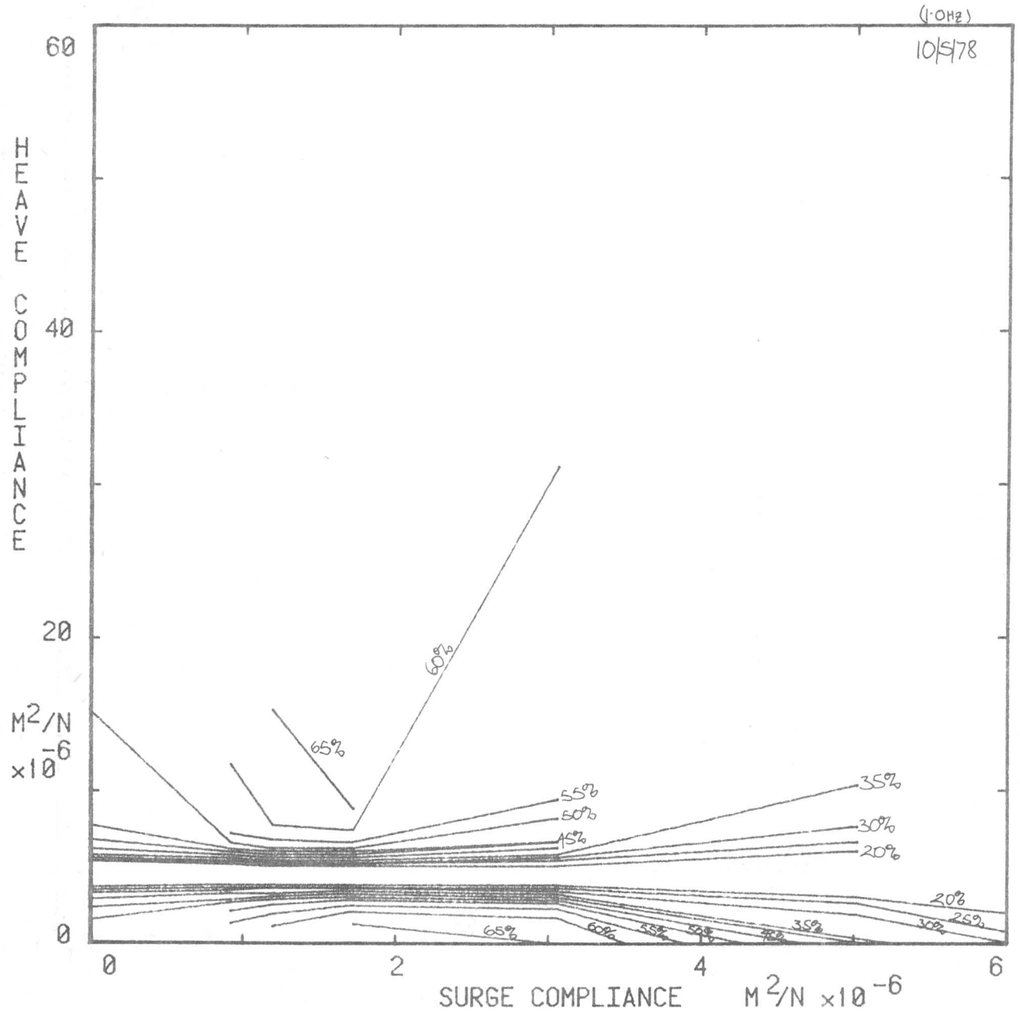

D0019

total surge inertia: 374 tonnes/m total heave inertia: 909 tonnes/m	nod damping: 7·7 MN/rad/s/m

DUCK EFFICIENCY on COMPLIANT AXIS

monochromatic sea: T=12·2 sec; L/d=15·6
Added INERTIA in Surge & Heave
parameters scaled up to represent 15m dia duck

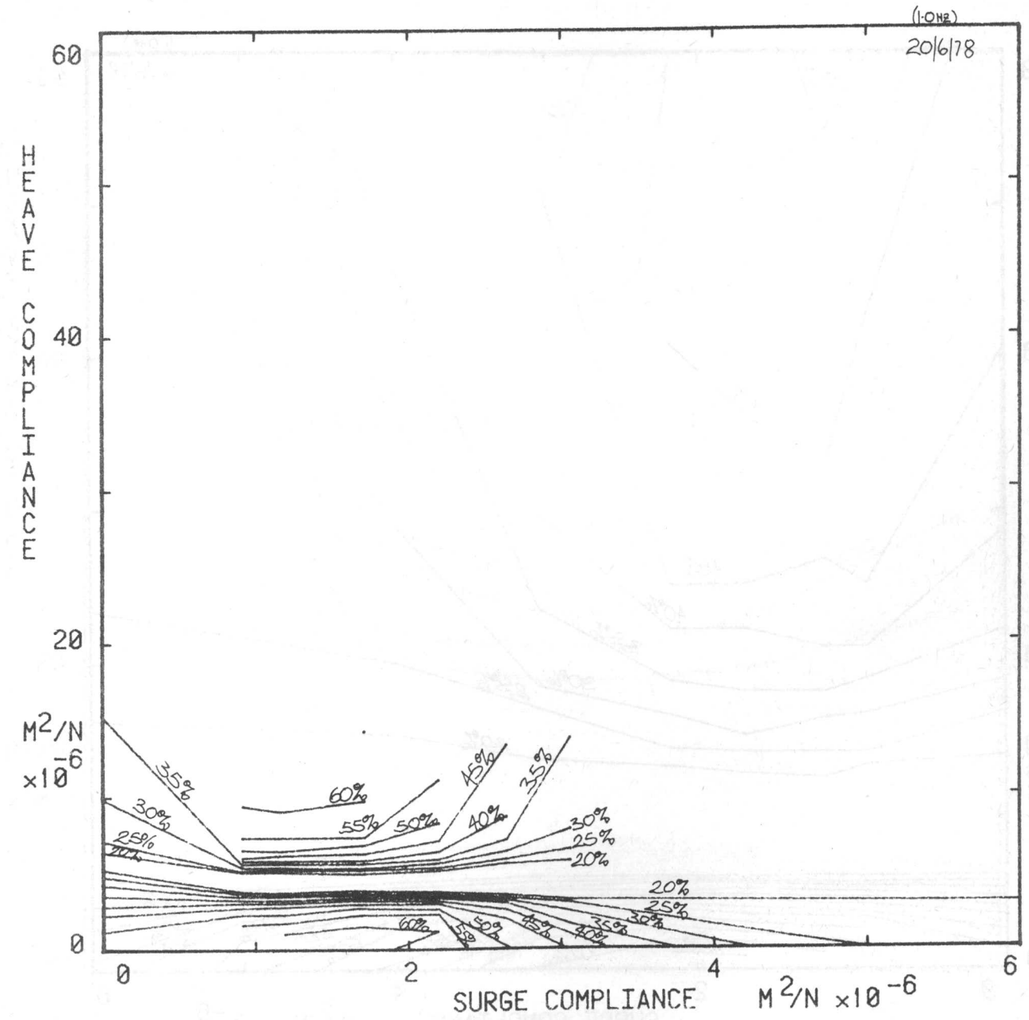

D0019

total surge inertia: 758 tonnes/m total heave inertia: 909 tonnes/m	nod damping: 7·7 MN/rad/s/m

DUCK EFFICIENCY on COMPLIANT AXIS

monochromatic sea: T=12·2 sec; L/d=15·6
With negative NOD SPRING

parameters scaled up to represent 15m dia duck

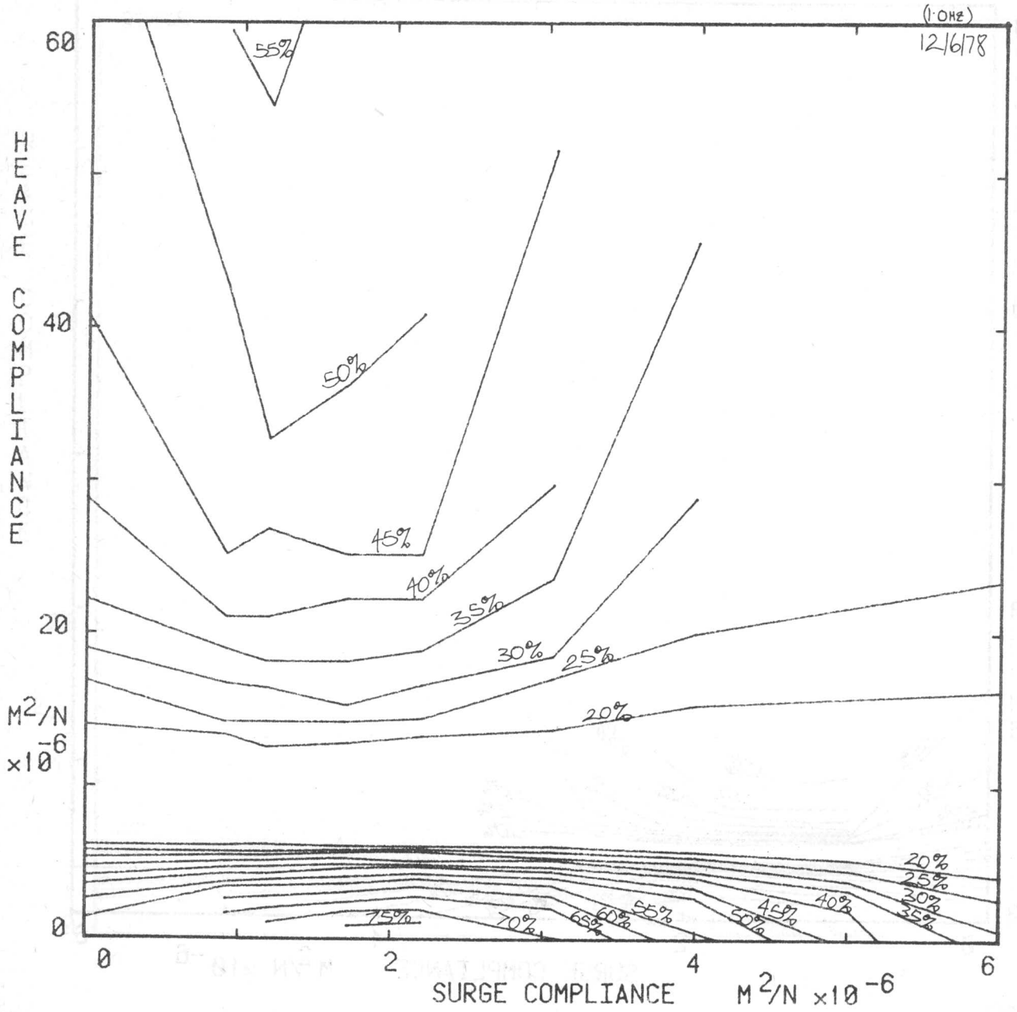

D0019

total surge inertia: 374 tonnes/m	nod damping: 7·7 MN/rad/s/m
total heave inertia: 542 tonnes/m	nod spring :2·29MN/rad/m

DUCK EFFICIENCY on COMPLIANT AXIS

monochromatic sea: T=14·4sec; L/d=21·6
With negative NOD SPRING

parameters scaled up to represent 15m dia duck

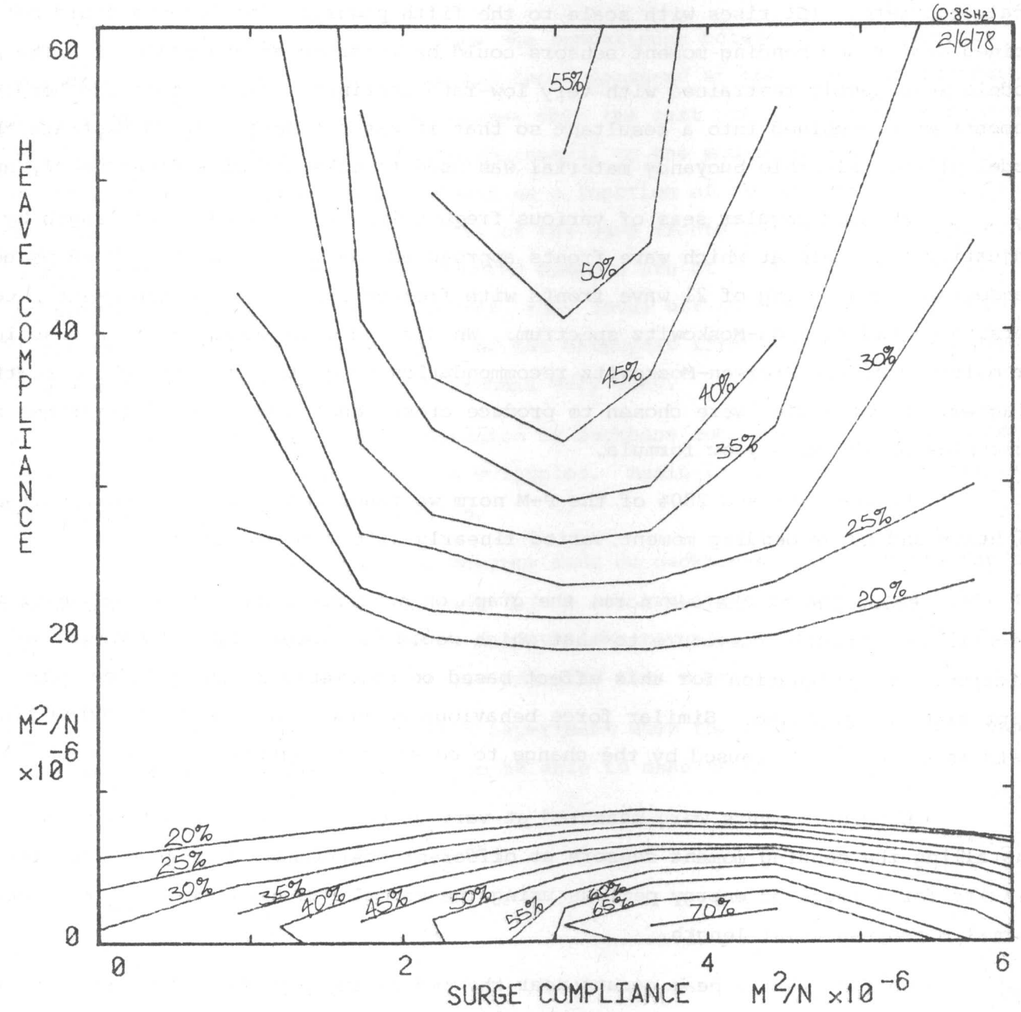

D0019

total surge inertia: 374 tonnes/m	nod damping: 10·8MN/rad/s/m
total heave inertia: 542 tonnes/m	nod spring :1·72MN/rad/m

PRELIMINARY BENDING MOMENT TESTS ON PLAIN BACKBONES

OBJECTIVES

We wanted to learn how to test in a wide tank and to see if our first ideas on bending moment and crest length stood up to testing.

APPARATUS

The models were made from lengths of 83 mm x 3.4 mm wall thickness PVC. We measured its EI value as 2400 Nm^2 which is above five times too stiff for full scale concrete. (EI rises with scale to the fifth power.) The lengths could be joined easily and bending moment sensors could be inserted at any position. The models were gently restrained with very low-rate moorings. Heave and surge bending moments were combined into a resultant so that it was not necessary to restrain the model pitch. Flexible buoyancy material was used to make the pipe float nearly awash.

We used regular seas of various frequencies and changed crest length by adjusting the angle at which wave fronts approached the model. We also used pseudo-random seas consisting of 21 wave fronts with frequencies chosen to represent a comb version of the Pierson-Moskowitz spectrum. We altered wave amplitude as a fraction or multiple of the Pierson-Moskowitz recommendation so as to cover the whole scatter diagram. Front angles were chosen to produce crest lengths which were fractions and multiples of the Mitsuyasu formula.

Between 50% and 200% of the P-M norm we found that the combined resultant of heave and surge bending moment varied linearly with wave amplitude.

Below 50% of the P-M norm, the graph on page 5.3 shows some non-linearity which is the opposite curvature to that which would have been caused by wavemaker stiction. An explanation for this effect based on movements of the jubilee clip joint might be proposed. Similar force behaviour occurs in narrow tank moving rig tests (see page 2.53) caused by the change to constant restoring force above 230 kN/m.

Bending moments were measured at various points along the backbone by installing the bending moment sensors at different positions. Page 5.4 shows the results for a range of energy periods using the normal P-M value for H_{rms} and the normal Mitsuyasu crest length.

We find that a peak occurs near the end of the pipe but it is not obvious how the distance from the peak position to the end is related to wave characteristics.

In the middle of the pipe, bending moments level off and reduce except for the very longest sea. We had hoped for a reduction of 2 but a value of $\sqrt{2}$ looks more accurate. It is possible to speculate that more compliant pipes would

make a greater reduction of bending moment in the middle and make the long seas behave as the short ones do in this experiment. This an important next step.

Page 5.4 shows results for half the model. We checked that similar behaviour occurred for the half not shown.

At the end of the backbone, bending moments are determined by factors other than H_{rms} and T_e. At the centre of a long backbone the bending moments depend much more on H_{rms} than T_e. We conclude that ends of difficult to design and so we should have as few as possible.

The graphs on page 5.5 show the comparisons between bending moments measured at the three end stations and those measured at the three central points. The 13 second T_e records are just higher than the rest but not nearly as much as would occur if bending moment was proportional to the square of crest length. The graph on page 5.6 shows bending moment as a function of crest length. If T_e and H_{rms} are held constant and the angles of the wave fronts in the sea are changed to alter crest length, we find that bending moments are at first more or less proportional to crest length. However, they level off in seas which have crest lengths three or four times more than those of the Mitsuyasu formula. This is followed by a gradual decline as crest length becomes very long.

This phenomenon must be caused by backbone compliance. Floppier models should level off at lower Mitsuyasu multiples. Again it is difficult to fit results to a crest length squared prediction.

Measurements of bending moments made on backbones held at different angles show some unusual behaviour. On page 5.7 we see results from moving the pipe relative to the wave system, and also the more convenient movement of the wave system relative to a pipe. Computers are more easily adjusted than mooring lines.

We shall be repeating this experiment when the orchestration unit can produce more wave fronts. We hope to be able to make about 70.

Bending Moment Linearity

for a 21m long pipe in irregular seas

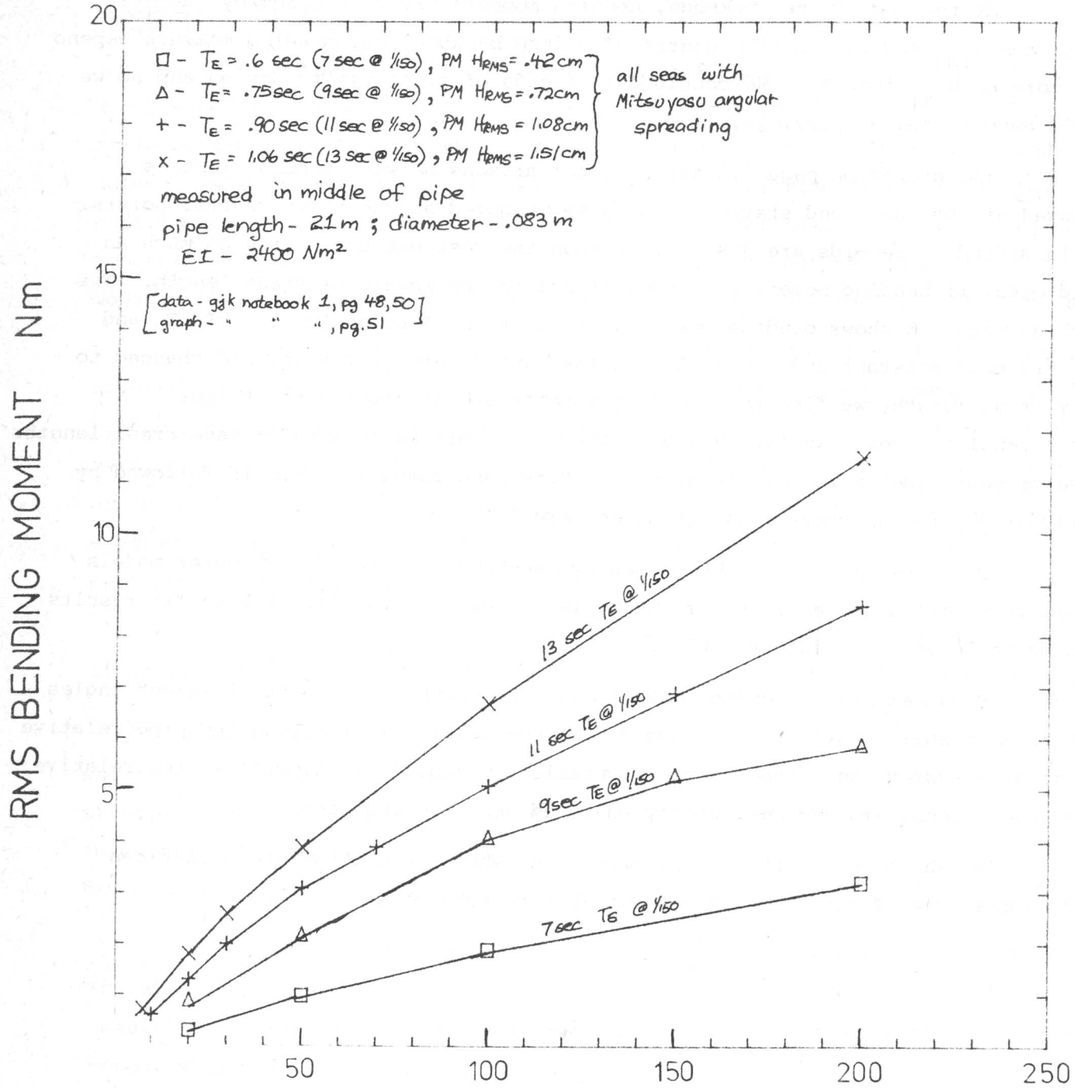

Bending Moment vs Position

for a 21m long pipe in irregular seas

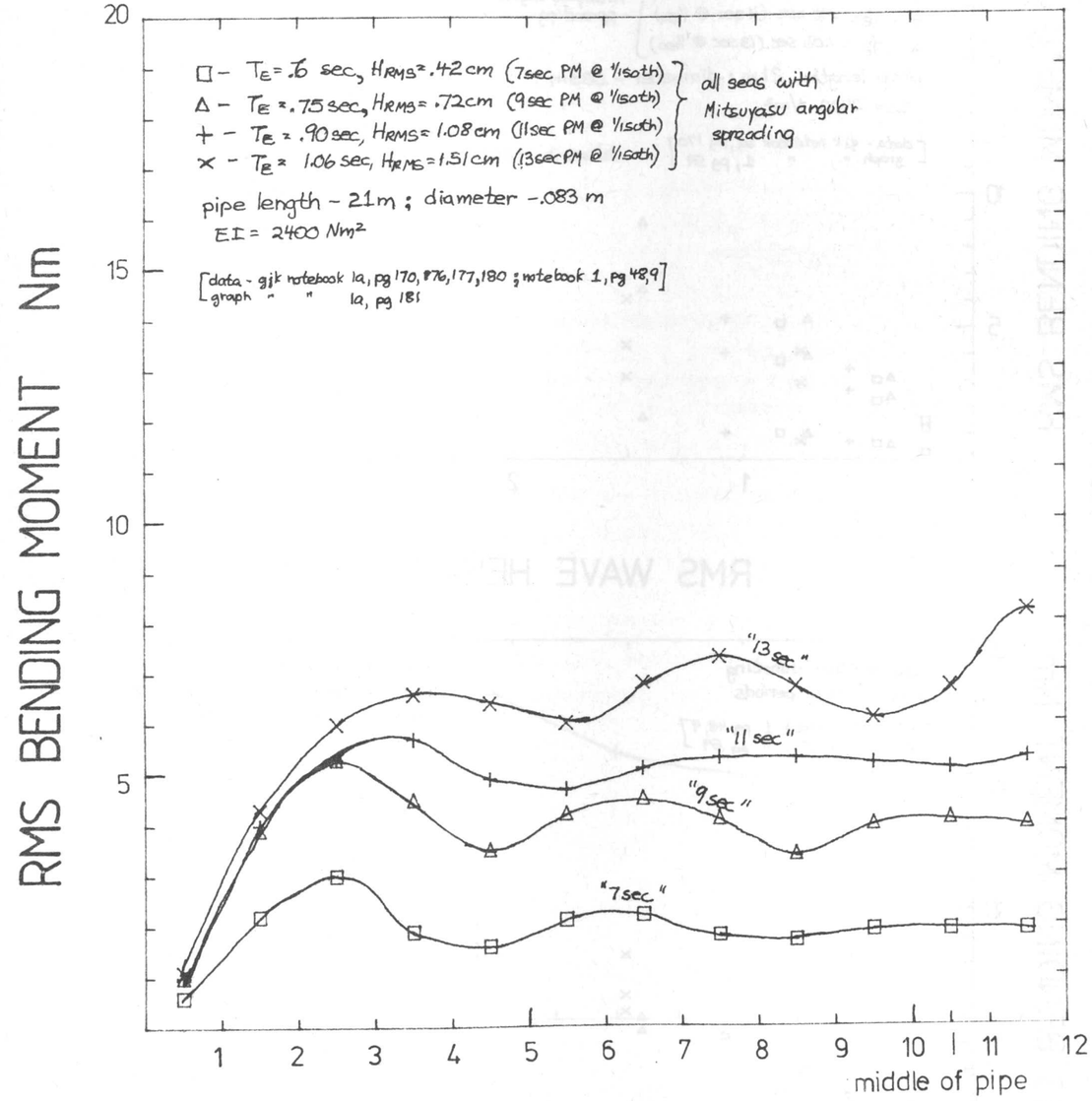

Bending Moment vs Wave Amplitude

for a 21m long pipe in irregular seas

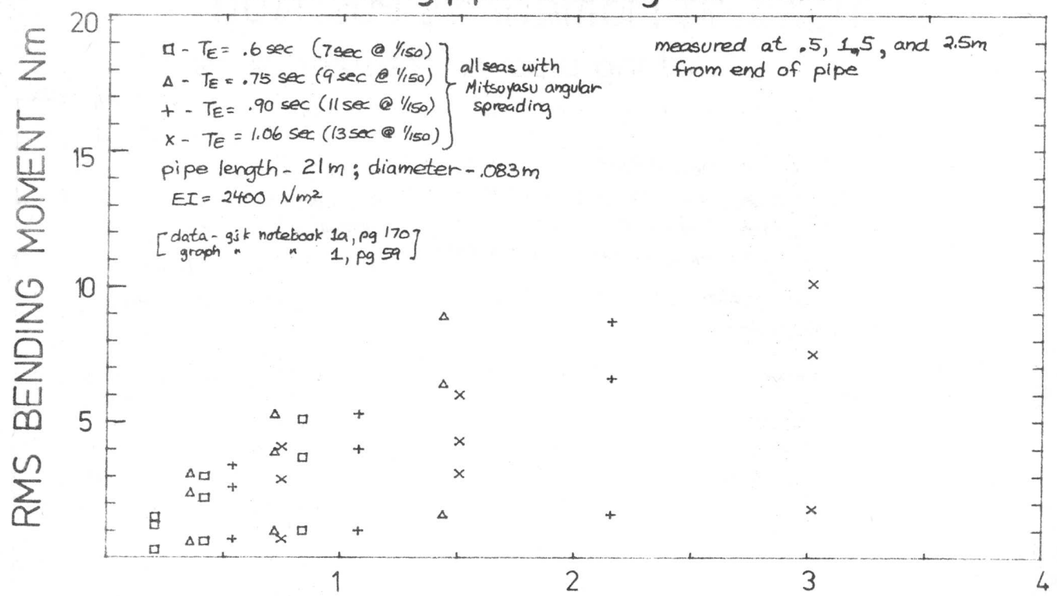

RMS WAVE HEIGHT cm

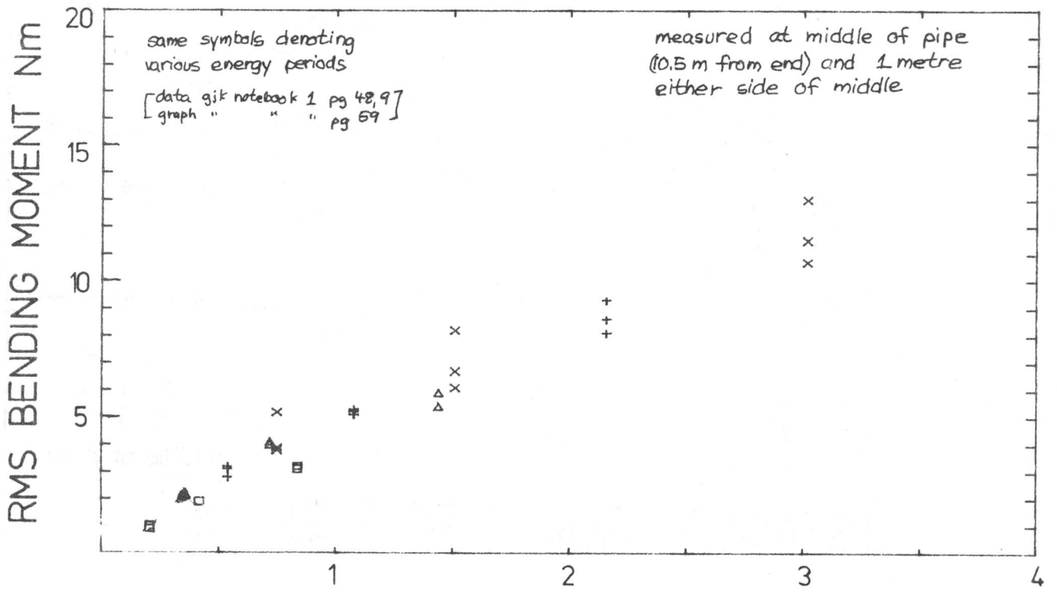

RMS WAVE HEIGHT cm

Bending Moment vs Crest Length

for a 21m long pipe in irregular seas

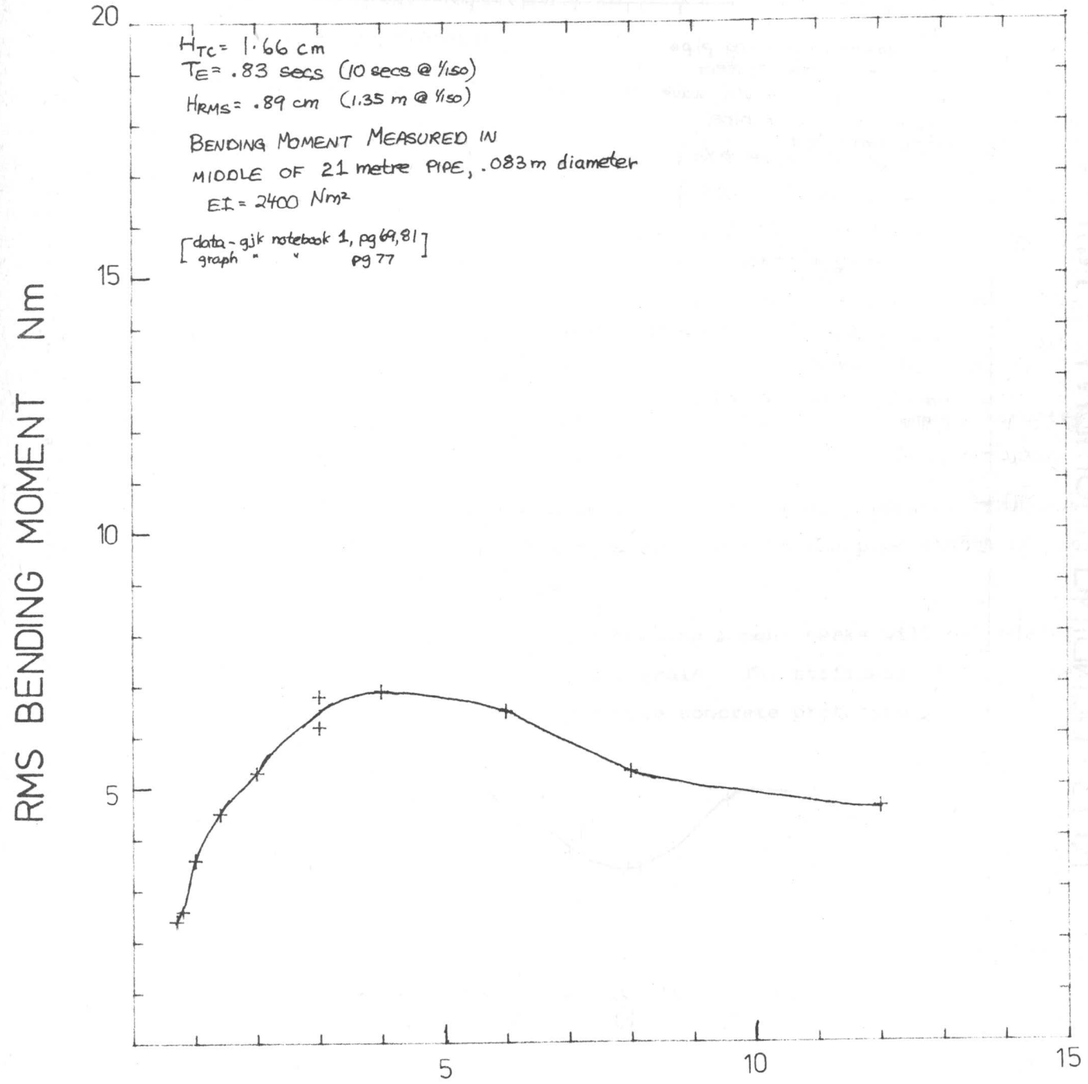

MULTIPLE OF MITSUYASU CREST LENGTHS

Bending Moment vs Mean Sea Angle

for a 21m long pipe in irregular seas

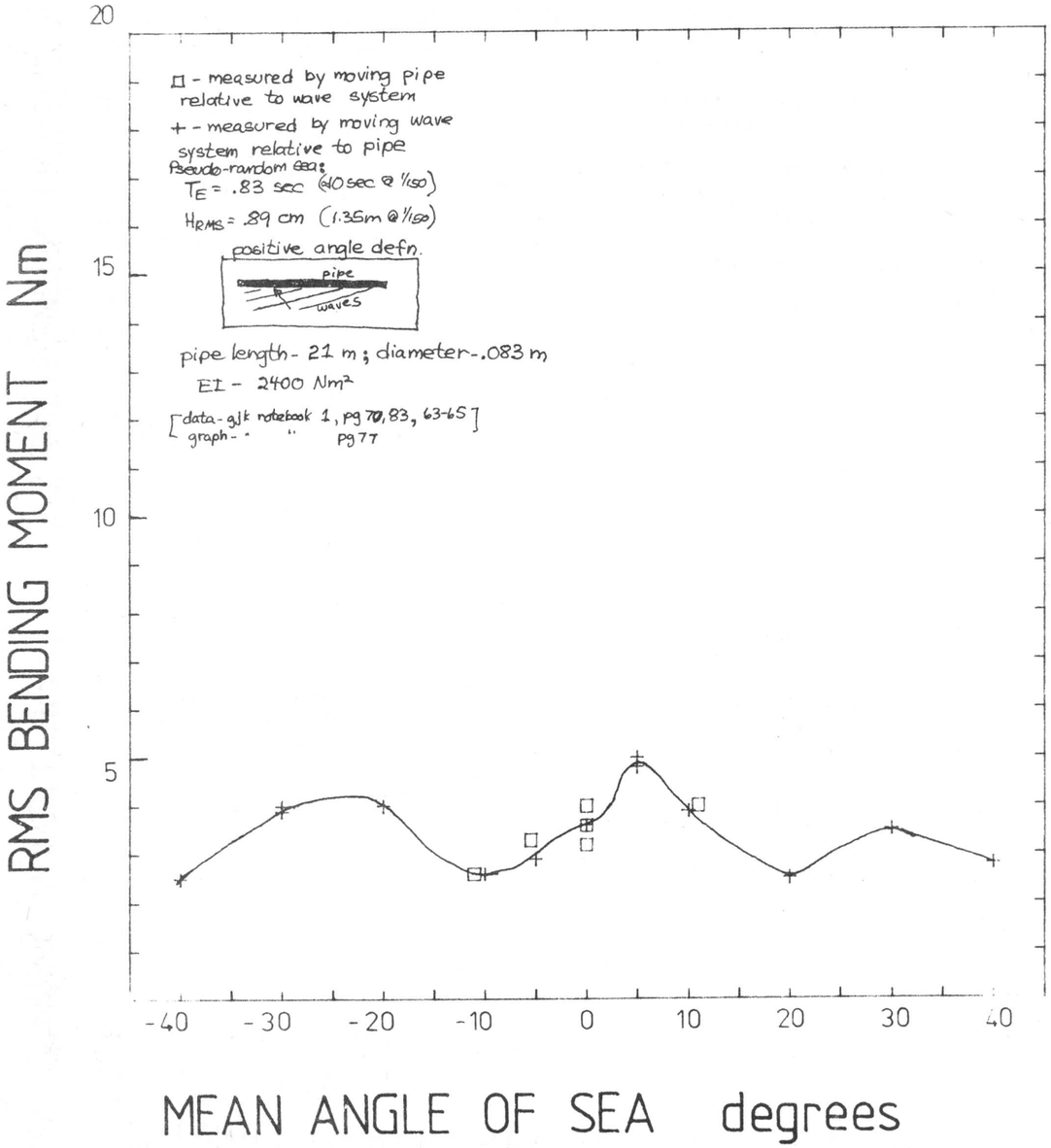

THE SEARCH FOR PEAKS IN THE CREST LENGTH/FREQUENCY PLANE FOR VARIOUS PIPE LENGTHS

We tested models of pipes of length 3, 9, 15 and 21 metres. We changed wave frequency and crest length to find the maximum bending moment at the centre of each length. We used oblique single wave fronts so that all points along the pipe received the same wave amplitude. We used a constant wave amplitude of one-tenth of a backbone diameter.

The results are tabulated as follows:

	LOW FREQUENCY				HIGH FREQUENCY				
PIPE LENGTH	3	9	15	21	3	9	15	21	m
FREQUENCY FOR MAXIMUM	-	0.5	-	0.5	1.2	1.3	1.1	1.1	Hz
CREST LENGTH FOR MAXIMUM	-	11.0	-	11.0	3.0	8.0	9.0	8.0	m
VALUE OF MAXIMUM	-	12.3	-	10.3	2.5	5.2	12.3	10.3	Nm

Some pipe lengths showed peaks at two frequencies. We were surprised to find no double peaks for the 15 m length despite a very thorough search.

The longest pipe does not have the largest bending moment. For the two shortest pipes, the worst crest length was close to the pipe length but it did not rise to match the longer pipes.

It is highly probably that the bending moment peaks will be reduced for any compliance which could be made at full scale. The stiffness of this model is five times greater than the stiffest possible concrete prototype.

BENDING MOMENT FOR A LONG PIPE AS A FUNCTION OF FREQUENCY AND CREST LENGTH

We measured the bending moment at the centre of a 21 metre length of pipe.

We varied the frequency from .4 to 2 Hz in fourteen steps. For each frequency we varied the crest length from 2 to 22 metres in fourteen steps.

Since crest length cannot be shorter than wave length, some of the low frequency short crest lengths are impossible.

The results are shown on pages 5.10 to 5.13 as views of a three-dimensional shape with crest length and frequency in the horizontal plane and bending moment to wave height ratio as the altitude. Views are shown for two directions with and without smoothing.

There are two prominent peaks of similar height and enough minor ones forming sytematic ridges to test any dynamicist's theories.

The graph on page 5.14 shows a section of the shape through the 1.2 Hz plane.

BENDING MOMENT

for a 21 metre long pipe in regular waves

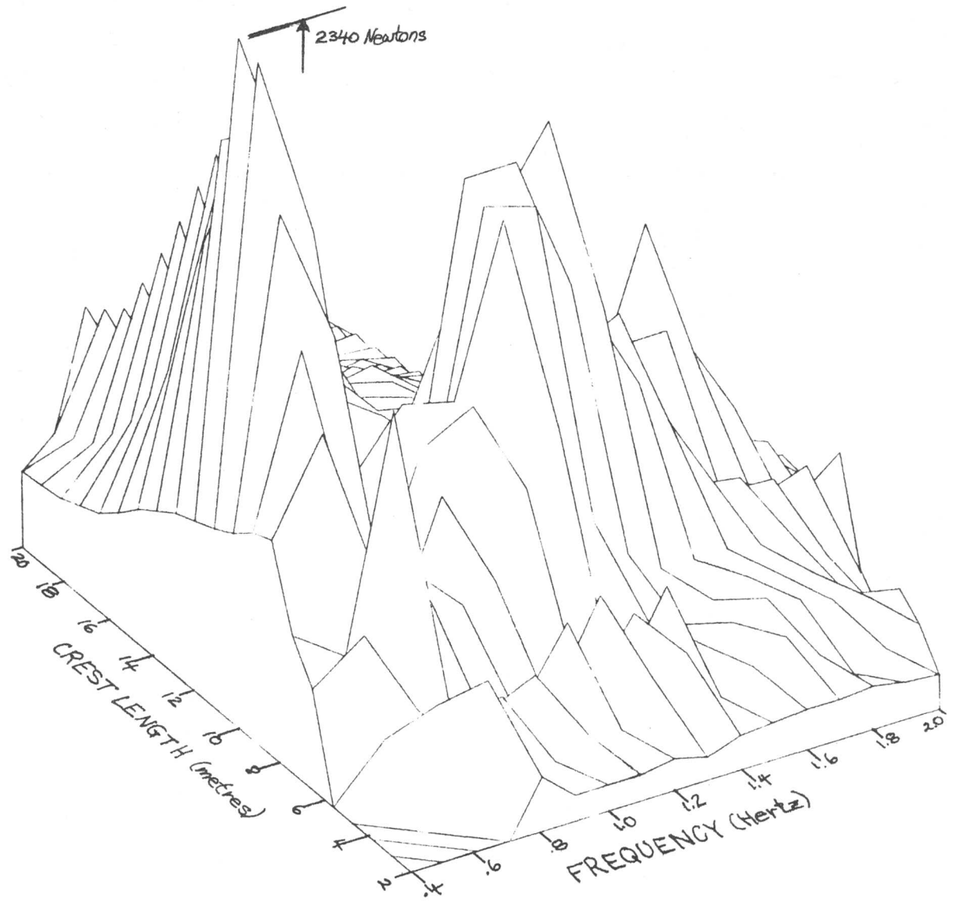

View from the short crest length low frequency corner - unsmoothed

BENDING MOMENT

for a 21 metre long pipe in regular waves

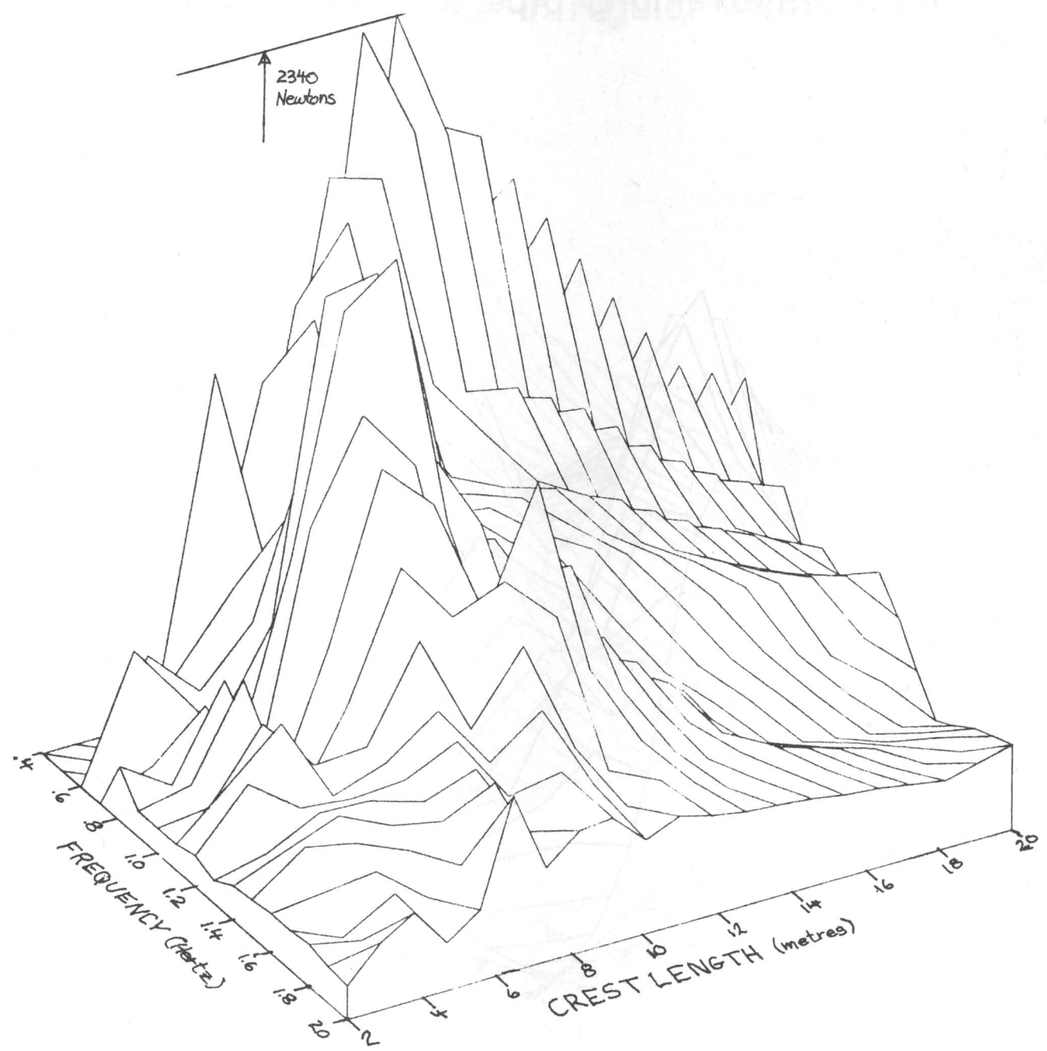

View from the short crest length high frequency corner - unsmoothed.

BENDING MOMENT

for a 21 metre long pipe in regular waves

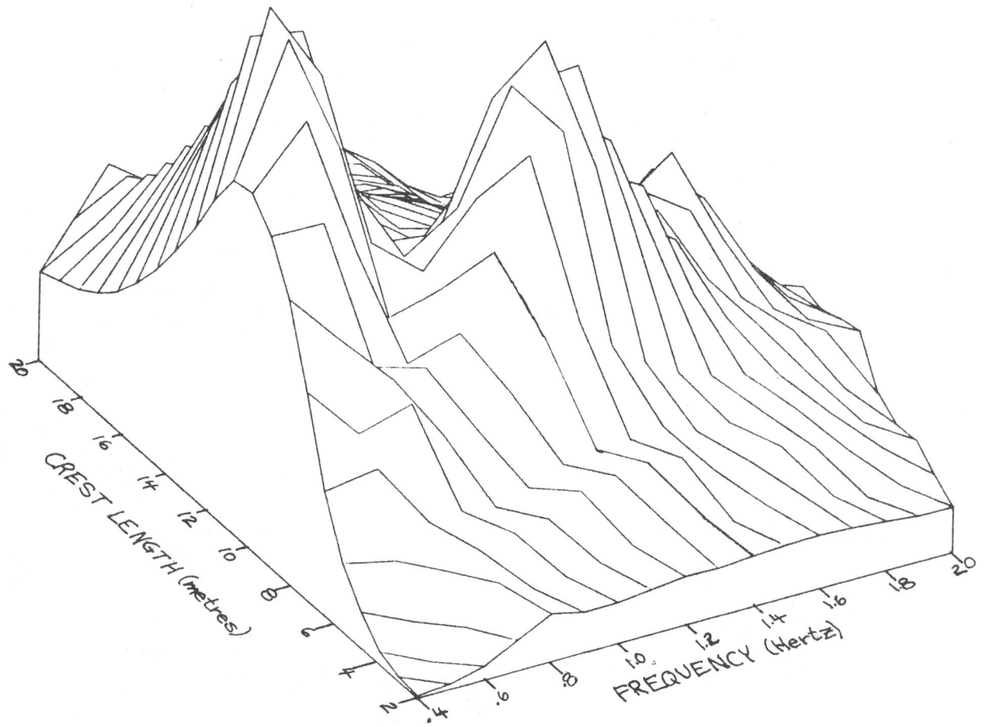

View from the short crest length low frequency corner - computer smoothing.

BENDING MOMENT

for a 21 metre long pipe in regular waves

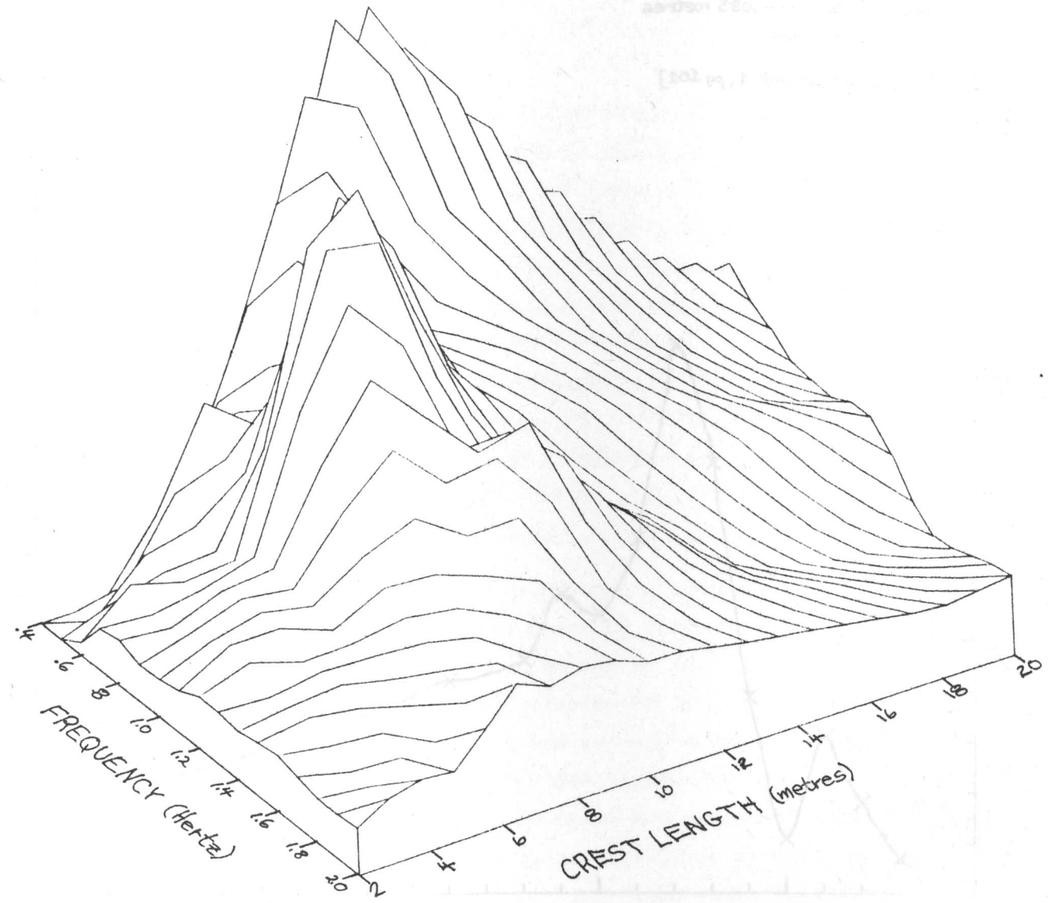

View from the short crest length high frequency corner = computer smoothing.

Bending Moment vs Crest Length

for a 21m long pipe in regular waves

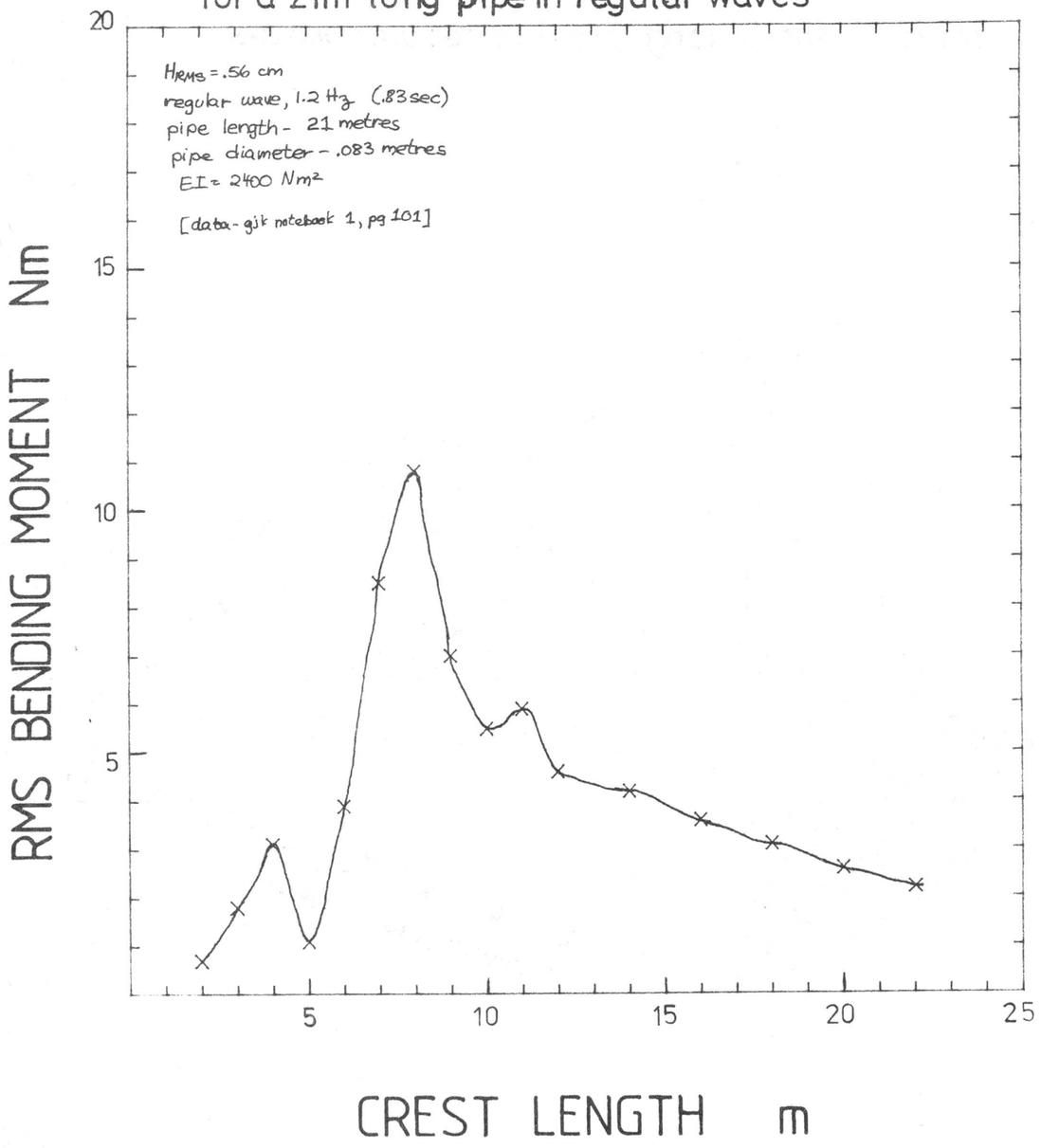

EXPLANATION OF TERMS

(If you know about waves, please skip this section.)

ROOT MEAN SQUARE WAVE HEIGHT, H_{rms}

Traditionally, wave size has been presented using 'significant wave height' (abbreviated H_{sig}, H_s or H1/3). One definition is 'the average height of the highest third of the waves'. This may sound confusing but there were good reasons for using H_{sig}. One big advantage is that it could be estimated without instruments. An explanation of this method of measurement should make the definition clearer.

The old way to measure H_{sig} was to climb to a point in your ship at which one wave in three appeared to come above the horizon. The level of your eyes above the still waterline of the ship was the significant wave height. After the development of the shipborne waverecorder[3] measurements became more convenient but enormous lengths of paper record were produced. Oceanographers devised techniques to analyse the data by hand[4]. They were very quick and worked much better than newcomers to the field might expect. It is easy to spot the highest and second highest peaks and also the lowest and second lowest troughs. With some clever statistics[5], this gives enough information for quite an accurate wave height estimate, particularly as the errors cancel over a long period. The bulk of wave data now available (1978) used this method and all the present marine structures are designed for wave climates based on it.

There is a common process used in dealing with many signals which involves taking a set of measurements, squaring them, taking the mean of the square, and then taking the square root of the mean. This is abbreviated as root mean square or RMS. It comes into lots of calculations of power and energy, gets over difficulties with negative numbers and pays more attention to the extreme values in a record. The oceanographers noticed that their significant wave heights were often about four times the RMS value of the water displacement signal and so they decided to redefine it as being exactly that. We now have four separate ways of estimating H_{sig}. They are:

(1) climbing the mast

(2) averaging the highest third

(3) taking highest peaks and lowest troughs

(4) taking four times the RMS signal.

If you say H_{sig}, nobody can tell which you are using.

The 'four times RMS' procedure is the most rigorous and there seems to be a general move towards it. It is less sensitive to noise than the peak/trough method. In this report we have decided to present data directly in terms of RMS since that is what we are measuring and it saves us having to explain what sort of H_{sig} we mean.

The symbol H makes people think of trough-to-crest rather than amplitudes or displacements which are measured from a central zero. Draper[6] suggested D_{rms} rather than H_{rms} and it is a pity that this has not caught on. We have been using D for duck diameter so we decided that H_{rms} was the best symbol. Top theoreticians use $M_0^{\frac{1}{2}}$ but this upsets the novice.

Longuet-Higgins[7] has shown how to estimate the highest wave in a record in terms of the length of the record and H_{rms}. It is useful to remember that in the usual length of record (20 minutes at sea), H_{Tc} max will be seven or eight times H_{rms}. Over a very long period we may expect a wave about ten times H_{rms}. Checking the ratio of peak to RMS is a quick pointer to the shape of a probability distribution. If wave power people could choose the weather, we would have H_{rms} = 1 metre except during maintenance periods. At H_{rms} = 2 metres, we would all be sick. H_{rms} = 4 metres is frightening even at 1/150th scale. If you want to use our results for H_{sig} wave climate, just multiply our numbers by four. But is it easier to count the sheep in a field or the number of hooves?

ENERGY PERIOD, T_e

Another important parameter in the description of a sea state is an average period. Several definitions of average period are in use but the most common one is called 'zero crossing period' (abbreviated T_z).

The records from shipborne wave recorders are the primary source of information for T_z. A line is drawn on the record corresponding to a guess of mean sea level. Then the number of times the trace crosses the zero line on the way up is counted. The total period of the record is divided by the number of crossings to get T_z.

This technique would be fine if all wave measurements were made with recorders of the same bandwidth. But if you increase the bandwidth of a recorder then more fast little waves get measured. The difference is shown in Figure 1.

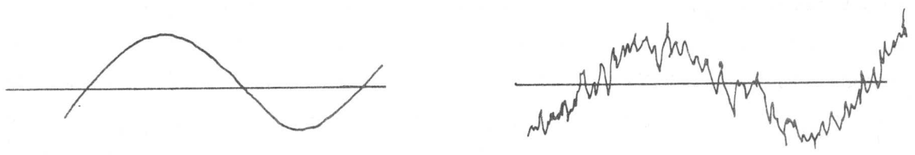

(a) Low bandwidth recorder looking at oily swell

(b) High bandwidth recorder looking at frothy waves

FIGURE 1

As the number of waves goes up the T_z goes down (and so does H_{sig}) even though there is hardly any power in the little waves.

What we need is a definition of period which will be less affected by changes of instrument bandwidth, small amounts of noise and hum in a record or froth on the surface of the water.

Mollison[8] has suggested that to calculate an 'energy period' T_e from a record would be more convenient than T_z for wave power work, provided that there is a way of measuring power.

In a regular sinusoidal wave there are no arguments about power or period. Where T = period, ρ = density of water, g = acceleration of gravity, H_{rms} = RMS wave height,

$$\text{Power density } P = \frac{\rho g^2}{4\pi} H^2_{rms} T$$

It is useful to remember that $\frac{\rho g^2}{4\pi} = 7.82$ for kilowatts/metre.

For a mixture of waves of different periods T_i and root mean square heights H_i, both the energy and power densities are additive. Thus:

$$H^2_{rms} = \Sigma H_i^2$$

$$\text{Power} = \frac{\rho g^2}{4\pi} \Sigma H_i^2 T_i$$

If we define the energy period $T_e = \Sigma H_i^2 T_i / H^2_{rms}$.

Random seas are commonly described as a mixture of an infinite number of components, or spectrum S(T). S(T) dT is the contribution to H^2_{rms} from periods between T and T + dT. Thus:

$$H^2_{rms} = \int_0^\infty S(T)\, dT$$

$$\text{Power} = \frac{\rho g^2}{4\pi} \int_0^\infty TS(T)\, dT$$

$$= \frac{\rho g^2}{4\pi} H^2_{rms} T_e \quad \text{(as before)}$$

T_e is usually 15-20% higher than T_z for the sampling rates and recorders commonly used. Thus Power $\doteqdot 9.2\, H^2_{rms} T_z = .57\, H^2_s T_z$ (using $H_s = 4 H_{rms}$).

To calculate T_e, and hence the exact power density of a random sea we have first to calculate the spectrum. We cannot evaluate a continuous spectrum exactly, but a good discrete approximation can be found using the Fast Fourier Transform (FFT) (see Newland[9] for a good account of this method). A record of N observations at time-intervals t (typically N = 2048, t = .5 secs) is thereby decomposed into components of period Nt/n (n = 1, 2, ... N). For real seas, the FFT is only an approximation, though a good one. If, however, our mixed sea consists purely of components with such periods (i.e. with frequencies all multiples of the basic frequency (1/Nt), analysis will recover those exact components. This can be achieved in a wide tank.

SCATTER DIAGRAMS

To understand the results of this report it is important to be familiar with scatter diagrams. The oceanographers who collect wave data use scatter diagrams to show the statistics of a wave climate. The vertical axis of the diagram is marked in wave size and the horizontal axis in wave period. The area inside the diagram is divided into cells each of which is indentified by height and period information. The cells contain a number which gives the probability, usually in parts per thousand, of getting that particular combination of amplitude and period.

Two numbers for each cell are not much to specify something as complicated as a sea state but Mollison[8] has shown that in the long run most of the errors cancel one another.

The scatter diagram on the opposite page is made from Institute of Oceanographic Sciences data from OWS India analysed by Hoffman and Mollison. H_{rms} and T_e are calculated from a set of 307 spectra which are chosen to be representative of the long term wind data. The family of curved lines are power density contours. We have also drawn in another line corresponding to the values of H_{rms} and T_e predicted in terms of wind speed with a model developed by Pierson and Moskowitz (see page 6.8).

H_{RMS} AND T_E AT O.W.S. INDIA WITH POWER CONTOURS (kW/M)

(DATA FOR WHOLE YEAR)

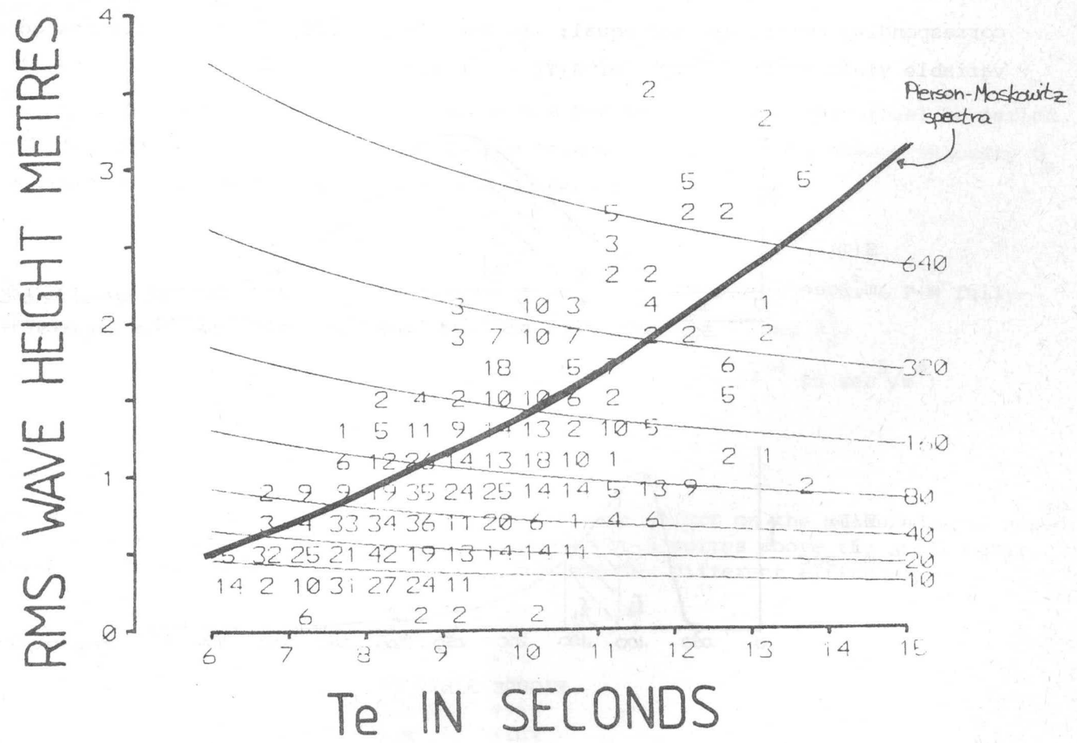

SPECTRA

A spectrum describes how the mean square height H_{rms}^2 (which we can call energy for short as it is proportional to the energy) is apportioned between periods or frequencies. It can be plotted as a function S(T) of period (Figure 3(a)) or E(f) of frequency (Figure 3(b)). The total area under each curve

$$\int_0^\infty S(T)\ dT = \int_0^\infty E(f)\ df = H_{rms}^2.$$

The energy between T_1 and T_2 is

$$\int_{T_1}^{T_2} T\ S(T)\ dT.$$

If f_1 and f_2 are the corresponding frequencies, (i.e. $f_1 = 1/T_1$, $f_2 = 1/T_2$), this energy is also

$$\int_{f_2}^{f_1} E(f)\ df$$

Note that it is the two areas which are equal. The heights of the curves at corresponding points are not equal; in fact if T = 1/f, the rules for change of variable yield $E(f) = T^2 S(T)$, or $S(T) = f^2 E(f)$.

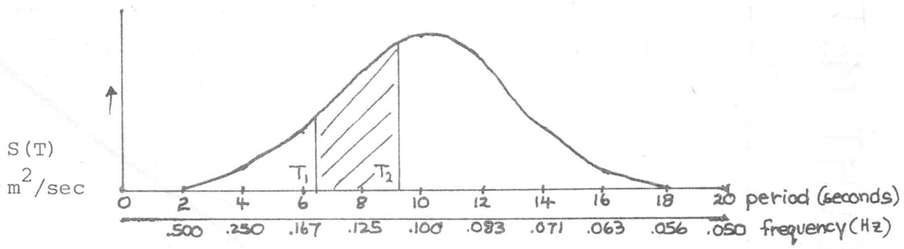

FIGURE 3(a)

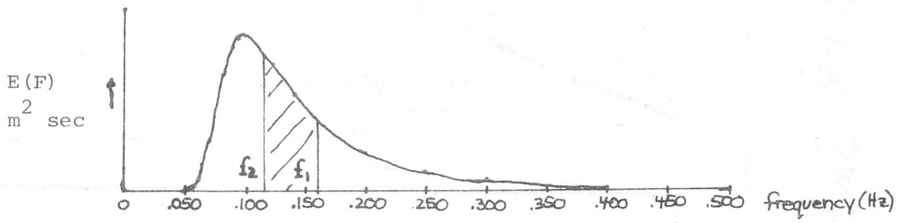

FIGURE 3(b)

PIERSON-MOSKOWITZ SPECTRUM

This is a single-parameter spectrum, suggested by Pierson and Moskowitz (10) (1964) as appropriate to a fully-developed wind created sea, i.e. one in which wind has been blowing steadily over a long enough time (6-18 hours) and a long enough space (200-600 km) for the sea to have reached a steady state condition. The energy and spectrum shape of the sea are constants. Before a sea gets to this state, it tends to have less energy and a narrower frequency spread. The model does not include swell from far away storms.

The Pierson-Moskowitz spectrum is defined by

$$E(\omega) = \alpha g^2 \omega^{-5} \exp(-\beta\ (\omega_o/\omega)^4)$$

where ω is the frequency in radians per second ($T = 1/f = 2\pi/\omega$), and α, = .0081, and β, = .74, are dimensionless constants. $\omega_o = g/U_o$, where U_o is the wind speed (the one parameter.)* The principal feature of this spectrum is that it is invariant under change of scale: in particular any measure of steepness, such as the ratio of height to wavelength, is a constant,

$$H_{rms}/\lambda e - 1/115$$

($\lambda e = gTe^2/2\pi$, the wavelength corresponding to the energy period). Hence height is proportional to period squared,

$$H_{rms} = cTe^2 \qquad (c = .0136\ m/sec^2).$$

The windspeed U_o associated with a P-M spectrum is proportional to period and in particular to T_e, which is closely related to the average energy velocity U_e (= Power density divided by kinetic energy density),

$$U_e = gTe/2 = .9773\ U_o$$

Remembering that power P is proportional to $H_{rms}^2\ T_e$, we see that for a P-M fully-developed sea the power is proportional to each of $H_{rms}^{2.5}$, T_e^5 and U_o^5,

$$P = c\ U_o^5 \qquad (c = 1.40 \times 10^{-4}\ kW\ sec^5/m^4)$$

* Footnote

The altitude of wind measurement has a significant effect on the measured wind speed. The P-M spectrum model uses windspeeds measured 19.5 metres above the still water surface. These are some approximate corrections for different altitudes:

25 m	-3%
19.5 m	0%
15 m	+3%
10 m	+7%
7.5 m	+11%
5 m	+16%

Real seas are not often fully-developed wind seas. In particular, their values of H_{rms} and T_e are often far from the "P-M curve" ($H_{rms} = .01361\ T_e^2$); (see Figure 2, page 6.6). Also, for non-fully developed seas, the instantaneous local wind speed is a poor guide to T_e (i.e. $U_e \neq .9773\ U_o$).

We therefore used a modification of the P-M spectrum, which retains the same spectral shape, but allows H_{rms} and T_e to vary independently; also H_{rms} and T_e are treated as the basic parameters. Thus

$$S(T) = H_{rms}^2 \exp(-cT/T_e)^4 .\ 4\ cT^3T_e^{-4} \text{ where } c = 10.80.$$

Note that the proportion of energy contributed by periods greater than T is simply $\exp(-c(T/T_e)^4)$.

Real seas may have spectra which are either narrower or broader than the P-M spectrum; a sensible measured spectral width, for wave power work at least, is the 'proportional standard deviation' σ/T_e, where σ is defined by

$$\sigma^2 = \int (T-T_e)^2\ S(T)\ dT\ /\ H_{rms}^2$$

for the P-M spectrum (modified or otherwise), σ/T_e is invariant, = .27.

The JONSWAP spectrum is a peakier modification of the P-M formula, appropriate to growing seas, for which σ/T_e may be as low as .2. Many real seas, however, have less peaky spectra than P-M, because they are a mixture of local wind sea and swell. The modified P-M spectrum seems a reasonable compromise for wave power work. For example, Mollison, Buneman and Salter[8] compared predictions using real spectra from OWS India and modified P-M spectra with the same T_e and H_{rms} and found that predicted average outputs varied by at most about 1 kW/m.

MITSUYASU DIRECTIONAL SPECTRA

For a directional sea, the spectrum is a function $S(T,\Theta)$ of both period (T) and direction (Θ). Some theoretical forms have been suggested for which the distribution of directions is independent of the period. For example, $S(T,\Theta) = S(T)\ C^n \cos^n(\Theta-\Theta_o)$ for $-90^\circ \leq (\Theta-\Theta_o) \leq 90^\circ$, where Θ_o is the principal direction (often thought of as the wind direction) and common values of n are between 2 and 4. The value 2 used to be most common but an ISSC conference[11] suggested that n = 4, corresponding to a narrower spread of directions, would be more accurate.

More recently, (1975), Mitsuyasu[12] has suggested that the directional spread depends on the period, being narrowest at the period corresponding to the wind speed. His formula is

$$S(T,\Theta) = S(T)\ C_m \cos^m(\tfrac{1}{2}(\Theta-\Theta_o)) \qquad (-180 \leq \Theta-\Theta_o \leq 180)$$

$$m(T) = 15.85\ (\frac{T}{T_o})^{-5} \qquad T \geq T_o$$

$$m(T) = 15.85\ (\frac{T}{T_o})^{2.5} \qquad T \leq T_o$$

$$T_o = \frac{g}{U_o}$$

U_o = wind speed

g = gravity

C_m is chosen to make the integral of $C_m \cos^m(\frac{1}{2}(\Theta-\Theta_o))$ over all Θ equal to 1.

LARGEST WAVE PREDICTION

Another important parameter is the ratio of trough-to-crest wave height to the H_{rms} of the sea. Longuet-Higgins[7] has developed a theory for narrow spectra which predicts the maximum wave from a number of waves and the RMS wave amplitude. This theory has been found experimentally to work even for wide spectra.

The following table shows the relationship.

Number of waves	Peak-to-peak/H_{rms}
10	4.5
100	6.1
1000	7.5
10000	8.6
100000	9.6

Example: What was the largest trough-to-crest wave expected during the year at OWS India using the scatter diagram on page 6.6 ?

There are three blocks in the chart which are candidates for producing the largest wave.

(1) T_e = 13.7 secs, H_{rms} = 3 metres, 5/1000 of the year (1.58×10^5) seconds.

(2) T_e = 13.3 secs, H_{rms} = 3.3 metres, 2/1000 of the year (6.3×10^4) seconds.

(3) T_e = 11.7 secs, H_{rms} = 3.6 metres, 2/1000 of the year (6.3×10^4) seconds.

(1) T_e is 13.7 seconds so the zero crossing period (T_z) is about $\frac{13.7}{1.2}$ = 11.4 seconds

Number of waves is about $\frac{1.58 \times 10^5 \text{ secs}}{11.4 \text{ sec/wave}} = 1.3 \times 10^4$ waves

If we interpolate logarithmically between 10^4 and 10^5 waves, the multiplier is

$$8.6 + \frac{\log (13800) - \log (10000)}{\log (100000) - \log(10000)} (9.6 - 8.6) = 8.74$$

Highest expected wave is then 3 x 8.74 = 26.2 metres.

(2) T_z is $\frac{13.3}{1.2}$ = 11.1 seconds, number of waves $\frac{6.31 \times 10^4}{11.1} = 5693$

log interpolate $\frac{\log(5693) - \log(1000)}{\log(10000 - \log(1000)} (8.6 - 7.5) = 8.33$

Highest wave is 3.3 x 8.33 = 27.5 metres.

(3) T_z is $\frac{11.7}{1.2}$ =9.75 seconds, number of waves $\frac{.6.3 \times 10^4}{9.75 \text{ sec/wave}} = 6471$

log interpolate $7.5 + \frac{\log (6471) - 3}{4-3} (8.6 - 7.5) = 8.39$

trough-crest wave is 3.6 x 8.39 = 30.2 metres

So the expected peak wave at India during the year in which the waves were measured was about 30 metres (trough to crest). This is only a point measurement, however. What about the expected wave that would have hit a duck string? We have not seen any theoretical work on this but one very crude method can be used. Assume a crest length for the sea, then assume that a duck string n crest lengths long gets about n times the number of waves that a point measurer does. An approximation for crest length is 1.7 times the wavelength of the energy period[13].

Then for the third big storm:

Crest length about $1.7 \times \frac{11.7^2 \ 9.81}{2} = 363$ metres

If we have a 4 kilometre duck string, so that number of waves

$$= 6471 \times \frac{4}{.363} = 71{,}300 \text{ waves}$$

long interpolate as before $8.6 + \frac{\log(71{,}300 - 4)}{1} (9.6 - 8.6) = 9.45$

Highest wave is 3.6 x 9.45 = 34 metres.

A crude rule for extrapolating beyond the table is that a factor of 10 increase in the number of waves gives about 10% increase in the maximum wave.

All the numbers up to now in this section have been concerned with predicting the maximum wave in a previously measured sea. This should be kept separate from the problem of predicting a "100 year storm", or the "100 year wave". A method for doing this is given by Draper[14].

FORCE COEFFICIENTS

During our work at Edinburgh we have discovered that a convenient way to express duck forces is by a 'force coefficient'. This coefficient relates duck diameter and wave height to the surge and heave forces on the duck. Details are explained on page 2.2 of our 1976 report. The merit of this coefficient is that it remains fairly constant over the whole range of operating conditions. It can be used to predict duck forces with the simplest possible equation.

We define the coefficient as follows:

$$C_f = \frac{\text{Force}}{\rho g \text{ (duck diameter) (duck width) (wave height)}}$$ ρg = (density)(gravity

The wave height is trough-to-crest, and the force is zero-to-peak in a regular sea.

For the work in random seas, we used two separate coefficients; the peak-derived coefficient and the RMS-derived coefficient.

The peak coefficient is calculated using the maximum force divided by the difference between the highest crest and the lowest trough wherever they may have occurred.

The RMS-derived coefficient is calculated using the RMS force divided by two times the H_{rms} of the sea.

$$C_{fp} = \frac{F \text{ peak}}{\rho g \text{ DW (highest crest-lowest trough}}$$

D = duck diameter

W - width of duck

$$C_{frms} = \frac{F_{rms}}{2\rho g D W \ H_{rms}}$$

If there is good agreement between peak-derived and RMS-derived coefficients we can take it as a sign that extrapolations and interpolations will be safe. But if the two coefficients disagree then we should do more tests to discover why.

Example:

What is the approximate peak surge force on a fixed-axis duck in an average 10 second sea if $C_f = .5$?

From the P-M section: $H_{rms} = 1.36$ m

From the H_{rms} section: H_{TC} max = 10 H_{rms} = 13.6 m

For a 15 m duck $F_p = C_{fp} \rho g D H_{TC}$

$= .5(1027 \text{ kg/m}^3)$ (9.81 m/sec^2) (15m) (13.6)

= 1.03 MN/m.

USEFUL EQUATIONS

A NOTE ON SCALE

If dynamic similarity exists between model and prototype, we can get full-scale figures from model figures with the right scaling factor. This is best described by some index of scale.

PARAMETER	INDEX OF SCALE
Wave height and length	1
Period	.5
Frequency	- .5
Nod angle	0
Angular velocity	- .5
Angular acceleration	-1
Buoyancy	3
Inertial forces	3
Velocity forces	3
Drift forces	3
Torque	4
Power	3.5
Power per unit length	2.5
Force per unit length	2
Torque per unit length	3
Mass	3
Inertia per unit length	4
Buoyancy spring per unit length	3
Damping per unit length	3.5
Heave and surge distances	1
Heave and surge velocities	.5
Heave and surge accelerations	0
Stiffness density	1
Compliance density	-1
Beam stiffness EI	5

The ratio of wavelength to diameter L/D is the most useful indicator of dynamic similarity. The ratio of wave height to diameter should also be considered. Scale effects should be less of a worry for inertia-dominated wave behaviour than in other fields.

$H_{RMS} = \frac{H_{sig}}{4} = \frac{H_{\frac{1}{3}}}{4} = \sqrt{M_o}$ For P.M. norm $H_{RMS} = .0136\, T_e^2$

$T_e = .977\, U_{19.5}$

$P_{ower} = \frac{\rho g^2}{4\pi} H_{RMS}^2 T_e$ For P.M. $= 1.4 \times 10^{-4}\, U_{19.5}^5 = 1.57 \times 10^{-4}\, T_e^5$

$\frac{\rho g^2}{4\pi} = 7.82$ for kW/m.

For deep water phase vel $= \sqrt{\frac{g\lambda}{2\pi}} = \frac{gT}{2\pi} = 2 \times$ group vel

For shallow phase vel $= \sqrt{gZ} =$ group vel. $\frac{Z}{\lambda} \tanh \frac{2\pi Z}{\lambda} = \frac{Z}{\lambda}$

Universal Beam Equation: $\frac{M}{I} = \frac{\sigma}{y} = \frac{E}{R}$

E concrete $= 40 \times 10^9$ N/M²

steel $= 200 \times 10^9$ N/M²

Floatation

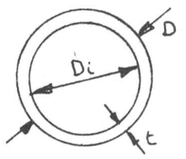

$\frac{Di}{D} = \sqrt{1 - \frac{1}{\gamma}}$

γ concrete $= 2.4$

$\frac{Di}{D} = .76$ max .8 probable

Section Moment $I = \frac{\pi (D^4 - Di^4)}{64} \simeq \frac{\pi D^3 t}{8}$ $I \simeq .03\, D^4$

$EI_{13.5} = 4 \times 10^{13}$ Nm²

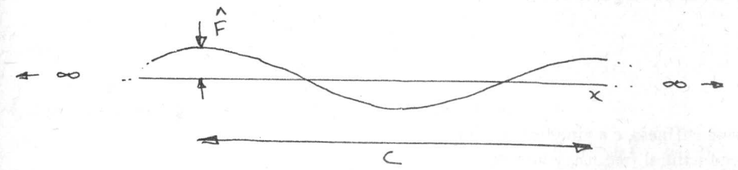

Static force field 'rigid' beam

$\lambda < C < \infty$; $C \simeq 1.7\lambda$?

Local Force density $F = \rho g D H_{Tc} f_p = \hat{F} \cos \frac{2\pi x}{C} = \frac{d\,\text{Shear}}{dx}$

Shear $= \frac{C\hat{F}}{2\pi} \sin \frac{2\pi x}{C} + k_1$

M $= -\frac{C^2 \hat{F}}{4\pi^2} \cos \frac{2\pi x}{C} + k_1 x + k_2 = EI \frac{d^2y}{dx^2} = \frac{EI}{R}$

Slope $= \frac{dy}{dx} = -\frac{C^3 \hat{F}}{8\pi^3 EI} \sin \frac{2\pi x}{C} + \frac{k_1 x^2}{2} + k_2 x + k_3$

$y = \frac{C^4 \hat{F}}{16\pi^4 EI} \cos \frac{2\pi x}{C} + \frac{C_1 x^3}{6} + \frac{C_2 x^2}{2} + C_3 x + C_4$

Stiffness $= \frac{\hat{F}}{y} = \frac{16\pi^4 EI}{C^4}$ EI for 13.5 concrete $= 4 \times 10^{13}$ Nm²

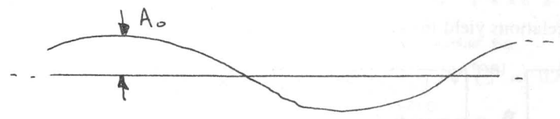

Flexible beam.

Deflection $y = A_o \cos \frac{2\pi x}{C}$

Slope $\frac{dy}{dx} = -\frac{2\pi A_o}{C} \sin \frac{2\pi x}{C}$

Curvature $\frac{d^2y}{dx^2} = -\frac{4\pi^2 A_o}{C^2} \cos \frac{2\pi x}{C} = \frac{1}{R}$

Strain $\epsilon = \frac{\sigma}{E} = \frac{MD}{2IE} = \frac{D}{2R} = \frac{2\pi^2}{C^2} D A$

Joint angle

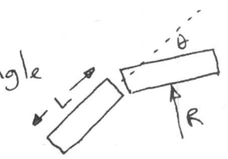

$\theta = \frac{L}{R} = \frac{LA}{C^2} 4\pi^2$

Vibrations

In the following, k is spring stiffness, c a viscous damping constant, ω_n an undamped natural frequency and m, M masses.

Free vibration with viscous damping

For a mass m the undamped natural frequency is

$$\omega_n = \sqrt{(k/m)}$$

the critical damping constant is

$$c_c = 2\sqrt{(km)}$$

the damping ratio is $\zeta = c/c_c$ and the logarithmic decrement is

$$\delta = 2\pi\zeta/\sqrt{(1-\zeta^2)} \approx 2\pi\zeta$$

Steady-state vibration with viscous damping

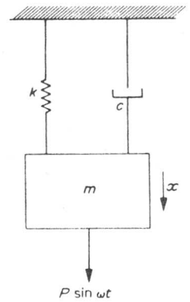

The ratio of peak amplitude X to the steady displacement $X_0 = P/k$ is

$$\frac{X}{X_0} = \frac{1}{[\{1-(\omega/\omega_n)^2\}^2 + \{2\zeta\omega/\omega_n\}^2]^{1/2}}$$

and the phase angle ϕ is given by

$$\tan\phi = \frac{2\zeta\omega/\omega_n}{1-(\omega/\omega_n)^2}$$

These relations yield the curves given below.

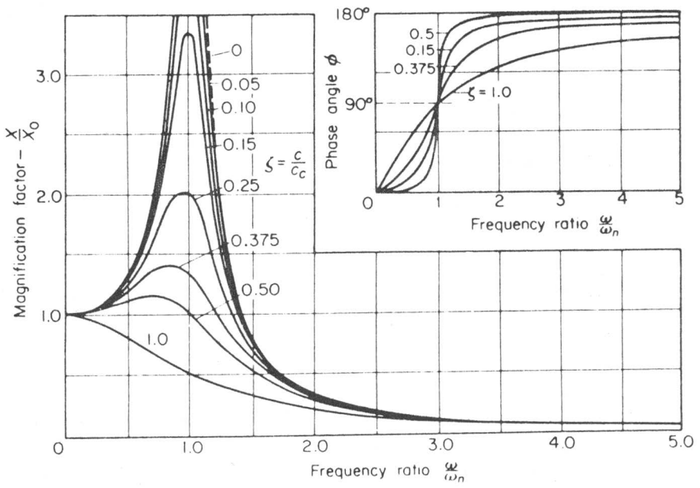

1st 2nd 3rd

Free beam. ω_{nat} = 22.4 , 61.7, 121 $\sqrt{\frac{EI}{mL^4}}$

m = mass / unit length. (inc added mass)

Coefficient of friction for pipes

The coefficient of friction f gives the head loss for an average flow velocity V in a pipe of radius r_0 and length L according to Darcy's equation:

$$h_L = f\frac{LV^2}{4r_0 g} \qquad \therefore P_L = \frac{f L V^2 \rho}{2D}$$

$D = 2r_0$

in which $f = 4C_f$ and C_f is the friction coefficient given by $\tau/\frac{1}{2}\rho V^2$ where τ is the shear stress at the wall. The curves show f as a function of Re for various values of r_0/ϵ, where ϵ is the effective surface roughness.

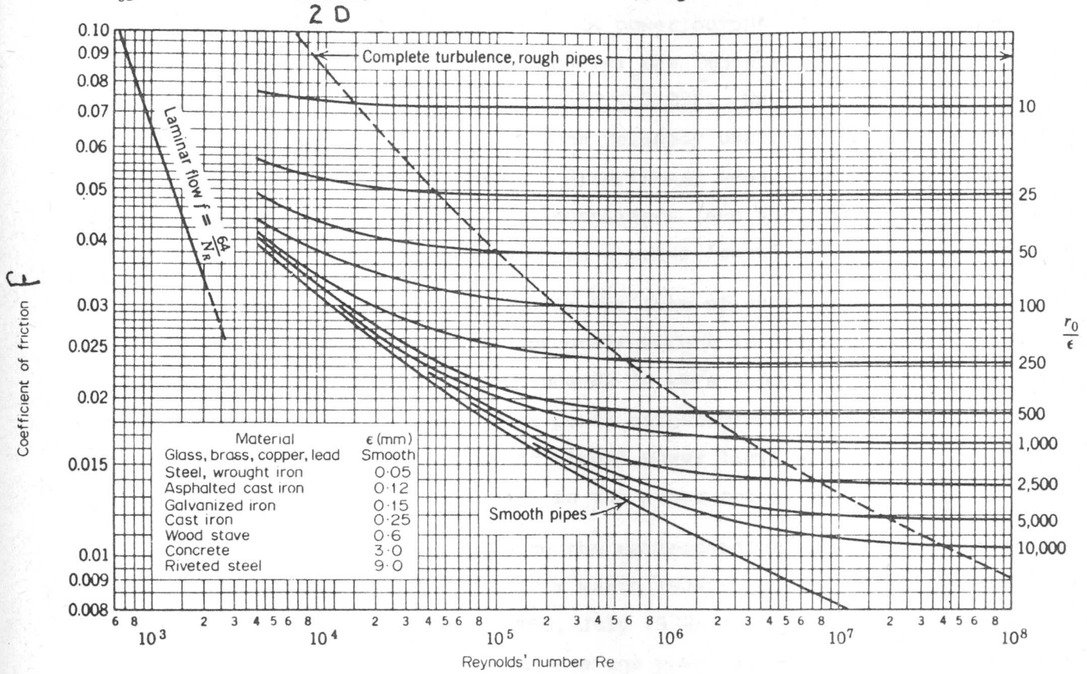

Re for water = V D × 10^6

Coefficients of loss for pipe fittings

The loss of head incurred by fittings, valves or sudden contractions of area is given by the loss coefficient C_L according to the relation

$$h_L = C_L(V^2/2g) \qquad \therefore P_L = C_L\frac{V^2\rho}{2}$$

where V is the average flow velocity. Values of C_L for fittings, valves and contractions of area ratio A_2/A_1 are given below

	C_L
Globe valve, fully open	10·0
Angle valve, fully open	5·0
Swing check valve, fully open	2·5
Gate valve, fully open	0·19
Three-quarters open	1·15
One-half open	5·6
One-quarter open	24·0

	C_L
Close return bend	2·2
Standard tee	1·8
Standard 90° elbow	0·9
Medium sweep 90° elbow	0·75
Long sweep 90° elbow	0·60
45° elbow	0·42
Rounded inlet	0·04
Re-entrant inlet	0·8
Sharp-edged inlet	0·5
Contraction, A_2/A_1 = 0·1	0·37
= 0·2	0·35
= 0·4	0·27
= 0·6	0·17
= 0·8	0·06
= 0·9	0·02

Power = $P V \frac{\pi D^2}{4}$

Pressure max = $\frac{2\sigma t}{D}$ ≃ 34·5 × 10^6 N/m² (For B.T.R. hose)

≃ 5000 lb/in²

≃ 345 bar

PREDICTED POWER AT SEA

The results from the scatter diagram tests have been integrated with the Hoffman India data[8] to predict duck power output over the year. We have used the fixed rig performance figures; however the (more recent) moving rig tests give very similar efficiencies (see pages 2.17 - 2.23). We have not made any allowance for directionality: this cannot be done reliably until we have experimental data on the performance of duck strings in directional seas. The most we can say is that NMI calculations and the heave/surge compliance (see Section 4) encourage us to believe that we will not lose as much as a naive 'cosθ' calculation would suggest.

Page 8.3 shows the results in the form of exceedance curves. These curves show the percentage of times the duck power output is greater than a certain level. For example, the duck power output exceeds 30 kW/m about 55% of the time. The table on page 8.4 shows average duck power output broken down by season as a function of duck torque limit and also an additional power limit which could be imposed by the cables to shore or some other device in the power chain.

The tables on page 8.5 give the corresponding figures for an inshore South Uist site, using IOS's data from March 1976 - February 1978, weighted as suggested by Mollison (Report to ETSU, July 1978) to make them representative of long term conditions. This gives an average power of about 40 kW/m, less than half that at OWS India. This site is somewhat sheltered by shoals both north and south, so it is possible that other inshore sites nearby may have significantly higher average power levels, of perhaps 50-60 kW/m. (The average power level at Fitzroy, about 50 miles west of Shetland, has been estimated at 60-70 kW/m (Mollison, EWPP Report No. 47).

In any case, predicted power output levels fall by less than half in going from India to S. Uist data, because much of the difference in power available is attributable to overload conditions.

For the S. Uist data we have given output tables for 10, 12 and 15 m diameter ducks (page 8.5). Output time series for two sample months are shown on page 8.7.

Even without detailed costings, some clear conclusions on optimal characteristics for ducks can be drawn. Because torque-limited ducks have a fairly well-defined maximum output (see page 2.17 et seq.) which is attained for a significant proportion of the year, it makes sense to match the power limit to this maximum: this implies a power limit of approximately 100 kW/m per MNm/m of torque limit.

The optimal torque limit depends more on the duck diameter chosen than on the wave climate: for South Uist the optimum torque limit is about 1 MNm/m for 15 m ducks and probably less than .5 MNm/m for 10 m ducks (see page 8.6).

The basic parameter is likely to be duck diameter, for both economic and structural reasons. Note that output increases less than linearly with diameter; so if we assume that duck costs increase linearly (or still worse quadratically) with diameter we find that the 10 m diameter ducks are the best value. Perhaps the optimal diameter is zero! However, this does not take into account any fixed overheads in construction costs, nor more importantly spine characteristics: experiments in progress suggest a diameter of at least 1/40th of typical crest lengths is necessary for our assumed efficiencies to apply. Also the relative costs of making spines sufficiently stiff may <u>increase</u> for smaller ducks.

We conclude that while these figures suggest that 10m or smaller ducks may be appropriate for a site such as South Uist, such an inference depends critically on assumptions about the behaviour of duck strings in directionally-spread seas.

FIGURE 1

PREDICTED OUTPUT FOR 15M DUCKS AT O.W.S. INDIA WITH TORQUE LIMITS 1,2,3 MN/M (CURVES IN ASCENDING ORDER)

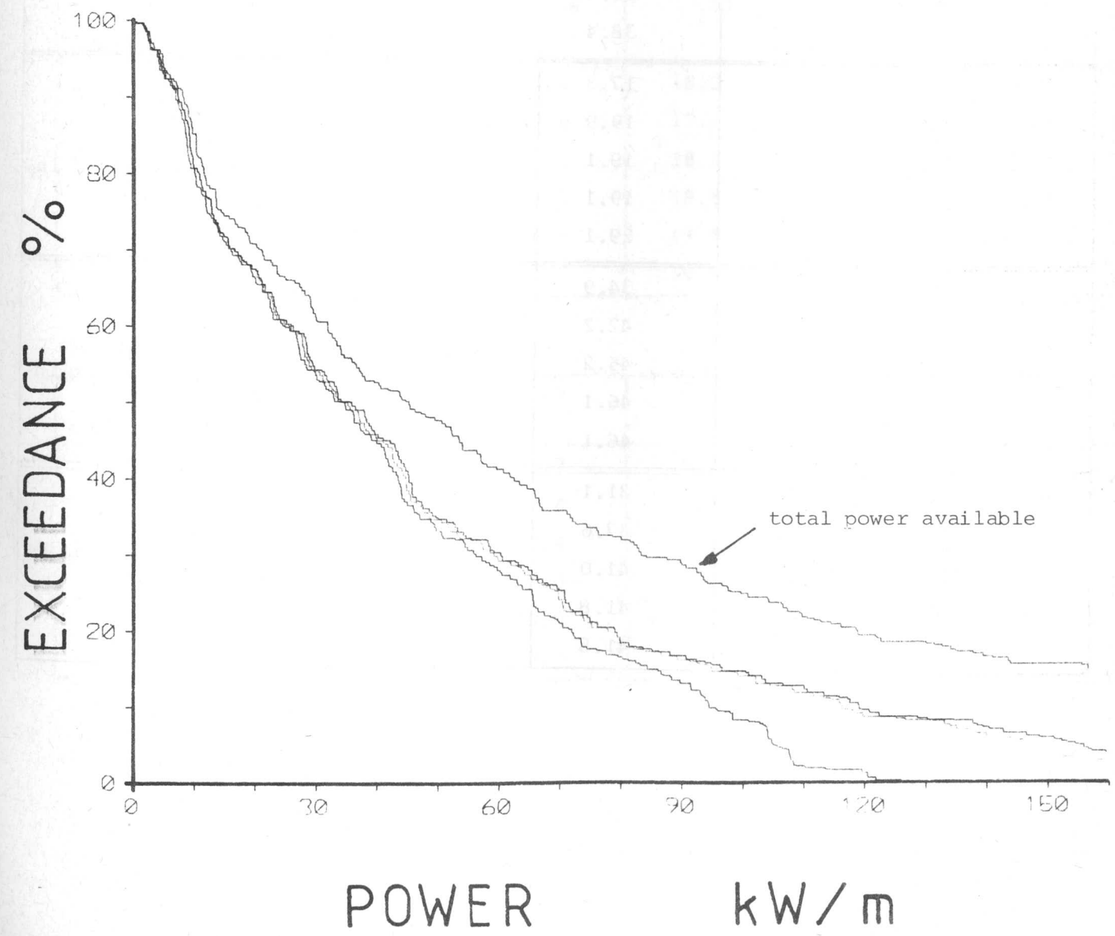

DUCK POWER OUTPUT (kW/m) AT OWS INDIA FOR VARIOUS TORQUE & POWER LIMITS

POWER LIMIT (kW/m) \ TORQUE LIMIT MNm/m)	1	2	3	
50	42,0	42.3	42.5	
75	54.2	55.1	55.4	WINTER DEC-FEB Average power in 177.1 kW/m
100	61.9	64.6	65.0	
200	63.6	77.3	79.3	
	63.6	77.3	80.0	
50	30.3	30.8	31.1	
75	35.2	36.2	36.6	SPRING MAR- MAY Average power in 68.4 kW/m
100	37.9	39.6	40.0	
200	38.4	43.4	44.6	
	38.4	43.4	44.6	
50	17.3	17.8	18.0	
75	19.9	19.8	20.0	SUMMER JUN-AUG Average power in 26.7 kW/m
100	19.1	20.2	20.4	
200	19.1	20.3	20.6	
	29.1	20.3	20.6	
50	34.9	35.4	35.6	
75	42.2	43.6	44.0	AUTUMN SEPT-NOV Average power in 91.3 kW/m
100	45.2	47.2	47.8	
200	46.1	51.9	53.4	
	46.1	51.9	53.4	
50	31.1	31.6	31.8	
75	37.6	38.7	39.0	WHOLE YEAR Average power in 90.9 kW/m
100	41.0	42.9	43.3	
200	41.8	48.2	49.5	
	41.8	48.2	49.7	

DUCK POWER OUTPUT (kW/m) AT SOUTH UIST FOR DUCK DIAMETERS 10 - 15m AND VARIOUS TORQUE LIMITS.

(Average power in is approximately 40 kW/m)

FIGURE 1(a) DUCK DIAMETER : 10m

POWER LIMIT \ TORQUE LIMIT MNm/m	.15	.30	.59	.89
30	11.6	14.8	15.2	15.3
40	11.6	15.8	16.7	16.9
50	11.6	15.8	17.6	17.8
75	11.6	15.8	18.3	18.6
- ∞	11.6	15.8	18.3	18.7

FIGURE 1(b) DUCK DIAMETER : 12m

POWER LIMIT \ TORQUE LIMIT	.26	.51	1.02	1.54
30	14.2	16.0	16.3	16.4
40	14.8	17.8	18.2	18.4
50	14.8	18.9	19.5	19.7
75	14.8	19.5	21.2	21.4
100	14.8	19.5	21.5	21.8
- ∞	14.8	19.5	21.6	21.9

FIGURE 1(c) DUCK DIAMETER : 15m

POWER LIMIT \ TORQUE LIMIT	.5	1.0	2.0	3.0
30	15.7	16.8	17.2	17.2
40	17.4	19.2	19.6	19.7
50	18.4	20.8	21.3	21.5
75	19.0	23.1	23.9	24.1
100	19.0	23.9	25.0	25.3
- ∞	19.0	24.0	25.6	26.0

DUCK POWER OUTPUT AS A FUNCTION OF TORQUE LIMIT

(In each case a 'saturation' power limit has been assumed, i.e. 100 kW/m per MNm/m of torque limit.)

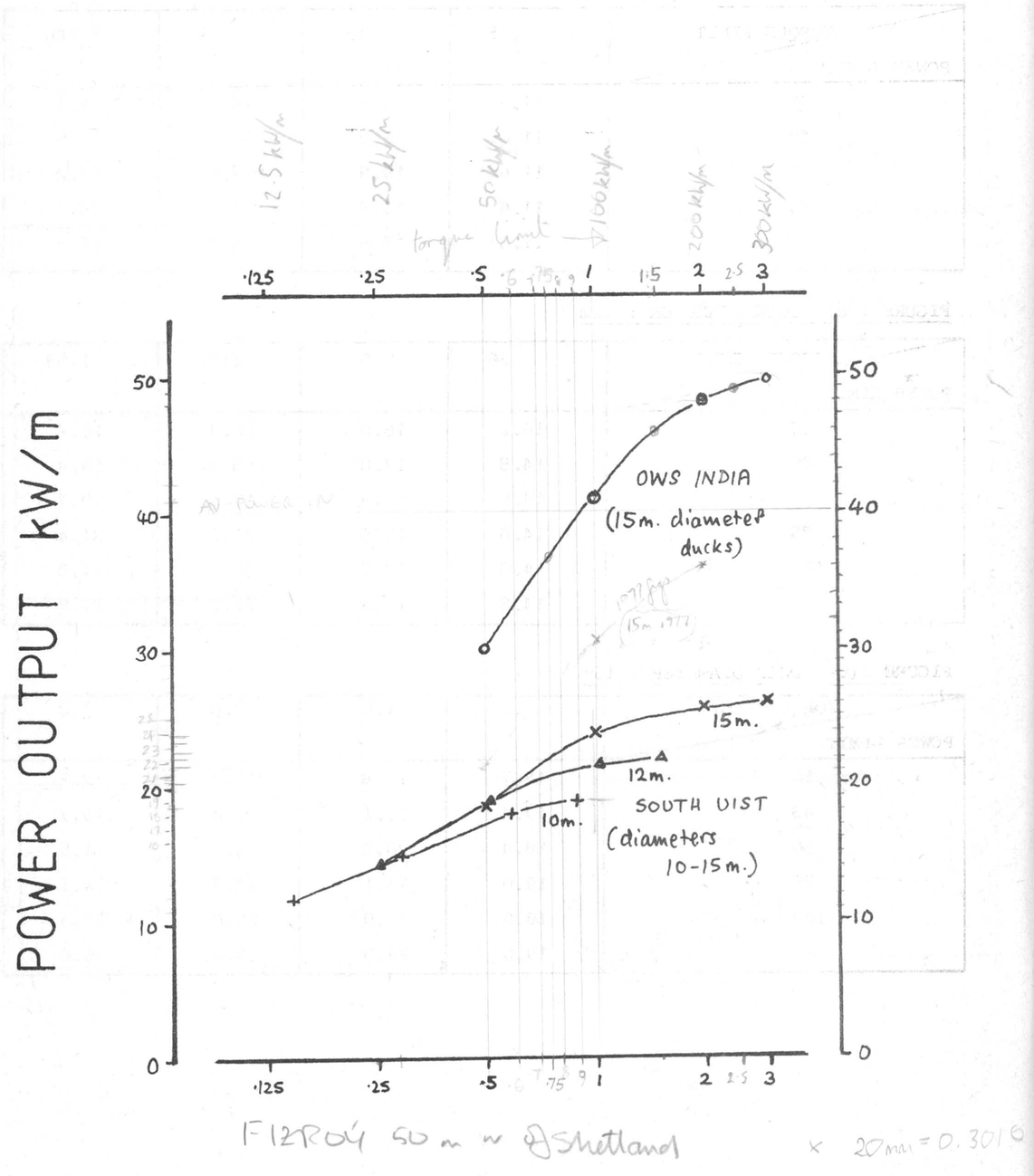

FIGURE 3

TWO SAMPLE MONTHS FROM IOS'S SOUTH UIST DATA FROM MARCH 1976 - FEBRUARY 1978

The top curve shows power in; predicted outputs are also shown for 15 m diameter ducks with torque limits .5, 1, 2 and 3 MNm/m (lower four curves in ascending order).

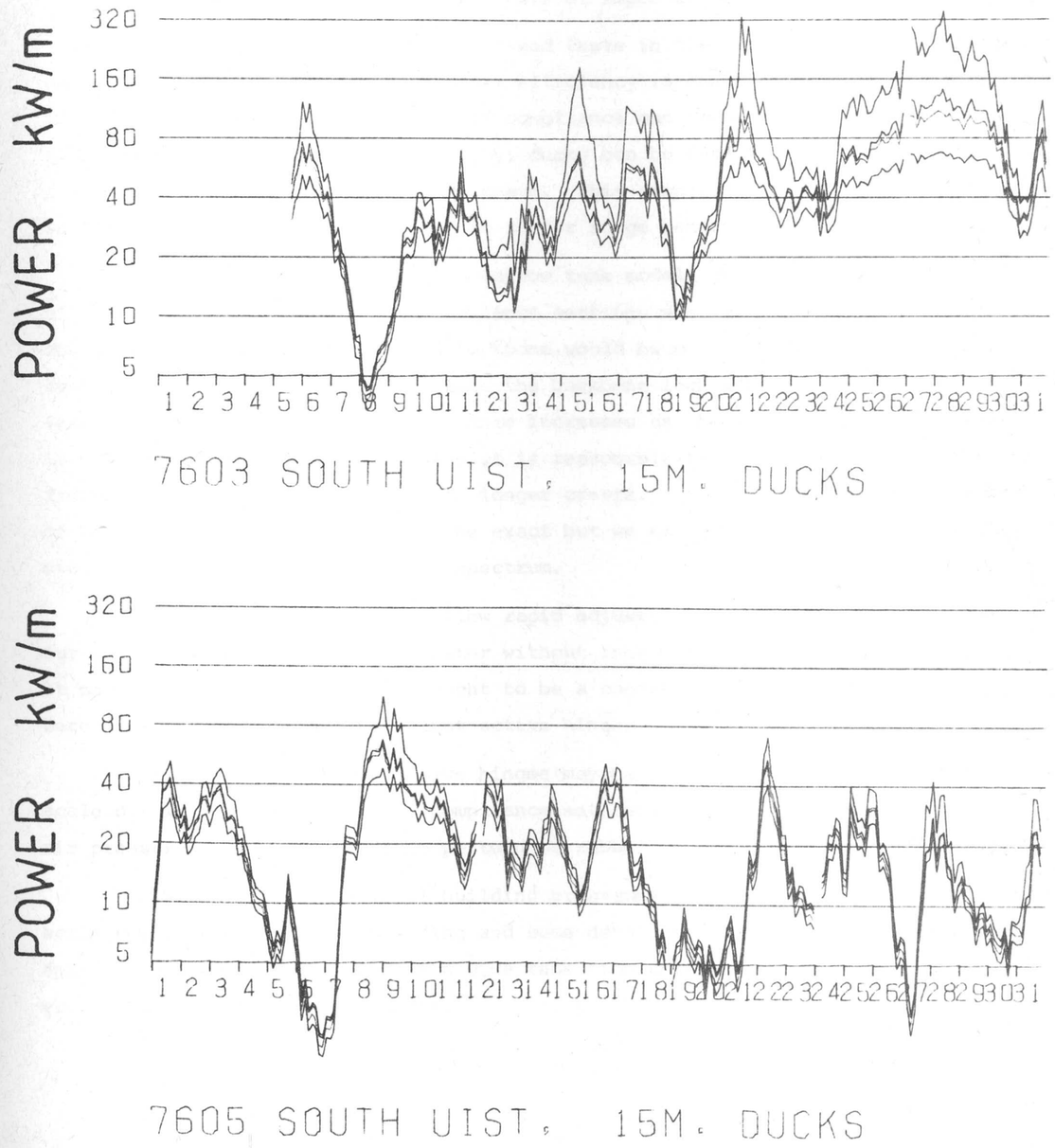

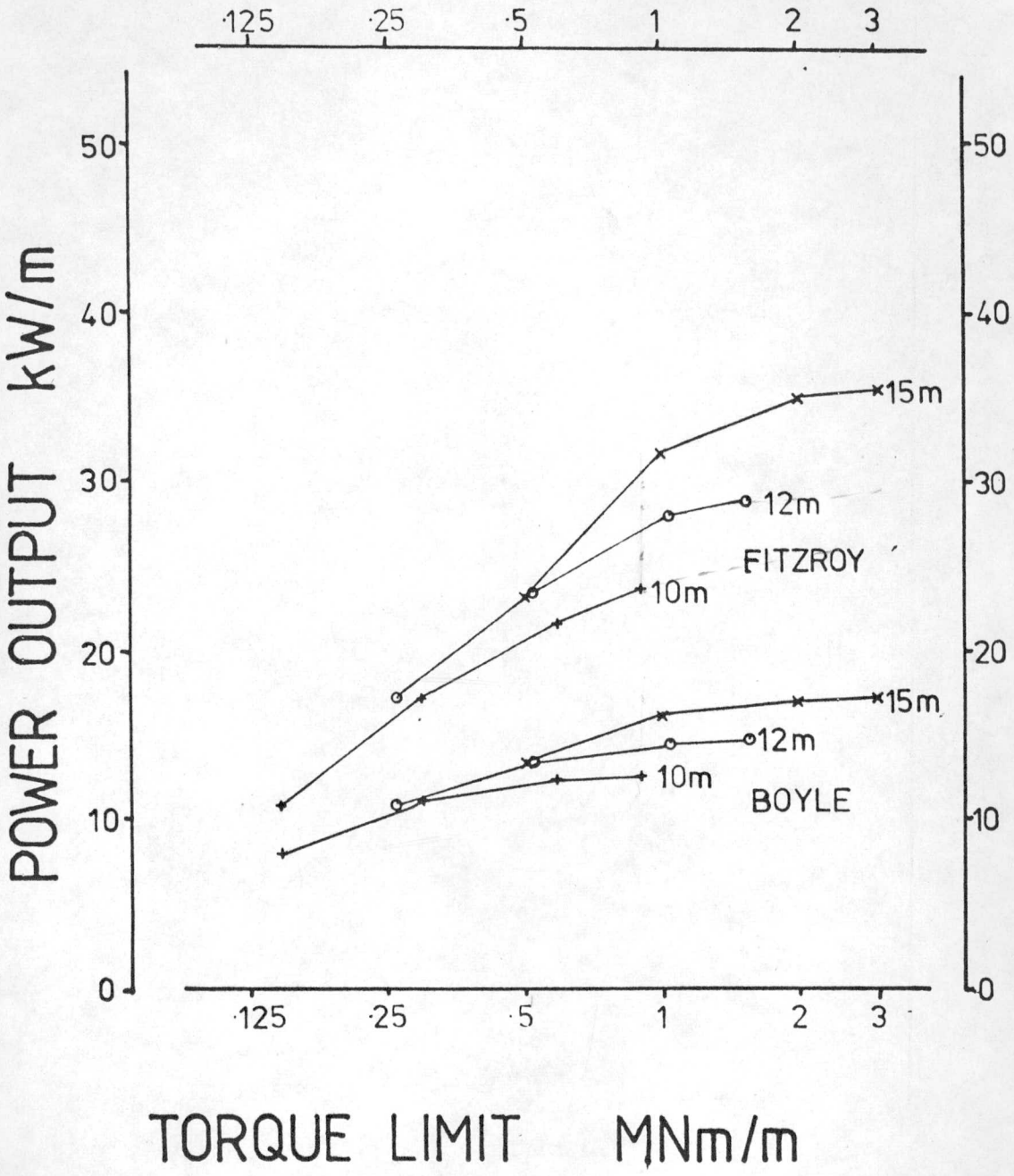

FIGURE 3

PREDICTED AVERAGE POWER OUTPUTS FOR DUCKS OF DIAMETERS 10-15 m AT FITZROY AND BOYLE STATIONS PLOTTED AS A FUNCTION OF THE TORQUE LIMIT OF THEIR POWER TAKE-OFF MACHINERY. DATA ARE FOR THE YEAR Mar 1975 - Feb 1976.

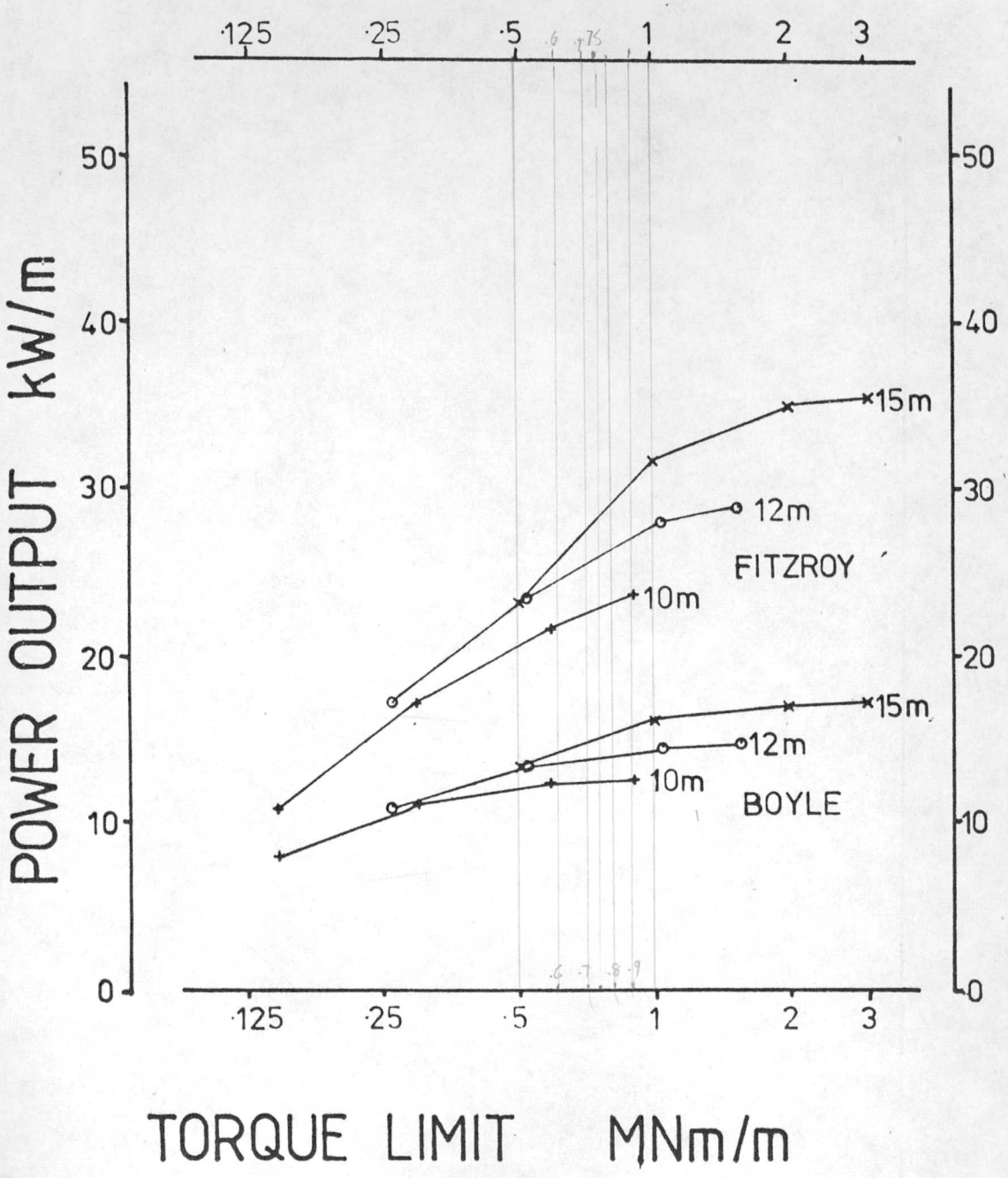

FIGURE 3

PREDICTED AVERAGE POWER OUTPUTS FOR DUCKS OF DIAMETERS 10-15 m AT FITZROY AND BOYLE STATIONS PLOTTED AS A FUNCTION OF THE TORQUE LIMIT OF THEIR POWER TAKE-OFF MACHINERY. DATA ARE FOR THE YEAR Mar 1975 - Feb 1976.

AIMS AND MILESTONES FOR WORK ON DUCKS AFTER OCTOBER 1978

(1) BACKBONE COMPLIANCE TESTS

AIM: To understand what joints have to do.

Before any pronouncements can be made on the feasibility of making backbones, it is necessary to have a clear specification of what the joints have to achieve and knowledge of the costs of imperfections.

In this report we have described tests in the narrow tank in which the effect of backbone compliance on model efficiency is explored. The work shows that practically achievable values of compliance can produce better results than rigid mountings and that, surprisingly, ducks can be made to work very well with a mounting which is totally free in heave. This simplifies the design of full scale joints which now have 'only' to resist surge bending moments and torque.

Irregular wave tests with narrow tank models suffer from a limitation of the pitch/heave/surge rig: compliance settings are not frequency dependent. The compliance of a free-floating backbone would be strongly dependent on crest length. Long-crested waves will make the backbone look more compliant. We find that the optimum setting for compliance increases as the frequency falls. This is the way we would like it because it is reasonable to expect that the lower frequencies will be associated with longer crests. It turns out that the matching of compliance to frequency cannot be exact but we can straddle the optimum values over the most useful parts of the spectrum.

The ideal model would allow rapid adjustment of compliances to be carried out while the models are in the water without interfering with normal duck operation. It may turn out that compliance ought to be a controlled variable rather than a carefully chosen constant, and that active hinges ought to be given some thought.

It looks as though active hinges may be difficult to make at 1/150th scale but we are confident that compliance settings can be changed by controlling air pressures inside a cruciform pattern of rubber tubes in each backbone joint.

We hope that the model building programme (which has to include 1/150th scale power take-off, duck building and some data collection) will be finished by April 1979. We will not need much wide tank time until then but after that we would like an intensive programme.

MILESTONES

1. Development of new large rotation dynamometer for free-floating backbone. DEC 1978
2. Development of compliance variation techniques. DEC 1978
3. Construction of 80 units. APRIL 1979
4. Joint specification to include degrees of freedom, values of torque and bending moment as a function of sea state, effects of safety limits, angle of movement and number of operations. As crest lengths at sea are uncertain, the results may have to be given as a function of crest length. DEC 1979

AREAS NOT COVERED BY THIS PROGRAMME

We may want to investigate active hinges, power take-off from hinges and ultra-smart computer-per-duck power take-off control designed for efficiency at low powers and survival at high powers. The results may suggest that we should examine external appendages to assist the backbone in its work. We will design the model so that appendages may be easily attached.

(2) FULL SCALE POWER TAKE-OFF

AIM: To confront the problem of full scale power conversion.

If one could take a duck and cut a thin slice along a vertical plane parallel to the direction of wave propagation, dissect and remove the power take-off components and lay them out flat on the floor of a heavy testing laboratory, one would have a clear image of our objective.

Our power take-off scheme uses pairs of wide thin tapes wrapped half a turn around the backbone and eight times round the body of a wheel pump/motor. Their thinness reduces problems with fatigue. (We accept, for the time being, the unfortunate feature that each pump works for only half the cycle, although we may decide at some time in the future to devise a differential unit to allow two inputs to drive a single pump.)

The pumps contain no valve gear. Instead, a reciprocating oil flow is taken to a pressure exchange unit where it is converted to a reciprocating water flow. Polymers, anti-fouling and anti-corrosion additives can be added. Flow is rectified with poppet valves into a constant high pressure main common to many ducks. The benefits of a variable displacement primary pump are obtained by foiling the closure of the water inlet valve. An accumulator, which may use expansion against vacuum rather than compression of air, is used to provide some local short-term storage. A single local 2 MW generator is run at a constant output and the energy surplus or deficit is sent as high pressure water to other ducks via the constant pressure main.

The advantages of the scheme are as follows:

1. The tapes do not conflict with duck location and are tolerant of misalignment.
2. Power is taken over the whole duck width, so that stress concentrations are avoided.
3. No high friction coefficients are required, very little rubbing occurs.
4. Fatigue is avoided by the thin tape section.
5. Each pump lives in its own oil which can be chosen for long life rather than efficient energy transport. Infection cannot spread.
6. We have the option to change pressure at the border between oil and water.
7. Water is cheaper than oil. Losses are lower and leaks more tolerable.
8. Poppet valves are more resistant to wear than face valves and can show a better volumetric efficiency.
9. There is lots of room around the valves for pump displacement control gear.
10. There are no pressure fluctuations in the hydraulic mains.
11. Machinery weight is concentrated at the place where duck dynamics demand.
12. A fair outside shape is preserved.

The disadvantages are as follows:

1. Power is on a moving duck rather than a steady backbone.
2. Complicated mechanism is required to make the pumps work over the full cycle.

Work on full scale power modules faces the continual problem of the high price of energy. We have to design rigs with large power ratings which can work for long periods of time. A module rating of .2 MW running for a year would cost £40,000 in electricity. It is important to build loops which re-circulate the energy so that we need only pay for the losses.

We propose to begin work on the oil-to-water conversion and the poppet valve gear. The loop will take the form:

electric motor - eccentric - oil piston - oil - inter-piston - water - valve gear - smoothing accumulator - Pelton wheel - electrical generator.

The rig will be static and we hope to have it running by the end of 1979.

The work on oil-to-water conversion and poppet valve control is of possible relevance to other devices and so it seems better to do it before work which is peculiar to ducks. The rig does not require as much space as the rest of the system which has to await the completion of a test building.

The second rig will be designed to test the tape-to-pump idea. We will build a bogey running on rubber tyres like a small segment of duck innards. It will carry four motor/pump units running on oil. Two will work alternately against one another as motors and pumps, while the other two test the condition of idle running and tape re-winding.

The laboratory floor will have a sloping section leading to a trough of salt water into which the bogey can be run for submerged operation. (Fortunately, the natural lie of the ground near our new wave tank allows this unusual feature to be included without excessive excavation.)

It seems sensible to build a pair of bogeys so that tests can run on one while modifications are carried out on the other. We cannot begin tests on the first unit until the building is available. The earliest estimate for this is two years from the start of architectural planning.

When we are confident about both the tapes and the water valve-gear we will combine the two rigs so as to produce the final complete module.

Power can be sent from a moving duck to the backbone if a large reel is built into the end face of each duck. The reels can be nearly half the duck diameter and so bending stresses on hoses and cables are very small. There are strong interactions with final duck design which suggest that design of reel and hose should be deferred.

MILESTONES

1.	Oil-to-water and valve gear rig	DEC 1979
2.	Tape pump/motor and bogey assembly ready for testing (Building permitting)	JUNE 1980
3.	Combination of 1 & 2 to produce final module design	JUNE 1981

ITEMS NOT INCLUDED

We have not yet defined our turbine/generator. Most of the optimisation pointers favour very high pressures (35×10^6 N/M^2) for fluid energy transmission. This raises questions about turbine design. No Pelton wheels have been used at heads of 3,000 metres and industrial opinion is cautious. However, this may be because no geographical sites have such high heads. Extrapolations from present practice suggest very small (.5 M) diameter high speed (8,000) turbine/generator combinations producing a high frequency output.

While the later tests will include salt water, the final proof should come from a single duck tested at sea. We plan to borrow a ship and build on to it a linkage like a simple version of our pitch/heave/surge rig. The vessel weight should be about ten times the duck displacement. Inertial sensors will produce drive signals for actuators on the linkage so that the vessel movements can be compensated. We may then introduce other movements simulating backbone deflections. The scale should be large enough for the use of full-scale power modules. The cost of the experiment will be about £2 million, plus the cost of the ship.

The work on hose reels and polymer injection can be deferred until we know where to draw the boundary between electricity and water for power balancing.

(3) WAVE GAUGE ARRAY

AIM: To measure the width of waves at 1/150th, 1/15th and 1/1th scale.

While crest length information is very obviously needed for the design of duck backbones, it is also important in choosing spacing and side-to-side restraint for other devices and for the design of power smoothing equipment. Crest length has never been of much importance for ship safety and so less is known about it than about heights and periods.

The following characteristics are desirable in the measuring instrument:

1. The technique should allow easy transfer from scale to scale.
2. It should give engineers an easy route to bending moment and compliance calculations.
3. Its resolution should be good at long crest lengths.

Our approach is to use a linear array of height measuring probes. We want to develop a cheap unit so that large numbers can be used and the failure of a few need not be serious. We argue that it costs £50,000 to measure anything at sea but that increasing the number of things measured costs little more. We suggest that as many as one hundred sensors could be used along a four kilometre line.

Waverider buoys measure vertical acceleration and send data to land via a radio telemetry link. Bandwidth restrictions prevent the use of large numbers of waveriders and so we prefer a direct wire data collection system. We also wish to examine the possibility of a design using a pressure transducer dangling below a float about one half wavelength below the surface. Each unit would contain its own A/D conversion so that a distributed multiplexer system with digital communication can be used. If the surface float looks sufficiently commonplace it may escape unwelcome attention.

Arrays will at first be towed behind boats but they could be permanently deployed or even dropped as a free-floating line from aircraft. While sophisticated maximum likelihood methods could yield directional information, we plan to use a simpler analysis based on the change of correlation coefficient with probe separation. This is readily calculated in real time and needs very little computer memory.

MILESTONES

1.	Checking analysis software on resistive wire gauge array in the wide tank.	JUNE 1979
2.	Checking mooring design in the wide tank	JUNE 1979
3.	Single 1/10th scale transducer trial	JUNE 1979
4.	25 off 1/10th scale units ready for use	APRIL 1980
5.	Single full-scale unit test	SEPT 1980
6.	Full-scale array trials start	APRIL 1981
7.	First full-scale results analysed	DEC 1981

REFERENCES

(1) Ogilvie, T.F., First and second order forces on a cylinder submerged under a free surface. J. Fluid Mech. Vol. 16, pp 451-472, (1963).

(2) Evans, D.V., A theory for wave power absorption by oscillating bodies. J. Fluid Mech. Vol. 77, pp 1-25, (1976).

(3) Tucker, M.J., A shipborne wave recorder. Trans. Inst. Nav. Arch. Vol. 98, pp 236-250, (1956).

(4) Tucker, M.J., Analysis of records of sea waves. Proc. Inst. Civ. Engrs., Vol. 26, pp 305-316, (1963).

(5) Cartwright, D.E., On estimating the mean energy of sea waves from the highest waves in a record. Proc. Roy. Soc. A, Vol. 247, pp 22-48, (1958).

(6) Draper, L., The analysis and presentation of wave data - a plea for uniformity. 10th Conf. Coastal Eng., Tokyo 1966, Vol. 1, pp 1-11, (published by Am. Soc. Civ. Engrs., 1967).

(7) Cartwright, D.E. & Longuet-Higgins, M.S., The statistical distribution of the maxima of a random function. Proc. Roy. Soc. A., Vol. 237, pp 212-232, (1958).

(8) Mollison D. et al., Wave power availability in the N.E. Atlantic. Nature, Vol. 263, Nature, Vol. 263, pp 223-226, (1976).

(9) Newland, D.E., An introduction to random vibrations and spectral analysis, Longman (London).

(10) Pierson, W.J. & Moskowitz, L., A proposed spectral form for fully-developed wind seas based on the similarity theory of S.A. Kitaigorodski, J. Geophys. Res., Vol. 69, pp 5181-5190 (1964).

(11) Hogben, N. et al. Report of Environmental Conditions Committee to 4th International Ship Structures Congress (ISSC), Tokyo, (1970).

(12) Mitsuyasu, H. et al. Observations of the directional spectrum of ocean waves using a cloverleaf buoy, J. Phys. Oceanography, Vol. 5, pp 750-760, (1975).

(13) Longuet-Higgins, M.S., personal communication.

(14) Draper, L., Derivation of a 'design wave' from instrumental records of sea waves. Proc. Instn. Civ. Engrs. Vol. 26, pp 291-304, (1963).